The Functional Characterization of PCSK9's Binding Interactions with LDL and the LDL Receptor

Angela Matyas

Thesis submitted to the University of Ottawa in partial fulfillment of the requirements for the Master of Science in Biochemistry

Department of Biochemistry, Microbiology and Immunology

Faculty of Medicine

University of Ottawa

Abstract

Elevated plasma cholesterol is a risk factor for cardiovascular disease. Proprotein convertase subtilisin/kexin type 9 (PCSK9) hinders the uptake of low-density lipoprotein cholesterol (LDL-c) by mediating degradation of LDL receptors (LDLRs) in the liver. Gain-of-function (GOF) mutations in *PCSK9* cause familial hypercholesterolemia (FH). In normolipidemic human plasma, 30-40% of PCSK9 is bound to LDL particles, and this association with LDL inhibits PCSK9's ability to mediate LDLR degradation in cultured cells. To further investigate the physiological relevance of this interaction, we analyzed natural GOF mutations in *PCSK9* and assessed their effects *in vitro* on LDL binding, LDLR binding and LDLR degradation. Our results indicate that several GOF mutations severely inhibit LDL binding compared to wild type (WT) PCSK9, and only modestly affect LDLR affinity and LDLR degradation. These findings shed light on the potential physiological relevance of the PCSK9-LDL interaction, which may have an inhibitory effect on PCSK9 activity *in vivo*.

Acknowledgments

First, I would like to thank my supervisor and my lab members for all of their support. I have been very lucky to receive excellent guidance since starting in Dr. Tom Lagace's lab. I would like to thank him for giving me the opportunity to get my first ever research experience. I will always be thankful for his hands-on approach to teaching, for being there to help and for quickly answering any questions I had. I would also like to thank him for his patience with me during this learning experience. I have had the great opportunity to be published for the first time, and to attend a national conference where I represented our lab and presented a talk on our research. These are invaluable experiences that I will always be thankful for.

I would also like to thank our lab technician Tanja Kosenko for always being available and willing to go the extra mile in teaching me techniques or helping me when I did not understand something. She is incredibly kind, patient and hard working and my experience here would not have been the same without her. She helped me edit my materials and methods section, and has always been willing to provide me with valuable feedback for presentations and other research-related reports. I'd also like to thank Dr. Samantha Sarkar, our former PhD student, for mentoring me during my Honours and for teaching me many techniques, as well as for helping me with editing my Honours thesis. I would like to thank our PhD candidate Ikhuosho Asikhia for his help, constant moral support and for always being a kind and positive person to be around in the lab. Our post-doctoral fellow Dr. Zhenkun Hu has also helped me very much, and he is always a great team player when it

comes to helping other members of the lab, regardless of the situation at hand. I will definitely miss the lab once I am gone.

Next, I would like to thank my friends here at the UOHI. The help, advice, and support they have given me is something I will always cherish. I would also like to thank the trainee committee and Dr. Erin Mulvihill for allowing me to get more involved here, and to have given me the opportunity to meet new individuals and to organize events that brought the trainee community closer together. I would also like to thank my thesis advisory committee, Dr. Jyh-Yeuan Lee and Dr. Morgan Fullerton for taking the time to give me feedback and for always being supportive during my MSc project.

Last but certainly not least; I would like to thank my family and my friends outside of research. My parents have always given me support while I've been in school, and I hope that I have made them proud. None of this would have been possible without them. I'd also like to thank my close friends who have been kind and extremely supportive, continuously inquiring about how I am doing and how my project is going during the last year and a half. Lastly, I'd like to thank my partner for being my #1 cheerleader since starting my master's. His patience and support has really helped me through many difficult times. I certainly would not have made it this far without everyone's kindness and encouragement, so thank you very much!

Table of Contents

List of Abbreviations

AcCoA – acetyl coenzyme A

ADH – autosomal dominant hypercholesterolemia

ARH – autosomal recessive hypercholesterolemia adaptor protein

Apo A/B/C/E – apolipoprotein A/B/C/E

bHLH-Zip – basic helix-loop-helix leucine zipper domain

β-Me – beta mercaptoethanol

BSA – bovine serum albumin

CETP – cholesterol ester transfer protein

CHD / CVD – coronary heart disease / cardiovascular disease

CTD – C-terminal domain

ddH_2o – double distilled water

DMEM – Dulbecco's modified Eagle's medium

ECD – extracellular domain of the LDLR

EGF-A – epidermal growth factor-like A domain in LDLR

ELISA – enzyme linked immunosorbent assay

ER – endoplasmic reticulum

FBS – fetal bovine serum

FH / HoFH – familial hypercholesterolemia / homozygous FH

FPLC – fast protein liquid chromatography

GAM / GAR – goat anti mouse / goat anti rabbit

GOF – gain-of-function

HBS-C – HEPES buffered saline

HDL – high-density lipoprotein

Hepa1c1c7 – mouse hepatoma immortalized liver cell line

HepG2 – human hepatoma immortalized liver cell line

HEK293 – human embryonic kidney immortalized cell line

HMG CoA – 3-hydroxy-3-methylglutaryl-coenzyme A

HSPG / HLM – heparin sulfate proteoglycan / heparin-like molecule

HuH7 – human hepatoma immortalized liver cell line

IDL – intermediate-density lipoprotein

IDR – intrinsically disordered region

IP – immunoprecipitation

LDL / LDL-c – low-density lipoprotein / LDL-cholesterol

LDLR – low-density lipoprotein receptor

LOF – loss-of-function

LRP-1 – LDLR related protein 1

MTP – microsomal triglyceride transfer protein

MW – molecular weight

NARC-1 – neutral apoptosis-regulated convertase 1

NTR – N-terminal region

PBS / PBS-T – phosphate buffered saline / PBS and Tween-20

PC – proprotein convertase

PCR – polymerase chain reaction

PCSK9 – proprotein convertase subtilisin/kexin type 9

RCT – reverse cholesterol transport

S1P/S2P – site 1 protease / site 2 protease

SDS – sodium dodecyl sulfate

SPR – surface plasmon resonance

SRE – sterol response element

SREBP / SCAP – sterol regulatory element binding protein / SREBP cleavage activating protein

TBS-C – Tris buffered saline

TCA – trichloroacetic acid

TG – triglyceride

TXA_2 – thromboxane A_2

VLDL – very low-density lipoprotein

WT – wild type

List of Figures

List of Tables

1. Introduction

Cardiovascular diseases (CVDs) are the leading cause of death worldwide (1). An elevated level of plasma cholesterol packaged in the form of low-density lipoprotein (LDL) particles is a major risk factor for coronary heart disease (CHD) (2). Clearance of LDL particles from the blood occurs through receptor-mediated endocytosis by binding to the LDL receptor (LDLR); a cell surface glycoprotein (3). Proprotein convertase subtilisin/kexin type 9 (PCSK9) is known for its role in negatively regulating the life cycle of liver cell surface LDLRs (4, 5) by shuttling them towards lysosomal degradation, rather than allowing for receptor recycling to the cell surface. Therefore, PCSK9 indirectly hinders the uptake of LDL particles from the plasma. Very rare gain-of-function (GOF) mutations in *PCSK9* cause familial hypercholesterolemia (FH) (6, 7). Patients with FH suffer from abnormally high LDL-cholesterol (LDL-c) levels in the plasma, along with other cardiovascular complications. In recent years, anti-PCSK9 monoclonal antibody therapies that block the LDLR interaction have been shown to dramatically lower LDL-c levels by up to 70% in hypercholesterolemic patients (8). Although effective, these medications are not currently prescribed as a first-line therapy, but are reserved only for very severe cases, as they are extremely costly.

Because PCSK9 inhibition is highly effective for plasma LDL-c reduction, there is an incentive towards finding alternative ways to target PCSK9 for the development of more cost-efficient medications. To this end, we have found that PCSK9's direct association with LDL dampens its ability to mediate LDLR degradation in cell culture (9). To further investigate the role of PCSK9's association with LDL, we focused on characterizing various natural mutations in *PCSK9* and observed their effects on LDL binding. We also looked at

the consequences that these mutations have on LDLR degradation, LDLR binding, as well as PCSK9 processing and secretion. The work herein presents a detailed functional analysis of several *PCSK9* mutations associated with plasma LDL-c levels in humans, and characterizes how these mutations affect the activity of PCSK9. These studies ultimately allow us to better understand the complex structure-function relationship in PCSK9, through relating the LDL-c phenotype to the *PCSK9* genotype, which is a necessary step towards finding novel routes for PCSK9 inhibition.

1.1 Cholesterol Synthesis, Regulation, Metabolism and Transport

Cholesterol is a molecule with various vital roles in mammalian cell biology. In animal cells, it modulates flexibility in highly complex membrane bilayers. Cholesterol is also a precursor for the production of steroid derivatives such as bile acids, sex hormones and vitamin D (10). All cells in the human body are able to produce cholesterol endogenously; however, they can also obtain it through extracellular sources. Intracellular cholesterol synthesis involves the mevalonate pathway, where acetyl-coenzyme A (AcCoA) is used to form mevalonate (11). In this pathway, AcCoA is converted into 3-hydroxy-3-methyl-glutaryl coenzyme A (HMGCoA), an important intermediate, which is then further converted to mevalonate via the enzyme HMGCoA reductase in the endoplasmic reticulum (ER) (12). HMGCoA reductase controls this irreversible rate-limiting step of endogenous cholesterol synthesis (12). Five-carbon isoprene units are formed from mevalonate after various steps, and they eventually assemble to form the linear precursor of cholesterol called squalene. Squalene later becomes cyclic through chemical modifications to form lanosterol, which is eventually converted to the twenty-seven-carbon molecule of cholesterol (12).

This intracellular pathway of cholesterol synthesis is quite complex and starts off in the cytosol, ending with the formation of cholesterol in the ER. Alternatively, the extracellular pathway involves the uptake of dietary cholesterol sources (11). The major organs in the human body that regulate cholesterol absorption and packaging are the small intestine and the liver (10). It takes large amounts of cellular energy to synthesize cholesterol, and an excess amount of free, un-esterified cholesterol disrupts cellular homeostasis and is very toxic (12). Because of these consequences, the transcriptional regulation of the cholesterol synthesis pathways involves tightly regulated machinery.

1.1.1. The Transcriptional Regulation of Cholesterol Synthesis Pathways

Membrane-bound transcription factors called sterol regulatory element binding proteins (SREBPs) are responsible for modulating the transcription of genes coding for enzymes related to lipid metabolism (13). There are three mammalian isoforms of SREBPs: SREBP-1a, SREBP-1c, and SREBP-2 (14). SREBPs are synthesized as membrane proteins and are found in the ER. They function to bind enhancer elements called sterol response elements (SREs) in the promoter regions of lipogenic genes. SREBP-1c is the major SREBP-1 isoform in the liver, and is more active in promoting the transcription of genes related to fatty acid synthesis. SREBP-2 on the other hand, is the primary promoter for expression of cholesterol biosynthesis genes, such as those coding for the enzymes HMG-CoA reductase, HMG-CoA synthase, and mevalonate kinase (15, 16). Furthermore, SREBP-2 predominantly co-regulates the expression of both *LDLR* and *PCSK9* genes when cholesterol levels are low (17, 18). This seemingly counter-intuitive upregulation of both genes will become more logical in the subsequent sections when considering the larger

relationships between cholesterol regulation and PCSK9, specifically in the context of circulating plasma lipoproteins (19).

In order for SREBPs to be able to activate transcription in the nucleus, they must first be translocated from the ER to the Golgi apparatus, where they are then proteolytically activated. During conditions of sterol depletion, a protein called Insig-1 dissociates from the SREBP cleavage activating protein (SCAP) and Insig-1 becomes ubiquitinated and is degraded by a proteasome. SREBPs will then bind with SCAP and exit from the ER in COP-II coated vesicles towards the Golgi, where the site 1 protease (S1P) cleaves the SREBP. After this, a second Golgi enzyme called site 2 protease (S2P) cleaves the N-terminal basic helix-loop-helix leucine zipper (bHLH-Zip) domain of the SREBP (20). The N-terminal segment of the SREBP is then released and traffics to the nucleus (21), allowing it to activate the expression of target genes.

There exist two isoforms of Insig in mammalian cells: Insig-1 and Insig-2, both of which play a role in binding to SCAP, when SCAP itself is bound to cholesterol. When cholesterol accumulates inside of the ER, it can bind directly to SCAP (22), creating a conformational change, allowing SCAP to bind Insig. This prevents the SCAP/SREBP complex from exiting the ER, ultimately inhibiting the transcription of genes related to cholesterol synthesis (21). SCAP binding to sterols acts in a switch-like mechanism to block SREBP-2 activation when ER cholesterol rises above 5% of the total ER lipid content (23). Insig-1 is also a transcriptional target of SREBPs (24, 25), meaning that it is actively transcribed and degraded during sterol starvation conditions. The constitutive transcription, translation and degradation of Insig-1 provide a safeguard for when cholesterol slowly accumulates inside of cells. Once there is enough cholesterol made to bind SCAP, Insig-1 is

stabilized, and can thus shut down events that would lead to the cleavage of SREBPs, so that cholesterol levels do not over-accumulate and become toxic.

1.1.2. Lipoproteins in the Human Body: Exogenous vs. Endogenous Metabolism

Due to the hydrophobic nature of lipids, they require a unique form of transport in the hydrophilic plasma for movement to and from tissues. Lipoproteins modulate this process in the human body, moving lipids from mainly the liver to the peripheral tissues and vice versa (26). The general structure of a lipoprotein includes a core filled with various hydrophobic components such as triglycerides (TGs) and cholesterol esters. The outer layer is comprised of more amphipathic components, including phospholipids, proteins and some free cholesterol (27). There are five major classes of lipoproteins based on their densities, from largest and least dense to smallest and most dense: chylomicrons, very low-density lipoproteins (VLDLs), intermediate-density lipoproteins (IDLs), LDLs, and high-density lipoproteins (HDLs). The liver-derived VLDLs and the intestine-derived chylomicrons are very TG-rich, whereas LDLs and HDLs are the more cholesterol-rich lipoproteins (26).

Essential components of these lipoproteins are the major surface proteins, which are called apolipoproteins. They are crucial not only for structural roles, but also for roles related to assembly and metabolism of these particles (28). Some apolipoproteins act as ligands for cell surface receptors, which allows these particles to be taken up into cells and metabolized. In addition, they are able to form amphipathic helix motifs to be able to reversibly associate with the lipid components of lipoproteins, which ultimately allows for the flexibility and exchangeability of certain apolipoprotein subclasses (27). Apolipoprotein B (apoB) is the major structural protein component of chylomicrons, VLDL, IDL and LDL. ApoB is non-exchangeable and exists in two forms: apoB-100 and apoB-48, which are derived from the

same gene but are edited differently at the mRNA level, resulting in two different proteins. The APOB mRNA editing complex (APOBEC1) in the human intestines edits the apoB-100 mRNA, where a stop codon is created in the transcript (29), leading to the formation of the truncated version of the apoB-100 protein, making apoB-48. In humans, apoB-48 is found exclusively on chylomicrons, and full-length apoB-100 is on VLDL, IDL and LDL (30), with only one moiety of apoB per particle. The liver is responsible for synthesizing apoB-100. Apolipoprotein-E (apoE) is an example of an exchangeable lipoprotein that can be found in several copies on chylomicrons, VLDL, IDL and HDL, and it is an important player in the clearance of particles rich in TGs (31). In addition to apoE, apoC-II, apoC-III and apoA-V also play vital roles in the metabolism of these TG-rich lipoproteins (26).

There are both exogenous and endogenous pathways for the metabolism of lipoproteins. The exogenous pathway refers to the 1) absorption and 2) subsequent distribution of dietary fats to various sites within the human body. Upon absorption of free fatty acids and cholesterol from dietary sources, chylomicrons form in the small intestine and are packaged with TGs and cholesterol esters. The chylomicrons are secreted and transported to peripheral tissues for the distribution of cholesterol and TGs: a process that reduces the chylomicron size, as the hydrophobic core gets smaller (26). Lipoprotein lipase (LPL) is an enzyme responsible for hydrolyzing the TGs and for releasing free fatty acids, which allows for the remodeling of both chylomicrons and VLDLs (32). Chylomicron remnants can bind to apoE and be subsequently cleared through the liver via LDLR (33). There is also evidence to suggest that chylomicrons may be cleared secondarily through the LDLR-related protein 1 (LRP-1) (33, 34).

Thus, PCSK9's action on LDLR degradation becomes important when addressing lipoprotein remodeling. LDLR can influence the clearance of these chylomicron remnants, which means that PCSK9's action can perhaps function to limit the uptake of chylomicrons and VLDL remnant particles. From a more ancient perspective, one can imagine that when dietary fat sources were not so abundant in everyday meals, PCSK9's action on LDLRs meant that lipoproteins could be left circulating for longer periods of time without harmful consequences on cardiovascular health (19). Such a regulatory role by PCSK9 would therefore allow for increased circulatory time of certain lipoprotein classes for the benefit of the human body in conditions where meals were not readily available, and when extensive periods of starvation were more common during the hunter-gatherer days.

The endogenous pathway involves the secretion and metabolism of apoB-containing lipoproteins from hepatic tissue. The liver produces VLDL particles that are packaged rich with TGs and cholesterol esters with the help of microsomal TG transfer protein (MTP) (26). The outer layer of VLDL contains a phospholipid monolayer and intercalated apoB-100. Once secreted into the plasma, VLDL also acquires several copies of apoE and apolipoproteins of the C series (apoC) from HDL particles. TGs in VLDL are hydrolyzed by LPL (32), which mostly occurs in adipose and muscle tissues. The VLDL remnants following these modifications are termed IDLs, which have approximately equal amounts of TGs and cholesterol, and can be removed from the circulation by binding to LDLR via apoE (31). Hence, PCSK9's degradation of LDLR not only affects the *clearance* of LDL via apoB-100, but also the *production* of LDL from the VLDL precursor. Decreases in cell surface LDLRs would hinder the uptake of the LDL precursors VLDL and IDL, which normally occurs via ApoE binding to LDLR. This may in turn signal to the liver to increase

production and secretion of VLDLs, due to a lack of uptake of all three lipoproteins from the plasma, since all three can be cleared via LDLR by receptor-mediated endocytosis. However, LRP-1 (37) and the heparin sulfate proteoglycan (HSPG) syndecan-1 (38) can also participate in the clearance of TG-rich lipoproteins, meaning that decreases in levels of cell surface LDLRs will not completely hinder their uptake. An enzyme called hepatic lipase (HL) remodels IDL to make LDL, and the remaining TGs in IDL are hydrolyzed prior to the particle becoming LDL.

1.1.3. LDL: A Cholesterol Carrier

LDL is colloquially known as the "bad cholesterol", in opposition to HDL, which is termed the "good cholesterol". The density of LDL can vary between 1.019 – 1.063 g/mL, based mainly on the amount of residual TG. In whole, LDL is comprised of free or esterified cholesterol (50%) with some proteins (25%), phospholipids (20%) and triglycerides (5%) as well (39). LDL populations can vary in size, charge, density and protein content (40). Small dense LDL can have an overall greater negative charge because of lower neutral carbohydrate and sialic acid content. This is one of the reasons why small dense LDL is hypothesized to be more atherogenic than larger less dense LDL, due to its greater ability to interact with positively charged proteoglycans in the arterial wall (40). Furthermore, small dense LDL has been shown to increase superoxide generation, increase transendothelial filtration into the subendothelium, have higher susceptibility to oxidation, lower affinity for LDLRs, and increase the stimulation of thromboxane A_2 (TXA_2) synthesis; a factor that promotes platelet aggregation and vasoconstriction (40). Taken together, these heterogeneous factors surrounding LDL particle characteristics are likely to influence the risk of atherosclerosis in patients who have elevated plasma LDL-c levels.

As mentioned, LDL contains a single molecule of apoB-100, which is a large, insoluble ≈ 550 kDa protein synthesized in hepatocytes (41). ApoB-100 accounts for 95% of the protein mass of an LDL particle (39). Importantly, apoB-100 acts as LDL's ligand for binding to the LDLR during LDLR-mediated endocytosis (42), which is the primary mechanism of clearing circulating LDL from the plasma (26). The LDL and LDLR interaction was discovered by the seminal work of Goldstein and Brown in the 1970-1980s, which stemmed from an incentive to understand the relationship between LDL, HMGCoA reductase activity and the cause of FH (3).

1.1.4. The LDLR: Protein Function and FH-Associated Mutations

Goldstein and Brown hypothesized that FH is caused by defects in a cellular regulatory mechanism (3). They discovered the LDLR and found that FH is due to mutations in the gene coding for this receptor. They also established that the interaction between LDL and LDLR involved a process called receptor-mediated endocytosis via clathrin-coated pits, which is a mechanism central to many processes in cell biology known today. Furthermore, the internalization of the LDL-LDLR complex in liver cells requires the autosomal recessive hypercholesterolemia adaptor protein (ARH) (43). After internalization, the LDLRs undergo a conformational change and dissociate from LDL as the pH drops in endosomes. This allows the receptors to be recycled to the cell surface and be re-used for plasma LDL clearance several hundred times (3). The internalized LDL particles are shuttled towards lysosomes and the inner components are metabolized. It was found that homozygous FH mutations in the *LDLR* gene rendered this binding and uptake process non-functional, which resulted in a severe disease phenotype in patients. In the 1980s, the LDLR was purified, cloned, and the gene was isolated for studies in subsequent years, which later revealed

thousands of disease mutations in the *LDLR* gene responsible for FH (3). The five major classes of *LDLR* mutations are described by their effect on the protein and are as follows: 1) no LDLR synthesis, 2) no LDLR transport, 3) no LDL binding, 4) no LDL internalization, and 5) no LDLR recycling (44).

Mature human LDLR is made from an 839 amino acid sequence that contains five major domains: 1) the rigid N-terminal domain containing many negatively charged cysteine residues (the ligand binding site for apoB and apoE), 2) the epidermal growth factor (EGF)-like homology domain, 3) the serine-threonine rich domain containing carbohydrates attached in O-glycosidic linkages, 4) the transmembrane domain, and 5) the cytoplasmic tail (45). The LDLR is synthesized in the rough ER and is subsequently modified in the Golgi via the addition of oligosaccharides. On SDS-PAGE, the LDLR precursor migrates at 120 kDa, whereas its mature counterpart is at 160 kDa (45). The change in molecular weight is due in part to modification of O-linked sugars, which increase its overall mass in the mature form. In cells, LDLR's N-terminal region (NTR) is found on the outside of the membrane and the C-terminus is on the cytoplasmic side (45). The LDLR is a key determinant in the proper clearance of LDL-c from the plasma via apoB-100, and inefficient clearance can be a serious risk factor for cardiovascular complications.

1.1.5. Cholesterol in Human Disease: Atherosclerosis and FH

Atherosclerosis is a chronic disease characterized by pro-inflammatory markers, cell death, and elevated buildup of LDL in the blood vessels eventually leading to plaque formation (46). Plaques can disrupt blood flow and in turn lead to myocardial infarctions and strokes, which cause significant morbidity and mortality worldwide (47). An elevated level of blood LDL-c is a major risk factor for heart disease, and some individuals have a genetic

predisposition to developing this dangerous hypercholesterolemic lipid profile. FH is a Mendelian disorder and a form of autosomal dominant hypercholesterolemia (ADH) caused by mutations that impair the LDL-LDLR uptake mechanism. Specific mutations in not only the *LDLR* gene (44), but also the *APOB* (48) and *PCSK9* (49) genes have been identified as causal mutations for ADH, with *LDLR* being the most commonly affected gene. General hypercholesterolemia is marked by LDL-c > 100 mg/dL. FH on the other hand is usually identified with LDL-c levels > 190 mg/dL in adults, and in severe cases is associated with physical symptoms such as tendon xanthomas or corneal arcus (26).

Patients with FH are usually heterozygous for these mutations, meaning that only one of the inherited alleles contains the disease mutation. Heterozygous FH has a prevalence of ≈ 1/220 persons, whereas homozygous FH (HoFH) is very rare and often marked by LDL-c levels above 400 mg/dL (26). Individuals with HoFH are at an increased risk for premature death, and they can suffer from heart attacks and strokes starting in childhood, which demonstrates that severely elevated LDL-c alone is enough to cause atherosclerosis (3). Understanding the molecular mechanisms of LDL-c clearance along with the endogenous pathways of cholesterol synthesis have served as the building blocks for the development of the first-line of medications prescribed to treat hypercholesterolemia.

1.1.6. Conventional Cholesterol-Lowering Therapies

Statins are the first-line of therapy for lowering plasma LDL-c (51). These small molecule drugs are inhibitors of HMG CoA reductase, which is the rate-limiting enzyme of cholesterol synthesis in cells. The result of this inhibition is an upregulation of *LDLR* expression via the SREBP-2 pathway in order to increase LDL uptake from the plasma (50). Although there are significant reductions in morbidity and mortality with the use of statins,

they can also come with unpleasant side effects in some patients. Inhibition of HMGCoA reductase can potentially affect many alternative pathways that depend on the synthesis of mevalonate and its downstream intermediates. Some risks that come with the use of statins include myalgia and drug interactions, primarily with ones that inhibit the cytochrome p450 enzymes, leading to increased risk of drug toxicity (51). In addition to statins, the second-line of therapies include cholesterol-absorption inhibitors such as ezetimibe, and bile acid sequestrants (52). However, many patients still do not achieve the desired reductions of LDL-c with these conventional therapies, especially those suffering from FH (53). These difficulties shed light onto why the discovery of the *PCSK9* gene in the early 2000s led to excitement surrounding the emergence of a novel target for the reduction of plasma LDL-c.

1.2 PCSK9: A Novel Regulator of Plasma Cholesterol

In 2003, Seidah *et al* discovered a gene encoding a soluble protein that was found to be a key regulator of circulating plasma cholesterol levels in humans (6, 7). Initially it was called neural apoptosis regulated convertase-1 (NARC-1), but later renamed to PCSK9, as it was found to have similarities to bacterial subtilisin and yeast kexin (6). PCSK9 is the 9th member of a family of enzymes called proprotein convertases (PC) and is expressed mainly in the liver, with low levels in the kidney, intestine and brain tissues as well (6). PCSK9 is a protein of 692 amino acids that contains a signal sequence (aa 1-30) and three major domains: the prodomain (aa 31-152), the catalytic domain (aa 153-454) and the C-terminal domain (CTD aa 455-692) (54). It is synthesized as an inactive ≈ 74 kDa zymogen in the ER where the signal sequence is cleaved off prior to PCSK9's exit. PCSK9 undergoes autocatalytic cleavage between Gln152 and Ser153. Like other members of the PC family, PCSK9 performs cleavage of its own prodomain, which subsequently remains non-

covalently bound and blocks the active site. Unlike other PC enzymes that undergo a secondary cleavage reaction to release the inhibitory prodomain segment, the prodomain of PCSK9 remains bound to the active site in the catalytic domain, which contains the active triad of Asp186, His226, and Ser386 (55, 6, 56, 57). Thus, to this date, the only identified substrate of PCSK9 is itself, and this single cleavage event occurs in an autocatalytic manner.

Various post-translational modifications have been identified in PCSK9 and they occur in the ER and Golgi. These changes include phosphorylation of Ser47 (58), sulfation at Tyr38 (6, 54), and N-linked glycosylation at position Asn533 (6). The physiological consequences of these post-translational modifications on PCSK9 activity remains to be further investigated. PCSK9 has also been shown to be susceptible to cleavage by furin, another member of the PC family, which cleaves PCSK9 at Arg218. It has been reported that furin cleavage renders PCSK9 less active, and some GOF mutations lowered its susceptibility to cleavage, while some loss-of-function (LOF) mutations increased it (59). These post-translational modifications to PCSK9 are relevant when thinking of factors that modulate activity of the protein. PCSK9 activity is defined by its ability and role in mediating degradation of LDLRs.

1.2.1. PCSK9 Negatively Regulates the Life Cycle of Liver Cell Surface LDLRs

Once PCSK9 is secreted from cells, its primary site of action towards LDLRs is on hepatocytes (60), and this is commonly referred to as the extracellular route of degradation. PCSK9 associates with LDLR on the cell surface, followed by endocytosis of the receptor-protein complex, and migration within the endosomal system. Subsequently, lysosomal

degradation of the PCSK9-LDLR complex takes place rather than allowing for LDLR recycling to occur. This causes increased circulating LDL-c, as there is a decrease in the level of cell surface LDLRs to accommodate uptake (54). It has been shown that PCSK9 does not use enzymatic activity or proteolytic mechanisms to degrade the LDLR. Instead, it acts as a molecular chaperone for the LDLR in the endolysosomal system (60, 61). The importance of the PCSK9-LDLR interaction was also shown *in vivo*, where *Pcsk9* (-/-) mice infused with recombinant human PCSK9 had significantly reduced liver LDLR levels (90%) within just one hour (60). In addition to this extracellular pathway whereby secreted PCSK9 acts on LDLRs, it was hypothesized early on that an intracellular pathway also exists, where PCSK9 associates with LDLR in cells and directs LDLR from the trans-Golgi network to lysosomes for degradation, without ever being secreted (62). However, the FDA-approved anti-PCSK9 monoclonal antibody therapies work highly effectively in the circulation to lower plasma LDL-c in patients (53), meaning that the extracellular pathway of LDLR degradation must be the primary mechanism leading to reduced levels of cell surface LDLRs in the liver, since these antibodies do not enter liver cells.

The circulating levels of PCSK9 vary over a large range in human subjects. In one study involving an ethnically diverse population of 3138 individuals, PCSK9 levels in the blood ranged from ≈ 30-3000 ng/mL (63) when measured using an enzyme-linked immunosorbent assay (ELISA). It is therefore difficult to generalize an average value of circulating PCSK9 since it can vary over a 100-fold range. There is, however, a positive correlation between PCSK9 and total plasma cholesterol levels in humans (64, 65, 66). It has also been shown that circulating PCSK9 levels decrease during fasting conditions and increase for a short period after a meal (67). These findings, along with the previously

mentioned upregulation of *PCSK9* gene expression via SREBP-2 when cellular cholesterol levels are low, suggest that PCSK9's activity on LDLR serves in complex regulatory ways related to lipoprotein and cholesterol circulation in the human body. Such an ancient mechanism leading to increased LDL circulation in Western societies (where high-fat diets are prevalent) is no longer necessary, and instead contributes to increased risk of CVD (19). Thus, PCSK9 levels depend on complex genetic, metabolic, and environmental factors.

1.2.2. Transcriptional Regulation of *PCSK9*

The widely prescribed statin medications have been shown to induce *PCSK9* gene expression (68, 69). In addition, SREBP-2 (18) and the liver-specific hepatocyte nuclear factor 1α (HNF-1α) (70) are positive regulators of *PCSK9* transcription as shown in mouse liver (71), as well as in hamsters receiving rosuvastatin treatment (68). These findings on statin use and *PCSK9* gene expression suggest that these drugs do not fully favour the reduction of plasma LDL-c, as the increased expression of both *LDLR* and *PCSK9* genes via SREBP-2 lowers the net efficiency of these drugs. PCSK9's ultimate action is counter-productive to the upregulation of the LDLR protein. Furthermore, the use of statin therapy alone seldom works efficiently in patients with severe hypercholesterolemia, especially for those who suffer from rare GOF mutations in the *PCSK9* gene (53).

1.2.3. Natural Mutations in the *PCSK9* Gene: Risk vs. Protection

The link between mutations in *PCSK9* and FH was made in a study where researchers found a third independent locus associated with ADH in a cohort of hypercholesterolemic patients, excluding the *LDLR* and *APOB* loci (7). GOF mutations in *PCSK9* are extremely rare causes of FH. Patients with these GOF mutations generally have LDL-c levels ranging anywhere from ≈ 200-400 mg/dL (53) which is very high and severely

increases their risk of secondary cardiovascular complications. Disease mutations exist throughout various regions in the *PCSK9* gene, and generally involve amino acid substitutions that result in a more active form of PCSK9 through heterogeneous mechanisms. Some prodomain mutations include L108R (72), S127R (7), and D129G (73), whereas the catalytic domain contains the mutations F216L (7) and D374Y (74, 102). The CTD contains various mutations as well, including R469W (75), R496W (76), N513D (77), A514T (77), F515L and H553R (78).

There are also LOF mutations in the *PCSK9* gene, which in opposition to GOF mutations are cardio-protective and patients have low levels of circulating LDL-c (79, 80). An individual who was a compound heterozygote for two inactivating mutations in *PCSK9* (ΔR97 and Y142X) had LDL-c levels as low as 14 mg/dL, and she had no evidence of circulating PCSK9 in the blood (81). Despite this drastic phenotype, the woman was otherwise fertile and healthy. Some examples of other LOF mutations in *PCSK9* include R46L (80, 82, 78), G106R (83), L253F and A443T (78). Defective secretion is a prominent mechanism by which LOF mutations reduce levels of plasma PCSK9, where they disrupt its synthesis (Y142X), cleavage (L253F), or protein folding (C679X) (81), further supporting that PCSK9's action in the plasma is a major regulator of blood cholesterol levels.

The *in vitro* and *in vivo* analyses of these natural mutations have allowed research groups to gain a thorough understanding of how and why these mutations may cause disease or protect against disease with respect to the regulation of circulating LDL-c. For GOF variants, the molecular mechanisms understood thus far to cause disease range from events such as increased LDLR affinity (56), increased LDLR degradation rates (72) and/or increased secretion of apoB-100 *in vivo* (84). For LOF variants, some have been shown to

possess secretion and processing defects along with decreased LDLR degradative functions (85), while others result in non-functional proteins, such as the C679X nonsense truncation variant, which is not secreted from cells (78, 81). Despite these advances, the functional consequences of several *PCSK9* mutations associated with LDL-c alterations in humans remains unknown, as many of the mutant proteins display normal parameters for secretion, LDLR binding and LDLR degradation. Thus, continued study of these mutant proteins may reveal novel aspects of PCSK9 regulation. A summary of some natural GOF and LOF mutations is shown in the schematic below (Figure 1).

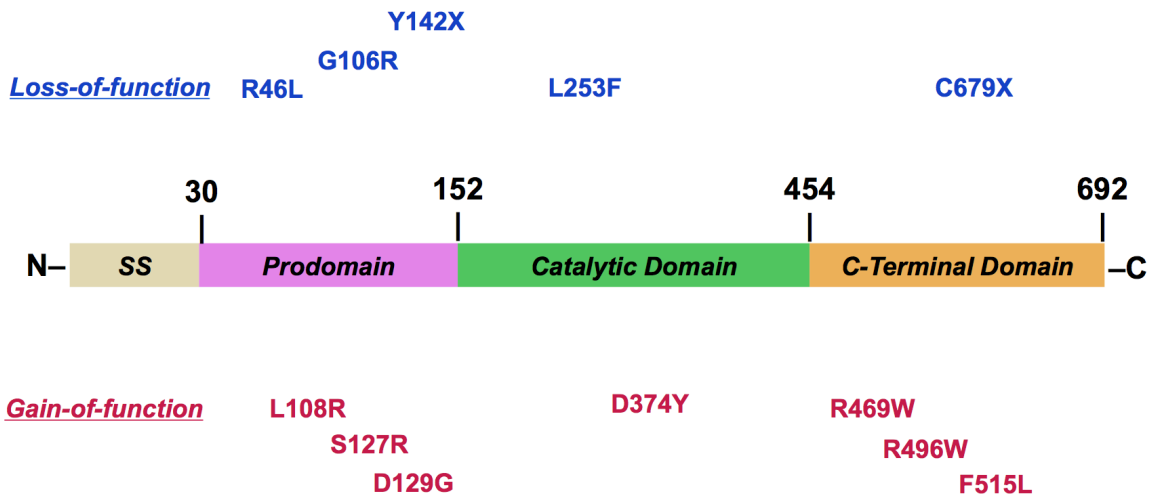

Figure 1. Natural mutations in PCSK9 and their approximate locations within the 3 major domains.

LOF mutations shown in blue above protein sequence, GOF mutations shown in red below protein sequence. SS = signal sequence from aa 1-30 (beige), followed by prodomain from aa 31-152 (magenta), catalytic domain from aa 153-454 (green), and C-terminal domain from aa 455-692 (orange).

1.2.4. PCSK9 and the LDLR: Details On Binding and Degradation

During binding, PCSK9's catalytic domain interacts with LDLR's first EGF-A like repeat in the extracellular domain (ECD) of the receptor (86). Many residues in PCSK9's catalytic domain (aa 153-381) directly associate with the LDLR. PCSK9's surface region involved in binding to the LDLR is more than 20 Å removed from the catalytic site, supporting that enzymatic activity is not needed for degradation of the LDLR (87). The binding between LDLR and PCSK9 is Ca^{2+} dependent as well as pH-dependent. There is evidence that PCSK9 binds to LDLR with a tighter affinity at low/acidic pH vs. neutral pH (56, 86, 88), which is thought to be reflective of the shift in pH from the cell surface to the endocytic compartment in cells. This mechanism has been hypothesized to prevent the dissociation between PCSK9 and LDLR intracellularly in hepatocytes, and is possibly the reason why receptor recycling is impaired. A summary of the PCSK9-LDLR interaction in cells is depicted in the schematic in Figure 2.

However, PCSK9 is not uniformly active in mediating LDLR degradation in all cell types (60). Previous work in our lab has shown that SV-589 fibroblasts are resistant to PCSK9-mediated LDLR degradation due to increased PCSK9 dissociation from LDLR in acidic early endosomes (89). Adrenal gland tissues are also resistant and do not respond to PCSK9 activity (60), meaning that there is a unique mechanism at play in these cells allowing for such resistance. The greater understanding and exploitation of this natural PCSK9 clearance mechanism, by allowing LDLR recycling to occur through nuances in the pH or Ca^{2+} levels, represents an optimal route for future therapies such as small molecule inhibitors that could be delivered into liver cells to inhibit PCSK9-mediated LDLR degradation.

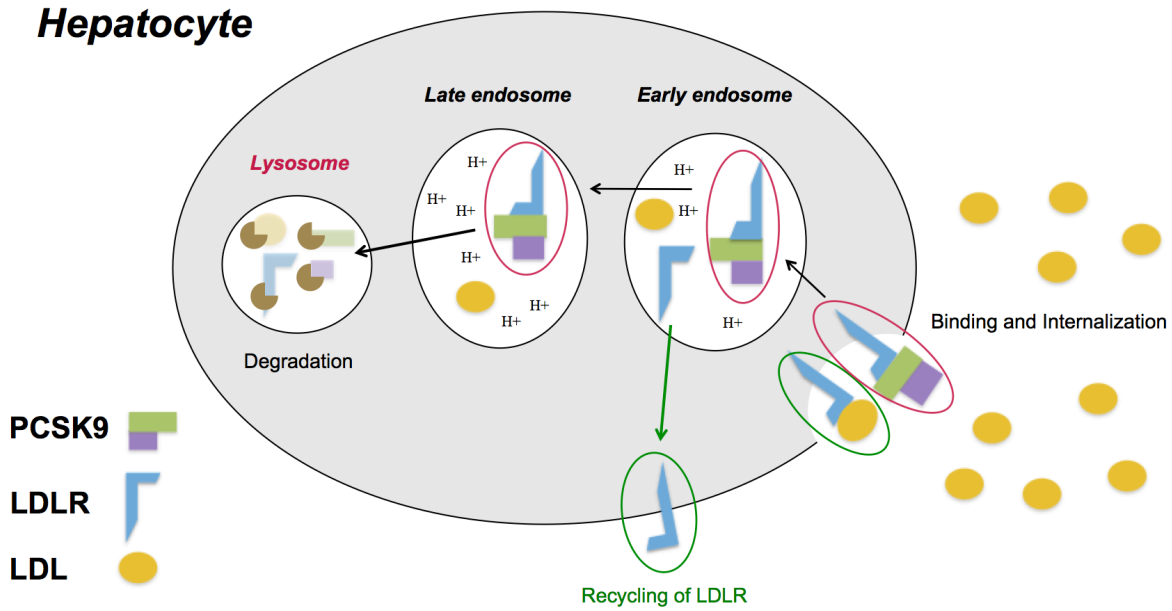

Figure 2. PCSK9 is a negative regulator of the life cycle of liver cell surface LDLRs.

In absence of PCSK9, LDL and LDLR interact freely and the complex is internalized via receptor-mediated endocytosis (green circle). Following internalization, the drop in pH causes LDL to dissociate from LDLR, and LDLR makes it back to the cell surface through recycling endosomes (green circle). The LDL and its components are metabolized in lysosomes. In the presence of PCSK9, LDLR and PCSK9 interact at the cell surface and are internalized (red circle). As the pH drops, there is a tighter affinity between LDLR-PCSK9 and the complex is shuttled towards lysosomes. This results in a lower abundance of cell surface LDLRs, which hinders uptake of plasma LDL-c.

The N-terminal region (NTR) of PCSK9 comprising residues 31-52 has been shown to negatively regulate binding to LDLR. Its deletion *increased* affinity for LDLR by 7-fold in studies that generated a Δ53 PCSK9 construct (missing aa 31-52 of the prodomain) for X-ray crystallography purposes (87). We predict that somehow this region of the protein is a negative allosteric regulator of LDLR binding, and may induce an auto-inhibitory conformation in PCSK9 when it is present. Although not conclusive, we have done preliminary tests using Δ53 PCSK9 in the context of pH-dependent binding, and found that the deletion of this stretch of acidic amino acids seems to blunt the pH effect (data not shown). This means that the difference in affinity for LDLR between acidic and neutral pH was not as large as in wild type (WT) PCSK9, which has been shown to be up to 170-fold greater at endosomal pH than at neutral pH (56). This leads us to believe that the NTR may somehow be directly or indirectly required in the pH-dependent binding to LDLR.

1.2.5. PCSK9 Inhibitors: Alirocumab and Evolocumab

Over the years, many research groups have been trying to develop therapies to inhibit PCSK9 in human plasma as a novel means of reducing LDL-c levels. As mentioned, inhibition of HMG CoA reductase via statins results in increased expression of *PCSK9* (69), showing that the effects of statins are counter-productive in reducing LDL-c. Two monoclonal antibodies were approved after ongoing clinical trials for a new line of treatment to use in patients with severe hypercholesterolemia who do not respond to conventional therapies. Alirocumab and Evolocumab are the first two FDA-approved injectable anti-PCSK9 drugs that function to block PCSK9's binding to LDLR *in vivo* by neutralizing plasma PCSK9 (8). These medications additionally lower LDL-c levels to ranges that are

unachievable with statin therapy alone, as shown with ≈ 60-70 % reduction in LDL-c after two weeks of treatment in patients with *PCSK9* GOF mutations (53).

Although effective, these medications are not an ideal therapy because they lack in exploiting any natural clearance mechanisms part of the PCSK9-LDLR interaction in cells, hence the neutralization currently occurring in the plasma. These drugs are reserved for use in severely hypercholesterolemic patients and are not routinely prescribed in clinical practice (8). Furthermore, they are extremely expensive as they are estimated to cost a patient around $14,000-15,000 USD per year (90). For these reasons, looking into alternative mechanisms to inhibit PCSK9's activity is still an important goal in the cardiovascular research field, because PCSK9 inhibition *does* have benefits with minimal side effects. With respect to such PCSK9 inhibition, our lab found that a proportion of PCSK9 in human plasma is associated with LDL, and that this association dampens PCSK9's ability to mediate LDLR degradation *in vitro* (9).

1.2.6. PCSK9's Interaction with LDL: A Novel Regulator of Activity

In earlier years, it was shown that PCSK9 was associated with larger complexes in the blood of mice fed a high fat diet, whereas there were more free forms of PCSK9 in those fed a normal chow diet (91). It has also been a question whether all PCSK9 in the plasma is uniformly active, or if there exist less or more active forms influenced by factors such as PCSK9 dimerization or oligomerization (92). Previous work from our lab has shown that 30-40% of plasma PCSK9 is bound to LDL particles in normolipidemic human subjects (9). The NTR from aa 31-52 was found to be crucial for this binding interaction *in vitro*, as the Δ53 PCSK9 construct lacked the ability to bind LDL. Importantly, PCSK9 associated with LDL can still bind to LDLR, meaning that the two binding sites are unlikely to overlap. It

was shown in HuH7 cells that the addition of exogenous LDL inhibits PCSK9's ability to mediate LDLR degradation in a dose-dependent manner. This effect is manifested through the LDL-PCSK9 interaction, because the binding between LDL and LDLR was unaffected. This leads us to believe that the PCSK9-LDL interaction allosterically regulates PCSK9's activity, and that it is not an issue related to steric hindrance in its binding to the LDLR. PCSK9's affinity for LDL is a slightly lower affinity interaction but still falls within a similar range when compared to PCSK9's affinity for the receptor. The K_d is ≈ 170 nM – 840 nM at neutral pH for LDLR binding (56, 57), and we found the K_d for LDL binding to be ≈ 325 nM as determined by a one-site binding model that follows specific and saturable binding kinetics (9).

Another group showed that adenoviral-overexpressed PCSK9 interacts with apoB in the secretory pathway of liver cells, and that PCSK9 affects apoB secretion in mice (93). This led to the hypothesis that PCSK9 may interact with apoB-100 on LDL. Indeed, co-IP experiments have shown the PCSK9-apoB-100 interaction (9, 94). However, we have yet to map the PCSK9-apoB-100 binding interface via cross-linking studies. Furthermore, it is important to consider that the regions available for PCSK9 to bind apoB-100 will likely differ between those in the secretory pathway of cells, compared to when apoB-100 is intercalated into a mature LDL particle found in the plasma.

The physiological relevance of the PCSK9-LDL interaction remains an important question. Based on our findings, we **hypothesized** that PCSK9 activity is subject to feedback regulation through binding to LDL, and that PCSK9-mediated LDLR degradation is negatively regulated by PCSK9-LDL binding in the plasma. When plasma LDL levels are high, PCSK9 is more likely to bind LDL and therefore be in an inhibited state, where it is

then less able to mediate LDLR degradation. However, when LDL levels are low, more of the "free" uninhibited PCSK9 may be present and can readily mediate LDLR degradation. In recent years, our lab has been identifying various regions of PCSK9 important for LDL binding. The detailed understanding of these locations in the protein might serve as a tool for the design of future pharmaceuticals, potentially helping to enhance this conformation or "less active" state that PCSK9 adopts when bound to LDL. This would represent a novel approach to PCSK9 inhibition without the need for exploiting the LDLR binding interface, which is a large and flat surface greater than 500Å (87), making it a very poor target for small molecules. To this end, we recently found evidence for a transient amphipathic helix in PCSK9's prodomain that plays a role in LDL binding (95).

1.2.7. Regions of PCSK9 Important for LDL Binding

Extensive work by our former PhD student Dr. Sarkar and collaborators showed that mimetic peptides corresponding to a predicted amphipathic helix in the NTR of the prodomain adopted an α-helical conformation in a membrane-like environment. The conditions used n-dodecylphosphocholine (DPC) micelles as a mimic for the outer surface of a lipoprotein particle. The helical propensity and hydrophobic face of this amphipathic helix was measured, and interestingly increased with the naturally cardio-protective R46L LOF *PCSK9* mutation. On the other hand, addition of a proline at position 44 (A44P) and 41 (L41P) both disrupted the predicted helical motif and lowered LDL binding affinity *in vitro*, but did not affect LDLR binding affinity. Dr. Ariela Vergara-Jaque performed computational modeling of PCSK9 to include this prodomain NTR, which is unavailable in crystal structures due to low electron density (95).

Dr. Vergara-Jaque's model showed that PCSK9's predicted α-helix in the NTR aligns with multiple residues in the CTD (Figure 3), perhaps modulating electrostatic and/or hydrophobic interactions important for the LDL binding conformation. Furthermore, we found that natural GOF mutations exist on this surface region of the CTD that is involved in the putative inter-domain interactions. The GOF mutations severely inhibited or abolished LDL binding *in vitro* (R469W, R496W and F515L) (95). The inhibitory effect that these GOF mutations have on LDL binding is novel information, and supports **the hypothesis** that LDL association of WT PCSK9 *in vivo* may have inhibitory effects on LDLR degradation. Based on these recent findings, we sought to further investigate other natural mutations and determine their effects on LDL binding and on other functional aspects of PCSK9 activity.

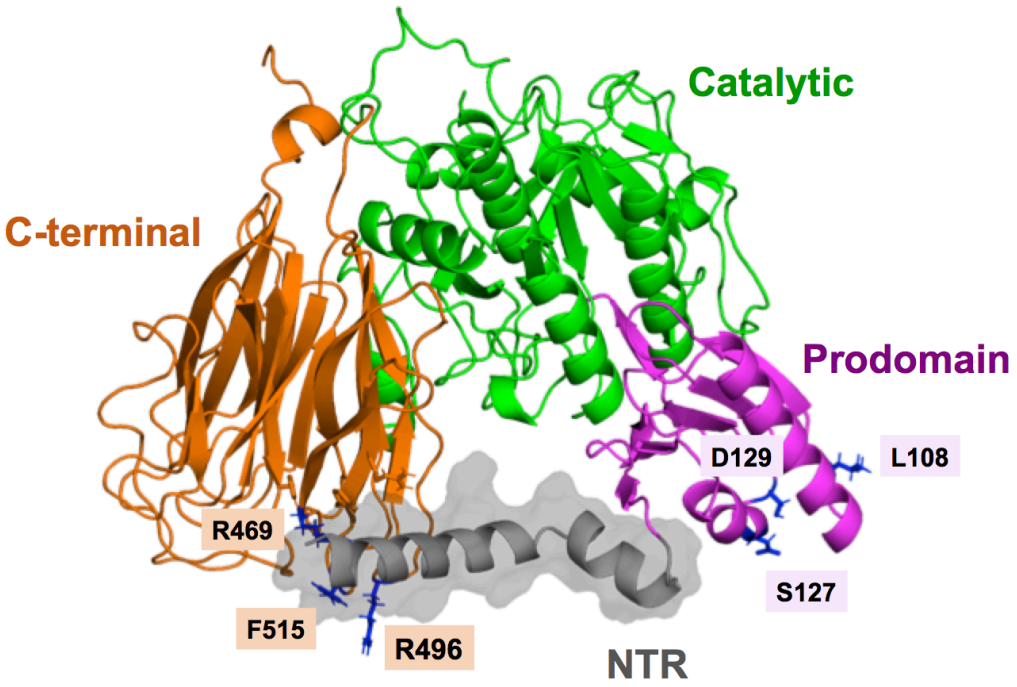

Figure 3. PCSK9 crystal structure at 1.9 Å in combination with the computationally modeled helix in the NTR.

Figure adapted from Sarkar *et al* (95). Residues associated with natural GOF mutations in CTD shown in orange (R469, R496, F515) and ones in prodomain shown in magenta (L108, S127, D129). The NTR's helix shown in grey, the prodomain in magenta, the catalytic domain in green, and the CTD in orange. The crystal structure is from Hampton *et al* (96) (PDB ID: 2QTW).

1.3 Statement of Objectives, Hypotheses and Predictions

The study of natural disease-causing mutations in *PCSK9* gives us a basis for validating how they may function on a molecular level. Early work on the D374Y PCSK9 GOF mutation showed that it binds with 25X higher affinity to LDLR when compared to WT PCSK9 using surface plasmon resonance (SPR) (56). This allowed for further understanding of the cellular mechanism used for manifestation of the severe FH phenotype in patients with D374Y PCSK9, and linked *in vitro* studies to clinically relevant data. In this project, the **overall goal** is to assess the consequences of mutations in *PCSK9* on the protein's function *in vitro* and in cell culture.

Objective 1: **Functional Characterization of CTD and NTR Mutations in PCSK9**

A) Based off the computational model, validate inter-domain interactions between PCSK9's CTD and prodomain NTR (aa 31-52) through LDL binding assays.

B) Test the effect of mutating histidines in PCSK9's CTD on pH-dependent binding to LDLR.

Hypothesis: Computational model-based inter-domain interactions between PCSK9's CTD and NTR may be required for LDL binding and in the pH-dependent binding to LDLR.
Predictions: Mutagenesis is expected to a) disrupt or b) enhance these interactions, and the overall effects on PCSK9 function are to be measured by *in vitro* assays looking at LDL binding and LDLR binding.

Objective 2: **Functional Characterization of Prodomain Mutations in PCSK9**

A) Assess the effect of GOF prodomain mutations L108R and S127R on LDLR binding and degradation, LDL binding, and PCSK9 processing and secretion.

B) Assess the effect of G106R, a LOF prodomain mutation, on LDL binding.

Hypothesis: WT PCSK9's association with LDL in the plasma is hypothesized to have an inhibitory effect on LDLR degradation. However, some patients with GOF *PCSK9* FH mutations may exhibit defective LDL binding, and they might in turn have a larger pool of free and active plasma PCSK9. This might be a mechanism contributing to their hypercholesterolemia.

Predictions: Natural GOF mutations in the prodomain of PCSK9 will disrupt LDL binding, and increase LDLR binding affinity or degradative events. LOF mutations may confer increased affinity for LDL, in opposition to what we have observed with some GOF variants.

Significance: Identifying the regions of PCSK9 required for LDL binding is an essential step towards understanding the physiological relevance of this interaction. Thus far, our findings show that several regions in PCSK9 play roles in LDL association: 1) the NTR from amino acids 31-52 and 2) the CTD surface region, comprising residues R469, R496 and F515. This MSc project has characterized **a third** region of interest in the prodomain containing residues G106, L108 and S127. Our *in vitro* data contributes novel information to the structure-function relationship of PCSK9, and supports the hypothesis that PCSK9-LDL association in the plasma inhibits LDLR degradation activity. Further validation of the effect of PCSK9-LDL association in animal models of dyslipidemia will provide evidence about whether this hypothesis is supported *in vivo*.

2. Materials and Methods

2.1 Materials – Media, Primers and Antibodies

Medium A – Dulbecco's Modified Eagle's Medium (DMEM, Gibco), 1mM sodium pyruvate (Gibco), 100 µg/mL streptomycin and 100 U/mL penicillin (Gibco) and 10% fetal bovine serum (FBS – Gibco)

Medium B – DMEM, 1% sodium pyruvate, 100 µg/mL streptomycin and 100 U/mL penicillin, 1X Insulin-Transferrin-Selenium (ITS- Sigma)

Medium C – DMEM

Medium D – DMEM, 1% sodium pyruvate, 100µg/mL streptomycin and 100U/mL penicillin

Medium E – DMEM, 20% FBS, 10% DMSO (Fisher Bioreagents)

Medium F – UltraDOMA™ medium supplemented with 10% FBS, 10 mM L-glutamine (Corning), 100 µg/mL streptomycin, and 100 U/mL penicillin

Medium G – Minimum Essentials Medium containing L-glutamine, ribonucleosides, and deoxyribonucleosides (MEM, Gibco), 100 µg/mL streptomycin and 100 U/mL penicillin, and 10% FBS

Medium H – MEM, 5% newborn calf lipoprotein deficient serum (NCLPDS), 100 µg/mL streptomycin and 100 U/mL penicillin, 50 µM sodium mevalonate, and 10 µM pravastatin (Sigma Aldrich)

Medium I – MEM, 5% NCLPDS, 100 µg/mL streptomycin and 100 U/mL penicillin, 1 ug/mL 25-OH cholesterol (Steraloids) and 10 ug/mL cholesterol (Steraloids)

Table 2. 1 Primers for mutagenesis and sequencing of PCSK9 cDNA.

Data shown only for variants created during this project. All other constructs mentioned were made by previous lab members prior to the start of this project. Base changes in mutagenesis primers are indicated by lowercase letters.

Primer	*Forward Primer Sequence (5' to 3')*	*Reverse Complement Sequence (5' to 3')*
E39P	GAGGACGGCGACTACccGGAGCTGGTGCTA	TAGCACCAGCTCCggGTAGTCGCCGTCCTC
E39A	GACGGCGACTACGcGGAGCTGGTGCTAGCC	GGCTAGCACCAGCTCCgCGTAGTCGCCGTC
H553R	ACTGCCgCCAACAGGGCCACGTCCT	AGGACGTGGCCCTGTTGGcGGCAGT
H553A	CGTGTCCACTGCgcCCAACAG	CTGTTGGgcGCAGTGGACACG
H565R	TGCAGCTCCcgCTGGGAGGT	ACCTCCCAGcgGGAGCTGCA
H565A	TGCAGCTCCgcCTGGGA	TCCCAGgcGGAGCTGCA
PCSK9-1	N/A	GAG GGG TAA TCC GCT CCA GGT (sequences reverse direction, upstream from AA 150 of prodomain
PCSK9-5	ACT GCA GCA CCT GCT TTG TGT (forward sequence primer from AA 400-680 of C terminal domain)	N/A

Table 2. 2 Primary antibodies used for western blotting.

Name	*Concentration*	*Dilution*	*Source*	*Molecular Weight*
TFR – mouse anti-human transferrin receptor	0.5 mg/mL	1 µg/mL	Invitrogen	95 kDa
Actin – mouse	Ascites fluid	1:500	Sigma	42 kDa
15A6 mouse anti-human PCSK9	5 µg/mL	1:10,000	Jay D. Horton (Dallas, TX)	63 kDa mature, 74 kDa pro
1A1 mouse anti PCSK9	0.9 mg/mL	1:10,000	Jay D. Horton (Dallas, TX)	14 kDa prodomain
3143 rabbit anti-LDLR	N/A	15 µL/10 mL	Jay D. Horton (Dallas, TX)	160 kDa mature, 120 kDa precursor

Table 2. 3 Secondary antibodies used for western blotting.

Name	*Concentration*	*Dilution*	*Source*
IRDye 800 conjugated affinity purified anti-mouse IgG	500 µg/mL	1:4,000	LI-COR
IRDye 800 conjugated affinity purified anti-rabbit IgG	500 µg/mL	1:4,000	LI-COR

2.2 Methods

2.2.1. Site-Directed Mutagenesis

Primers were generated by introducing point mutations into the pcDNA3.1 vector containing our WT PCSK9 sequence. All primers were designed on SeqBuilder Pro 15 and ordered through Life Technologies (See Table 2.1). Any variants for which the primers are not listed were made prior to this work. The polymerase chain reaction (PCR) was set up as follows: RNAse/DNAse-free Ultrapure water (Invitrogen), Q5 buffer (New England BioLabs), dNTP mixture (FroggaBio), dimethyl sulfoxide (DMSO; Fisher Scientific), WT PCSK9 FLAG-tagged template plasmid DNA at 10 ng/µL, forward and reverse primers at 10 µM each, and Q5 high fidelity hot start polymerase (New England BioLabs) in a 25 µL reaction. PCR was done in a thermocycler (GeneAmp PCR system 9700, Applied Biosciences). One cycle of PCR went as follows: initial denaturation for 30s at 98 °C, another denaturation for 10s at 98°C, annealing between 60-70°C depending on the melting temperature of the primers, and extension at 72°C for 6 minutes. This cycle was repeated 25 times. Following PCR, the samples were incubated with DpnI enzyme (New England BioLabs) at 10U/µL for 2 hours at 37°C to digest the methylated parental DNA.

XL10-Gold® Ultra Competent cells (Stratagene) were put into sterile Eppendorf tubes at 45 µL per transformation. XL10-Gold® β-mercaptoethanol (β-Me) mix was added at 2 µL to each bacterial aliquot, and tubes were swirled every 2 minutes, while placing them on ice between swirls for a total time of 10 minutes. 2 µL of each PCR reaction was added to a bacterial/β-Me aliquot, and mixed by flicking the tube, while placing the mixture on ice for 30 minutes afterwards. The bacteria were heat shocked at 42°C for 30s, and then put onto ice

for 2 minutes. Following heat shock, each bacterial aliquot was given 450µL of sterile SOC outgrowth medium (NEB), and cultures were left to grow for 1 hour in a 37°C incubator with shaking at 225rpm (Innova 42, New Brunswick Scientific). Once bacterial cultures grew, they were plated onto LB-agar plates with 200µL of bacteria per plate. Plates were made using LB-agar and 1 µg/mL ampicillin (Fisher Bioreagents).

Several distinct colonies were picked from each bacterial plate and grown in liquid LB broth base (Invitrogen) + ampicillin at 1 µg/mL overnight with shaking in an incubator (Forma Scientific – Orbital Shaker) at 225 rpm at 37°C. The cultures were collected and spun down at 3500rpm for 15 minutes. Bacterial pellets were then used for DNA purification using mini and/or maxi preps kits as per the manufacturer's instructions (Omega Bio-Tek). Plasmid DNA concentration and purity was determined using the NanoDrop® Spectrophotometer. Positive clones were confirmed by sequencing at the Centre for Applied Genomics in Toronto, ON.

2.2.2. Making A Stable HEK293S Cell Line Expressing PCSK9

HEK293S cells were plated in 100mm culture dishes (Corning) and grown to 80% confluency in Medium A. The plasmid expressing the PCSK9 construct of interest was then transfected into cells. The ratio of DNA to Lipofectamine-2000 (Invitrogen) was 1:3, and a 1:25 ratio of Lipofectamine-2000 to Opti-MEM™ (Gibco) was used for generating transfection complexes. The mixture was incubated at room temperature for 20 minutes. Meanwhile, old medium was aspirated off of cells and replaced with 5mL Medium B. The transfection complex was added to the dish and cells were incubated for 4-5hrs at 37°C in 5% CO_2 conditions. Afterwards, 5 mL of Medium D with 20% FBS was added to the cells

and they were incubated overnight. Fresh Medium A containing 750 µg/mL of Genticin (G418, Thermo Fisher) antibiotic was used to select for stably transfected cells. Fresh medium was supplied every 2 days (twice), and then only every 4-5 days until resistant colonies formed.

When resistant cells grew to confluency, they were maintained in 500 µg/mL G418. Some cells were frozen in Medium E for later use. Twenty dishes of PCSK9-expressing cells were grown to make a large-scale suspension culture in UltraDOMA™ medium (BioWhittaker) in 1L of Medium F in a 6L, longneck sterile flask with a stir bar. The cells were in suspension for 1 week with slow stirring at 37°C in 5% CO_2. The medium was collected in 500 mL centrifuge tubes (Corning) and cells were spun down at 3500rpm for 20 minutes in the Sorvall Legend XTR centrifuge. The medium was then filter-sterilized using a 0.22µM filter unit (Millipore), and stored at 4°C wrapped in foil.

2.2.3. Affinity Purification of PCSK9 from Conditioned Medium

Approximately 200 mL of medium containing secreted PCSK9 was adjusted to a pH of 7.0 by adding 1M Tris-Cl solution to a 50mM final concentration. A column with 4-5 mL of FLAG beads (Sigma) added was used to capture PCSK9 from the medium. PCSK9 constructs contain the FLAG tag at the C-terminus of the peptide, allowing for capturing of the protein. Medium was passed at a slow flow rate through the column overnight at 4°C. The column was washed with 20 column volumes (≈100 mL) of wash buffer (50 mM Tris-HCl pH 7.4, 150 mM NaCl, 2 mM $CaCl_2$). PCSK9 bound to the column's FLAG beads was then eluted at a slow rate with 30 mL of wash buffer + FLAG peptide (100µg/mL, Biomatik). Extra 10 mL of wash buffer was run through the column afterwards to collect any

residual PCSK9. The column was regenerated by using 10 column volumes (≈ 50mL) of 0.1M Glycine-HCl buffer (pH 3.5) to strip any bound PCSK9 from the beads. The glycine buffer was immediately washed out using wash buffer, and the column was stored with a gentle overlay of wash buffer + 50% glycerol and 0.02% sodium-azide. All steps were carried out at 4°C.

Eluted PCSK9 was pooled and concentrated using an Amicon Ultra concentrator tube with a 10kDa molecular weight cutoff (Millipore). The elution volume was concentrated and then passed through a 0.45μM filter unit. The Äkta Purifier System (GE Healthcare Life Sciences) with the Superdex 200 Column was used to purify our PCSK9 preps. The protein was concentrated again and aliquots were frozen to a 4 mg/mL final concentration in HBS-C and stored at -80 °C.

2.2.4. Concentrated Conditioned Medium Containing PCSK9

HEK293 cells were plated in 100mm dishes (Corning) and grown in Medium A to ≈80% confluency. Each dish was transfected with 3 μg DNA coding for the PCSK9 construct of interest and 10 μL of PolyJet transfection reagent (SignaGen Laboratories). The medium was aspirated off of the cells and replaced with 5 mL of Medium A. Transfection complexes were generated using Medium C and allowed to sit for 15 minutes at room temperature (25°C) prior to adding 200 μL onto each dish. The cells were then left to incubate overnight at 37°C in 5% CO_2. The next morning, the medium was aspirated off and cells were washed in 1X phosphate buffered saline (PBS; 8g NaCl, 0.2g KCl, 0.27g KH_2PO_4, and 2.05g Na_2HPO_4 for 1L solution using ddH_2O). Medium B was added to each dish. Secretion of PCSK9 occurred for 48 hours. Conditioned medium was collected and

spun down at 1000xG for 5 minutes. The medium was concentrated using an Amicon Ultra Centrifuge tube with a 10kDa cutoff (Millipore). The concentrated conditioned medium was frozen at -80 °C in aliquots following a PCSK9 expression check via western blot.

2.2.5. PCSK9 Expression Check on Conditioned Medium

To test for the levels of expression of PCSK9 in conditioned medium following transfections, a trichloroacetic acid (TCA; Sigma) precipitation was performed. 100% TCA was added at 10% to conditioned medium, mixed, and placed on ice for 15 minutes. The samples were then spun for 15 minutes at 4 °C at 13,300 rpm in the micro-centrifuge. The supernatant was removed, and samples were washed in cold acetone and spun again at 13,300rpm for 5 minutes. Residual acetone was removed and tubes were left to air dry for 5 minutes. Samples for gels were made in 1X SDS-PAGE + 6 M Urea loading dye and 1X of Bolt reducing agent (Novex – Life Technologies) and were vortexed for 1 minute at high speed to dissolve the pellets.

2.2.6. Harvesting Cells and Making Cell Lysates

Cells were washed in cold 1X PBS (4°C) and then scraped in 1X PBS. The cell suspension was spun down at 1000xG for 5 minutes at 4°C in a micro-centrifuge to pellet the cells. The supernatant was aspirated off and pellets were used to create whole cell extracts/lysates. The cells were resuspended in lysis buffer (Tris lysis buffer: 50 mM Tris pH 7.0, 5 mM EDTA, 150 mM NaCl, 1% NP-40, 0.5% DOC), 1% protease inhibitor (PI; Roche), 1mM phenylmethane sulphonyl fluoride (PMSF; Sigma), and 1mM dithiothreitol (DTT). The lysates were incubated on ice for 15 minutes, and then spun at 13,300rpm for 15 minutes. The supernatant was put into a new Eppendorf tube, and the pellet was discarded. A

μBCA protein assay was performed on the cell lysates to determine the total amount of protein according to the manufacturer's instructions.

2.2.7. Analysis of Proteins by Western Blotting

Gel samples contained 30-35 μg of protein per well and were boiled on a hot plate (Labnet International) at 96°C for 5 minutes. The molecular weight marker used was the Precision Plus Protein™ All Blue Standards ladder (BioRad). ***Bolt gels:*** 4-12% Bolt™ gradient Bis-Tris Plus gel (Thermo Fisher Scientific). Gels were run at 165 volts for 45 minutes. Running buffer consisted of the 20X Bolt MES SDS Running Buffer (Novex – Life Technologies) diluted to 1X in ddH_2O. ***Polyacrylamide gels:*** made to 9%, for which the running buffer consisted of 25 mM Tris pH 8.3, 192 mM glycine, and 0.1% SDS. The loading dye used for acrylamide gels consisted of 40% 0.5M Tris pH 6.8, 20% SDS, 20% glycerol, 8% of 0.5M EDTA, and 3.2% of 0.5% bromophenol blue, with 10% β-Me (OmniPur) added to each aliquot when thawed from -20 °C.

Samples run on protein gels were transferred to a nitrocellulose membrane (BioRad) via a wet transfer at 80 volts for 120 minutes in a cold room at 4°C. 1X transfer buffer (25 mM Tris pH 8.3, 192 mM glycine) was made using ddH_2O, with 10% total isopropanol or methanol added to the mixture. When finished, membranes were incubated with 1X PBS and 5% milk (non-fat, dry milk powder) for 1 hour at room temperature (25°C). Membranes were washed 3x for 10 minutes with 1X PBS + 0.1% Tween-20 (PBS-T; Tween-20 from Fisher Scientific). Primary antibodies were diluted in antibody dilution buffer (0.1% Tween-20, 5% Bovine Serum Albumin (BSA-Sigma), and 0.02% sodium azide in 1X PBS) to 1:10,000 and were left on the membranes overnight with shaking at 4°C (See Table 2.2).

Three 10-minute washes were done in PBS-T. The labeled secondary antibodies used are listed in Table 2.3. Secondary antibodies were diluted to a final concentration of 1:4,000 using Blotto buffer (1X PBS-Tween, 5% milk, and 5% newborn calf serum (Gibco)) and incubations were done at room temperature for 45 minutes on a shaker, with foil covering the membrane to protect it from light. The final three washes were done in PBS-T for 10 minutes each, followed by one rinse in 1X PBS. All membranes and gels were scanned using the LICOR scanner system (LICOR Biosciences). Data was analyzed using the Odyssey V3.0 software to quantify band intensities from blots and gels.

2.2.8. PCSK9-LDL Binding Affinity: Agarose Gel-Shift Assay

Two separate reaction series of 12 serial dilutions each were made for either **a)** WT-PCSK9 or **b)** the mutant of interest. Starting with 50 µg/ 26µL of purified PCSK9 in the first tube, two-fold serial dilutions were carried out. The tubes for each series contained the following: **1)** 1.5ng/µL DyLight 800-labelled WT-PCSK9 with 5% BSA and **2)** PCSK9-free LDL diluted to 7.5µg/µL in HBS-C. Increasing amounts of unlabeled PCSK9 (from tube 1 to 12) competed for binding to LDL against the DyLight 800-labeled WT PCSK9. All mixtures were incubated at 37°C for 90 minutes to allow PCSK9-LDL binding to reach equilibrium.

Ficoll loading dye (10% Ficoll-400 and 0.01% bromophenol blue made in 1X LDL buffer (450 mM Tris, 400 mM sodium borate, 10 mM calcium lactate, pH 8.0)) was added to each sample, followed by loading of samples onto a 0.7% agarose (SeaKem LE) gel made with 1X LDL buffer. Gels were run for 2 hours at 40V to allow for separation of labeled LDL-bound WT-PCSK9 and labeled unbound WT-PCSK9. The running buffer was 1X LDL buffer. Gels were immediately scanned using the LICOR scanner with a focus offset of 3mm

to account for the thickness of the gel. Band intensities for bound vs. unbound labeled WT-PCSK9 were quantified using the Odyssey V3.0 software. K_i values could subsequently be calculated with GraphPad Prism 5.0 using the function: [Binding – Competitive, One-site, Fit K_i] with setting the "hot" concentration of purified 800-WT PCSK9 to 10.8 nM, and the "cold" concentration of unlabeled competitor varied according to the serial dilutions of purified competitor (log nM X). The "hot" K_i was set to 350 nM for this assay, which is the theoretical, one-site K_i value for WT PCSK9's affinity to LDL.

2.2.9. PCSK9 and LDL Binding: Optiprep Density Gradient Separation

This assay allows in qualitatively assessing LDL binding of various PCSK9 mutants through the use of LDL incubated with conditioned medium containing PCSK9. Each incubation mixture contained 25mM Hepes-KOH buffer at pH 7.4, 0.5 mg of isolated, PCSK9-free LDL, HBS-C with 5% BSA, PCSK9 conditioned medium (200 µL or less) and HBS-C (20 mM Hepes-KOH, 150 mM NaCl and 2 mM $CaCl_2$) to make up the total volume to 1 mL. Tubes were mixed by inversion and incubated at 37°C for 1 hour. Each reaction was transferred to a falcon tube with the addition of 1.65 mL of 25 mM Hepes pH 7.4, and 450 µL of 60% Optiprep density gradient mixture for a 9% final concentration (Optiprep™). 3 mL of this total sample was added to 3.3 mL OptiSeal Polypropylene centrifuge tubes (Beckman Coulter). Each sample was overlaid with 25 mM HEPES. Sample tubes were loaded onto a TLN100 rotor (Beckman Coulter). Screws were tightened with a tension monitor to 120lbs and the samples were loaded into the Optima™ MAX-TL Ultracentrifuge (Beckman Coulter) for a 2-hour spin at 4°C at 100,000 rpm with the deceleration setting at 9. After the spin, the LDL layer was drawn off to capture the total ≈600 µL.

Immunoprecipitation (IP) was performed on the LDL layer to capture PCSK9 bound to LDL.

Reactions were prepared using the 600 µL of LDL layer, IP buffer (40 mM Hepes pH 7.4, 200 mM NaCl, 3mM $MgCl_2$, 2 mM $CaCl_2$, and 2% NP-40), Pureproteome Protein A magnetic beads (EMD Millipore Corp), and 2µL of diluted rabbit antiserum 1697 antibody raised against full-length human PCSK9 (Biomatik, Cambridge, ON, Canada). The total 1 mL reaction volumes were rotated overnight with end-over-end mixing at 4°C. The next morning, three washes were done in 1X IP wash buffer. The beads were resuspended in 1X Bolt dye, 1X Bolt reducing agent, and ddH_2O to make 60 µL samples. A western blot was done to probe for PCSK9 in the inputted medium and in the LDL layers.

2.3.0. PCSK9 Uptake in Cells Overexpressing LDLR

HEK293 cells were plated in 6-well dishes (Corning) and grown to ≈80% confluency in Medium A. Cells were transfected with vector pCMV empty plasmid or the full-length human pLDLR-17 plasmid. PolyJet transfection reagent was used to make transfection complexes in Medium C, to have a total of 1 µg DNA and 3 µL of PolyJet per well. Mixtures were incubated at room temperature for 15 minutes, and then 200 µL of each mixture was pipetted onto the cells. The cells were incubated overnight in 37°C at 5% CO_2, and the next day the medium was aspirated off and cells were washed twice in pre-warmed, sterile 1X PBS. In order to assess the ability of cells to take up exogenous PCSK9, conditioned medium made up in 1 mL total volume of Medium D was added to each of the wells to assess extent of uptake for different mutant PCSK9 variants. Chloroquine diphosphate salt (Sigma) was diluted to 0.05 mg/mL in ddH_2O and added to each plate 30

minutes before the PCSK9 treatments, in order to inhibit lysosomal degradation. Cells were incubated with PCSK9 conditioned medium for 2 hours at 37°C in 5% CO_2. Following incubation, the medium was aspirated off and cells were washed in cold 1X PBS and harvested for analysis by western blotting.

2.3.1. PCSK9 Processing and Secretion Assay

HEK293 cells were plated in a 6-well dish, grown in Medium A and transfected with 1.5 µg of PCSK9 plasmid once cells reached 60-70% confluency. PolyJet transfection reagent was used as previously described. Cells were washed in 1X PBS and fresh Medium B was added to each well. PCSK9 secretion was allowed to take place for 24 hours by leaving the cells to secrete protein at 37°C. The medium was collected and PCSK9 secretion was quantified from the medium using a TCA precipitation followed by western blot. The cells were harvested and lysates were made for analysis of PCSK9 processing.

2.3.2. Ligand Blotting of LDLR-ECD to Test PCSK9 Affinity

Nitrocellulose membranes were blotted with purified or partially purified LDLR-ECD at 1 µg/ well using a slot-blot apparatus (Bio-Rad). Duplicate slots were created on each membrane, and incubated for 30 minutes in TBS-C + 5% milk, followed by overnight incubation at 4°C. The following day, a mixture of 2.5% milk and purified 0.1 µg/mL DyLight 800-labeled WT PCSK9 made in low salt TBS-C (50mM Tris-Cl pH 7.0, 90mM NaCl, and 2mM $CaCl_2$) was generated as an incubation buffer. From membranes 12 - 1, purified, unlabeled PCSK9 (either WT or mutant) was diluted over a range of 3000 to 0.1 nM, acting as the competitor. Mixtures were added onto membranes, covered with foil, and incubated for 2 hours with gentle shaking at room temperature. Blots were then washed 2x

for 15 minutes in incubation buffer and scanned on the LICOR scanner, with intensities calculated using the Odyssey V3.0 software. Binding curves to determine a relative IC_{50} value for both WT and the mutant of interest were generated from averages of duplicate band intensity calculations (Y axis) vs. log [nM unlabeled competitor] (X axis) with the function: log(inhibitor) vs. response – variable slope in GraphPad Prism 5.0.

2.3.3. Delipidation of Serum for Cell Culture Experiments

The density of newborn calf serum was adjusted to 1.215 g/mL by addition of KBr. Serum was then spun for 45hrs at 55,000rpm to separate out all the lipoproteins in the top phase. The bottom phase of lipoprotein deficient serum was then dialysed 5 times against PBS and was filter-sterilized.

2.3.4. PCSK9's LDLR Degradation Activity: Biotinylation of Cell Surface Proteins

Mouse hepatoma (Hepa1c1c7) cells were plated in 60mm dishes and grown to 70-80% confluency in Medium G. Medium H was used to *induce* endogenous LDLR expression in cells, and a no-PCSK9 control plate was also included. Medium I was used to *suppress* LDLR expression as a negative control. The following day, treatments were prepared by making up mixtures of Medium H with various purified PCSK9 proteins of interest at a concentration of 5µg/mL. Cells were washed in warm 1X PBS and the appropriate medium added to each plate. Cells were then incubated for 4 hours with the treatment at 37°C to allow for LDLR degradation in the presence of exogenous PCSK9.

Fresh Sulfo-NHS-SS-Biotin (Campbell Science) was mixed to a 0.5mg/mL final concentration in biotinylation buffer (10mM triethanolamine pH 8.0 (triethanolamine 1.13 g/ml), 150 mM NaCl, 2 mM $CaCl_2$). Cells were immediately washed twice with cold 1X

PBS-CM (1X PBS, 1 mM $MgCl_2$, 0.1M $CaCl_2$). Biotinylation buffer with biotin was added to cells for 30 minutes with gentle shaking at 4°C. Cells were washed in PBS-CM and a second 30-minute incubation was repeated. After biotinylation of cell surface proteins, cells were washed with fresh quenching buffer (PBS-CM, 25 mM Tris-Cl pH 7.4, 192 mM Glycine) and incubated for 30 minutes at 4°C with gentle shaking. Cells were then washed and scraped in cold PBS-CM and spun down at 1000xG for 5 minutes at 4°C. The supernatant was aspirated off and PBS-CM was added to resuspend cells. Another spin was repeated to pellet cells prior to creating cell lysates.

Fresh lysis buffer containing 1mM PMSF and 1% PI made up in Tris lysis buffer was used and cell pellets were resuspended in 200µL of buffer. DTT was omitted from the buffer to minimize the risk of breaking disulfide bonds, which would release the biotin label. The suspensions were incubated on ice for 20mins, followed by a 20min spin at 13,000 rpm at 4°C. The cell lysate supernatant was added to a new tube, and ¾ of the mixture was used in an IP reaction done with slow rotation at 4°C overnight. The IP reactions contained cell lysate, 50µL of NeutrAvidin® Plus UltraLink® Resin beads (Thermo Scientific) and Tris lysis buffer to a volume of 500µL with 1X PI. The rest of the ¼ cell lysate was used in a µBCA protein assay according to the manufacturer's protocol, to determine the concentration of cellular proteins in preparation for western blotting. The following day, IP reactions were washed 3X with Tris lysis buffer, once with high salt wash buffer (50 mM Tris-Cl, pH 7.4, 500 mM NaCl), and once with low salt wash buffer (10 mM Tris-Cl pH 7.4). The beads were then resuspended in 1X SDS loading dye to a concentration of 3.5µg/µL according to µBCA assay results. Cell extracts were run on gels at a protein

concentration of 35µg/30µl using 5X SDS dye and ddH_2O. Gel and western protocols followed the procedures previously described.

2.3.5. Statistical Analyses

Statistical analyses involved a Student's t-test or a column statistics analysis with a one-sample t-test to compare mutants to the WT PCSK9 control. Statistical significance was relevant if $p < 0.05$. All statistical analyses and graphs were done using GraphPad Prism 5.0 software.

3. Results

3.1 CTD and NTR Mutations in PCSK9: Their Functional Consequences

The cysteine-histidine rich CTD of PCSK9 has been shown to be important for the degradation of LDLRs (97), but its effect on LDL association remained to be investigated. Our lab has shown that PCSK9's association with LDL has an inhibitory effect on LDLR degradation in cell culture (9). However, the physiological relevance of this interaction also remains to be elucidated. In a recent publication (95), we showed that peptides corresponding to a sequence within the NTR of PCSK9 adopt an α-helical conformation in a membrane mimetic environment similar to the surface of lipoprotein particles. Helical wheel modelling showed that an amphipathic helix likely forms in this region. Furthermore, molecular simulations showed that polar residues in this putative helix align with multiple positively charged residues in the CTD of PCSK9; thus, the helical conformation was predicted to facilitate an inter-domain interaction with the CTD. In addition, several natural FH mutations in PCSK9's CTD are found at this inter-domain interface. We wanted to characterize the effect that these disease-associated mutations have on LDL binding. In the first section of this MSc project, we investigated the role of the CTD on LDL association as well as on LDLR binding, and we attempted to characterize the predicted inter-domain interaction with the NTR based off the computational model. We performed site-directed mutagenesis to create natural as well as artificial mutations in *PCSK9,* and subsequently performed functional assays to determine the consequences that amino acid substitutions have on protein function.

3.1.1. FH Mutations in the CTD Inhibit LDL Binding, but Do Not Affect LDLR Binding or PCSK9 Uptake

To investigate the functional role of natural FH mutations in PCSK9's CTD on LDL association, LDL binding experiments were carried out with conditioned medium containing various PCSK9 constructs incubated with PCSK9-free LDL at 37°C. Incubations were followed by the addition of Optiprep density gradient solution and a 2-hour centrifugation, after which the LDL layer was isolated and an IP was performed to capture LDL-bound PCSK9. The amount of PCSK9 bound to LDL in each layer was analyzed via western blot (Figure 4A). This analysis shows that three natural FH-associated mutations in the CTD of PCSK9 (R469W, R496W and F515L) display defects in LDL binding compared to WT PCSK9. Quantification of this data indicates that LDL binding is diminished by ≈ 60-70% for R469W and F515L, whereas for R496W there is near complete lack of LDL binding (Figure 4B).

In order to confirm that protein misfolding was not the culprit of the lack of LDL binding, the uptake of PCSK9 into cells overexpressing LDLR indicated that these proteins were folded and otherwise functional. This experiment allowed in quantifying the amount of PCSK9 internalized into cells after addition of exogenous PCSK9 in conditioned medium onto cells for a 2-hour incubation. Cells were harvested and PCSK9 and LDLR were detected via western blot. Figure 4C shows that PCSK9 uptake and LDLR binding is unaffected by these three CTD FH mutations, as the amounts internalized are relatively the same based on band intensities when compared to WT PCSK9. Quantifications generated for bar graphs in Figure 4D reveal that the uptake of these CTD FH mutants is indeed not

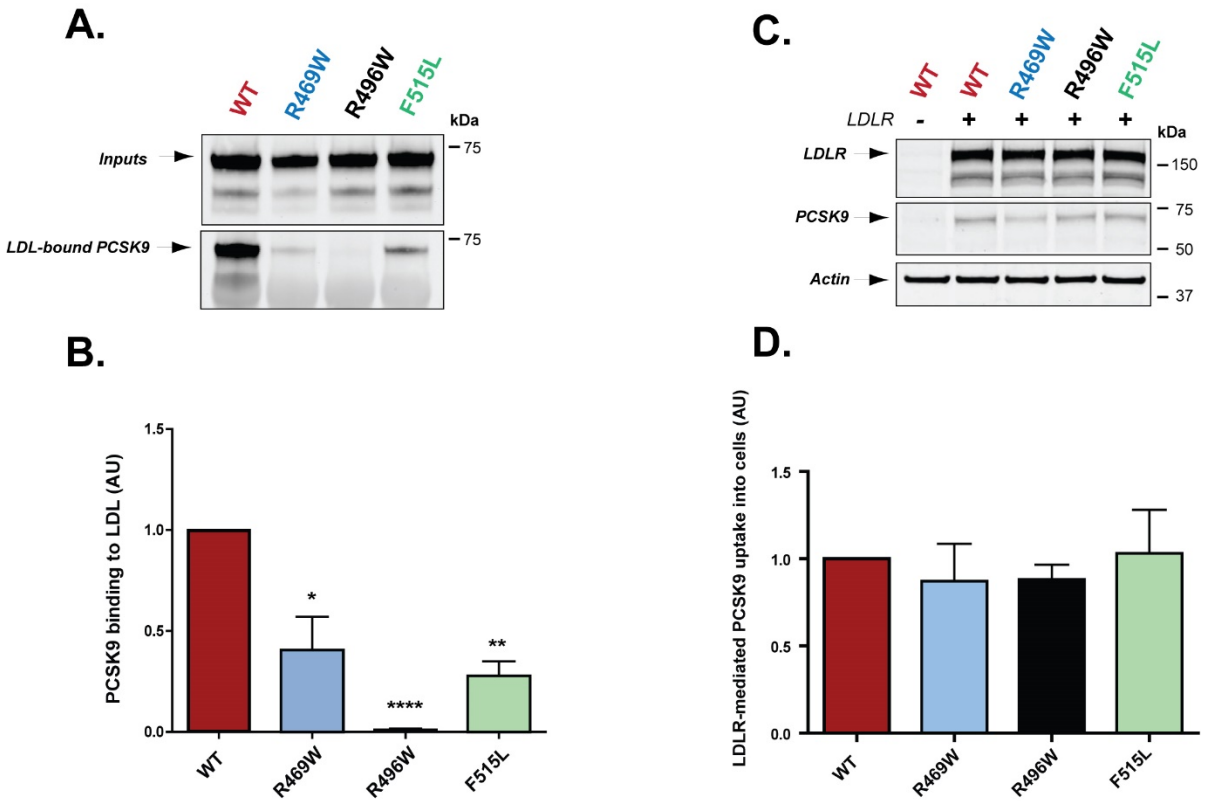

Figure 4. FH mutations located in PCSK9's CTD inhibit LDL binding but do not affect LDLR-mediated uptake into cells.

A. Western blot showing inputs of conditioned medium containing PCSK9 and LDL layers isolated following Optiprep density gradient ultracentrifugation. **B.** Quantifications of values from western blots done in 4 independent replicates for the LDL binding experiments, showing mean + SEM. A column statistics analysis with hypothetical value set to 1 determined after a one-sample t-test that R469W * $p = 0.037$, R496W **** $p < 0.0001$, and F515L ** $p = 0.0022$. Calculated as LDL bound/input band. **C.** Western blot depicting PCSK9 uptake into HEK293 cells overexpressing LDLR. **D.** Column analysis representative of 4 independent experiments of quantifications from western blots, calculated as PCSK9 band/LDLR band. WT value was set to 1 for column statistics and all other mutants are shown as relative to this via a one-sample t-test. Means were not significantly different. Data is published (95).

significantly different from WT PCSK9, meaning that these mutations appear to uniquely affect LDL association and do not affect protein folding or LDLR binding.

We next sought to measure the binding affinity of purified R496W PCSK9 for LDLR-ECD to confirm that the affinity was unchanged by this mutation. We immobilized purified LDLR-ECD onto nitrocellulose membranes and then used an excess of unlabeled WT or R496W purified protein competitors in the presence of DyLight 800-labeled WT PCSK9 in a homologous competition assay. The average intensity data from the membranes (Y-axis) was then plotted against log (nM unlabeled competitor) (X-axis) to generate sigmoidal binding curves in facilitating the calculation of relative IC_{50} values for WT and for R496W versions of PCSK9. Figure 5A and B reveal that purified R496W PCSK9's affinity for LDLR-ECD is not significantly different from WT PCSK9. Relative IC_{50} values of 377.5 nM and 375.5 nM were obtained for WT and R496W, respectively. In conclusion, the R496 residue is crucial in allowing PCSK9 to bind LDL, and mutating to the FH-associated R496W does not affect LDLR binding affinity. Based on our computational model created in collaboration with Dr. Ariela Vergara-Jaque (95), we further explored the role of the R496 residue in a possible inter-domain interaction with E39 in the NTR of PCSK9.

3.1.2. New Mutations Do Not Affect PCSK9 Processing or Secretion, but Some Substitution Mutations at Positions E39 and R496 Inhibit LDL Binding

Molecular simulations predicted that an inter-domain interaction within PCSK9 might be playing a role in aligning basic residues in the CTD with acidic residues with the proposed amphipathic α-helix of the NTR in a membrane-like environment. This included residues E39 and R496. Mutations were introduced at position E39 in the prodomain and R496 in the CTD of PCSK9, both of which are highly conserved residues among vertebrates

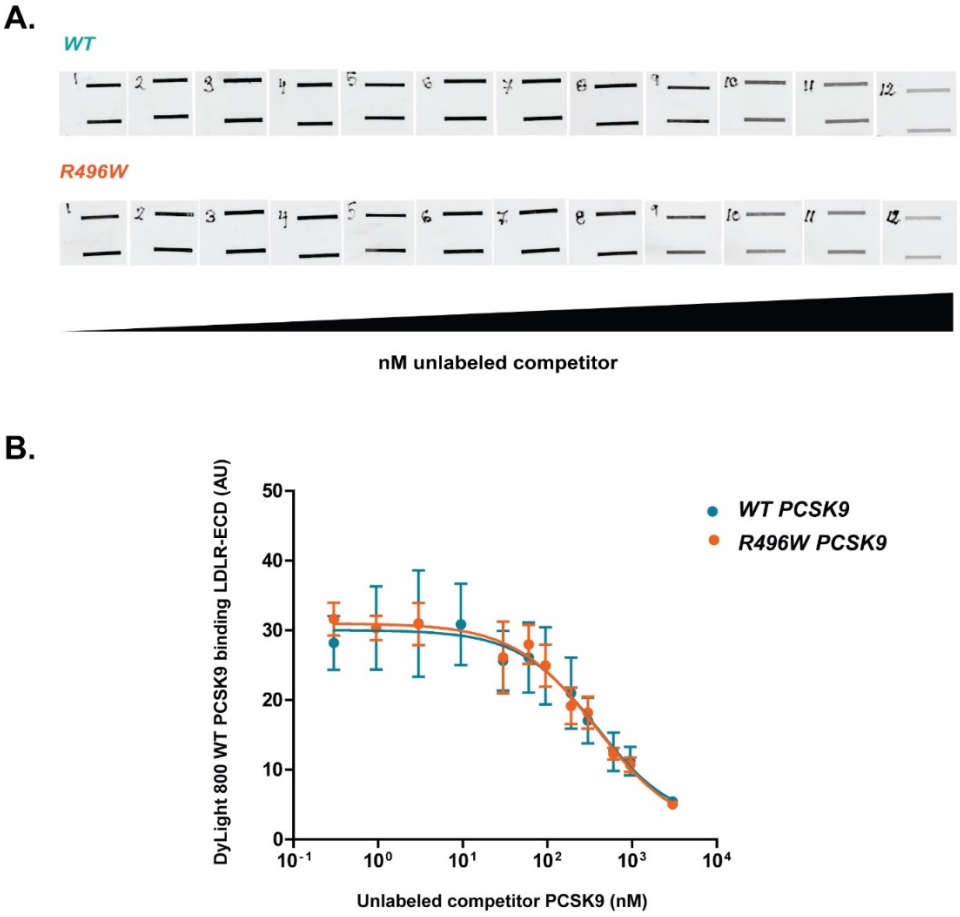

Figure 5. R496W PCSK9 FH mutation does not significantly alter affinity for LDLR-ECD.

A. Nitrocellulose membranes were blotted with purified LDLR-ECD using a slot-blot apparatus (Bio-Rad). From membranes 12 - 1, purified, unlabeled competitor PCSK9 was diluted over a range of 3000 to 0.1 nM, with the competitor being either WT or R496W, and DyLight 800-labeled WT-PCSK9 at 0.1 μg/mL was competed off. **B**. Binding curves generated from average band intensity calculations (Y) vs. nM unlabeled competitor (X) with the function log (inhibitor) vs. response – variable slope in GraphPad Prism 5. The relative IC_{50} values calculated from 3 trials are 377.5 nM for WT and 375.5 nM for R496W. Statistics were done using a paired, two-tailed Student's T-test, where $p > 0.05$ (not significantly different). Error bars show SEM. Data representative of n = 3. Data is published (95).

(109). We predicted that mutagenesis would disrupt the possible inter-domain interaction, and that this would be observable by proxy of inhibited LDL binding. We sought to create single E39A and E39P mutations, R496Y and R496Q mutations, and a double E39P-R496Q mutation representative of armadillo PCSK9. Interestingly, the armadillo sequence has different residues at *both* of these highly conserved positions, so we investigated whether this double mutation combination in human PCSK9 might compensate in the context of LDL binding.

In addition to these mutations, two histidines (H553 and H565) were mutated in the CTD for a second objective, which was to test the effect of pH on the LDLR binding function of PCSK9. It is hypothesized that histidines in the CTD play a role in PCSK9's activity towards LDLR degradation, and it has been shown that the overall basic charge in this region is important for proper LDLR degradation (97). In light of our recent computational model, we predicted that histidines in the CTD located in close proximity to R469, R496 and F515 might participate in the predicted inter-domain interaction with the NTR under certain conditions. We hypothesized that a change to lower pH may preferentially shift the NTR to bind positively charged histidine residues in the CTD, which may in turn relieve auto-inhibition in PCSK9-LDLR binding by shifting the site of the NTR-CTD interaction. Our premise for introducing H → R mutations was that due to a constitutive positive charge at neutral pH of 7.0 (the side chain of arginines harbor a pKa ≈ 12.5), we may observe increased binding to LDLR that we otherwise would only observe at lower pH with the natural histidines. Since the pKa of histidines is ≈ 6 (98), it may be why they are required in PCSK9-mediated LDLR degradation. The pH of endosomes is also close to / lower than 6 (5.5 – 5) (99), so there may be increased protonation of histidines in low pH

conditions due to the local environment, ultimately contributing to the increased binding affinity to LDLR (97) through relief of PCSK9 auto-inhibition.

All novel PCSK9 constructs were transfected into HEK293 cells and secretion took place for 24 hours before the collection of cultured medium and lysis of cells. We carried this analysis out in order to confirm that the secretion and processing of PCSK9 would be unaffected by these new mutations. The western blot in Figure 6A shows that processing of all new PCSK9 constructs was comparable to WT, meaning that none of these new mutations affected the folding or auto-processing of PCSK9 in cells. The R496Q and R496Y mutations were made and tested by other lab members prior to the start of this project. PCSK9 processing is measured by the quotient of the band intensities corresponding to mature/pro PCSK9. The smaller molecular weight (MW) band corresponding to mature PCSK9 (around 63 kDa) was significantly intense for all mutants. The secretion of PCSK9 into the medium is shown in the blot in Figure 6B, and no significant differences are observed between the mutants and WT. A band corresponding to mature PCSK9 missing the prodomain is observed below 75 kDa (around 63 kDa) for all samples, and a minor furin cleaved form is at a slightly lower MW than the mature form. The prodomain fragment that dissociates after boiling reducing SDS-PAGE samples is below 20 kDa. Figure 6C depicts LDL binding analysis done through Optiprep density gradient centrifugation as previously described, and abolishment of this function is observed with the E39P mutation as shown by lack of an LDL-bound PCSK9 band. However, the E39A mutation displays normal LDL binding and so does the FH variant H553R, as indicated by the LDL-bound PCSK9 band intensities comparable to WT.

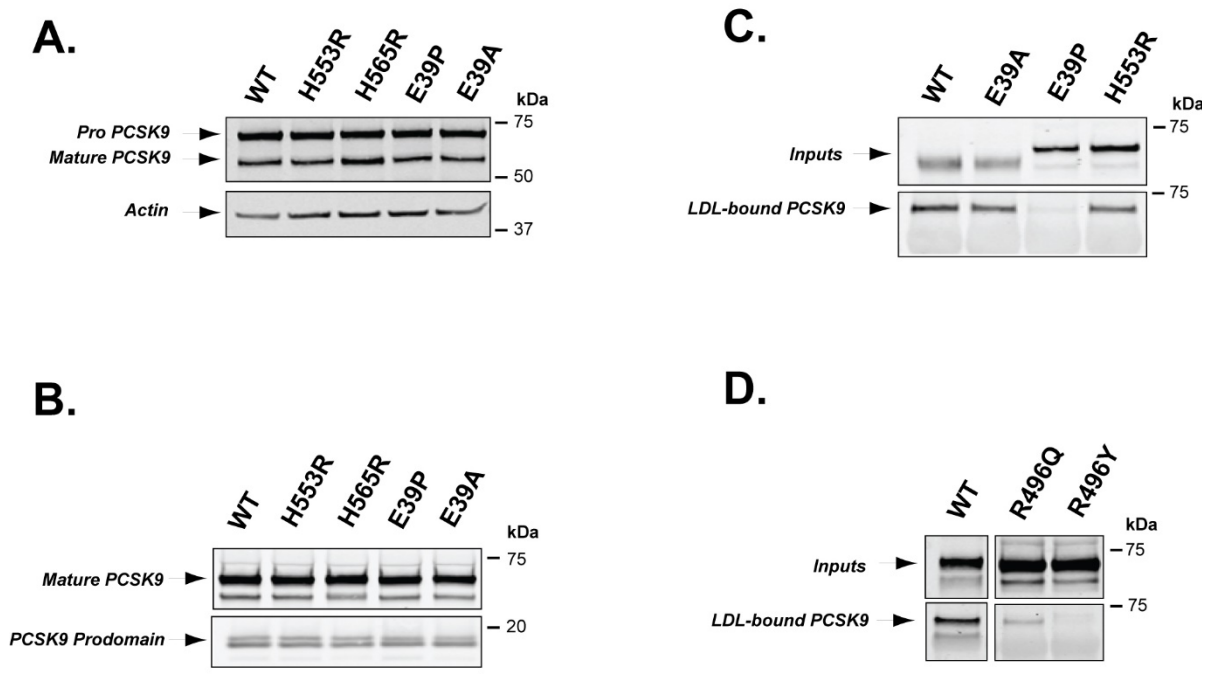

Figure 6. The effect of PCSK9 mutagenesis on secretion, processing and LDL binding.

A-B. ***Substitution mutations do not affect PCSK9 processing in cells or secretion into the cultured medium.*** Western blots depicting PCSK9 processing in cells and secretion of PCSK9 into cultured medium. HEK293 cells were transfected with 1 μg DNA per well in a 6 well dish, and medium was changed to serum free DMEM + ITS supplement. Secretion was allowed to take place for 24 hours, after which cell extracts were made and medium was collected and used in a TCA precipitation for quantification of PCSK9 secreted into the medium. **C**. ***E39P disrupts LDL binding while E39A and H553R do not***. Western blots showing inputs of conditioned medium containing PCSK9 and LDL layers isolated following Optiprep density gradient ultracentrifugation. Blot is from a representative experiment done two more times with similar results. **D.** ***R496Q rescues LDL binding by 10% and R496Y abolishes it.*** Western blots showing inputs of conditioned medium containing PCSK9 and LDL layers isolated following Optiprep density gradient ultracentrifugation. Blot is from a representative experiment done two more times with similar results.

Figure 6D depicts LDL binding done with two different PCSK9 proteins with other amino acids at position 496. We observed that placement of a Tyr (R496Y) abolished LDL binding; however, placement of a Gln (R496Q) restored LDL binding by ≈ 10% as shown in Figure 6D. R496Q PCSK9 is a natural mutant associated with type III hyperlipoproteinaemia in humans (85), and it was previously shown to exhibit normal secretion, processing and LDLR degradation in cell culture. Taken together, our results display that the natural arginine at position 496 is crucial for fully functional LDL association.

Mutating E39 to E39A does not inhibit LDL binding and therefore is unlikely to disrupt the potential charge-associated interaction with R496 (Figure 6C). However, the proline substitution E39P, similarly to L41P and A44P, likely disrupts the predicted α-helix in this region (95), as all three proline mutations abolish LDL binding *in vitro*. The E39P-R496Q armadillo double mutation was made by Dr. Sarkar, and it was determined that it does not compensate in the context of LDL binding (data not shown). To further investigate the functional roles of CTD mutations on PCSK9 activity, H553R and H565R single mutations were made to investigate the effect of placing constitutive positive charges in these two positions on PCSK9's interaction with LDLR.

3.1.3. The H553R FH Mutation Slightly Increases LDLR Binding At Neutral pH, but the H565R Mutation Does Not

The literature has reported that PCSK9 binds with increased affinity to LDLR at low pH (56, 87, 88). However, no mechanisms have been identified for this effect. As described above, we sought to investigate the role of pH on LDLR binding based on the inter-domain interaction presented in our computational model. With the Δ53 PCSK9 variant missing the NTR, we have observed that the pH effect trends towards being blunted, meaning there is

not as large of an increase in affinity between neutral and acidic pH with this mutant, as the 170-fold increase that has been reported for WT PCSK9 (56). We predicted that this difference might be due to the absence of the inter-domain interaction between the NTR and CTD. To this end, we mutated two separate histidines in the CTD of PCSK9 and assessed the impact on LDLR binding / PCSK9 uptake at neutral pH in cell culture. We selected His553 because it is naturally associated with increased plasma LDL-c when substituted to an arginine (H553R) (78). We also mutated His565 because it was one of the residues in the CTD predicted to align and potentially interact with the acidic region of the NTR in our model (95). We predicted that H → R substitutions at positions 553 and 565 might increase the binding affinity to LDLR at neutral pH. We overexpressed LDLR in HEK293 cells and treated them with chloroquine to inhibit lysosomal degradation. Exogenous PCSK9 was added to cells in conditioned medium for 2 hours to allow for uptake to occur. The cells were lysed for western blot analysis and PCSK9 uptake was detected.

Figure 7B demonstrates that uptake of PCSK9 into cells is modestly increased by ≈ 40% with H553R (78). This effect can be observed by the slight increase in band intensity corresponding to H553R PCSK9 below the 75kDa marker (Figure 7A). However, the H565R mutation did not significantly increase the uptake, as shown in Figures 7A and B. The quantifications for PCSK9 taken up into cells shows that the level for H565R is not significantly different from WT. D374Y PCSK9 is a very well characterized FH mutation and was used as a positive control in the assay to monitor the extent of increase in LDLR binding, which here is ≈ 7-fold higher than WT. In conclusion, we determined that mutating single histidines to arginines did not confer very large effects on LDLR binding affinity at neutral pH. It is possible that multiple histidines in this region are required for the pH effect,

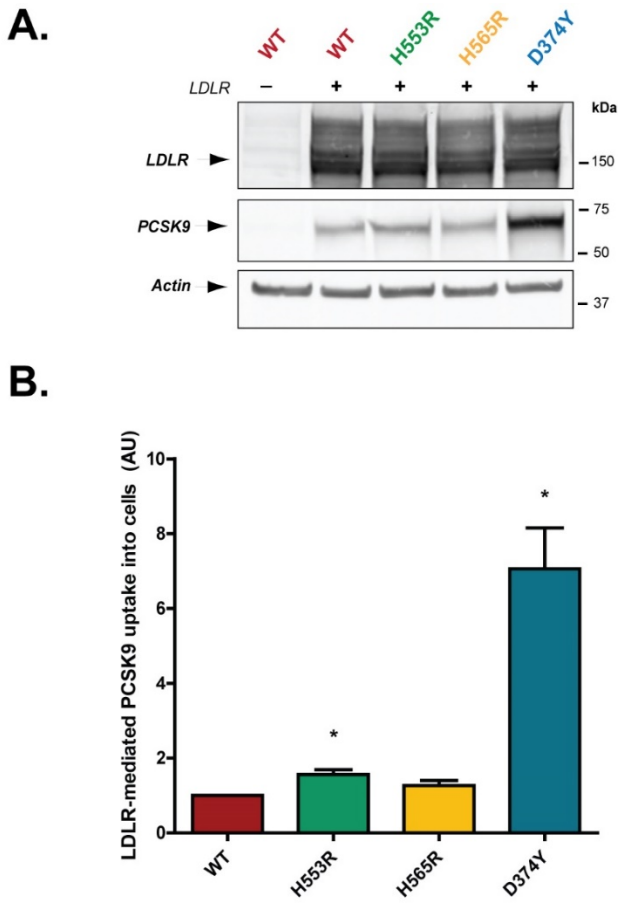

Figure 7. H553R FH mutation in PCSK9 slightly increases LDLR binding and PCSK9 uptake at neutral pH while the H565R mutation does not.

A. Western blot representative of LDLR-mediated PCSK9 uptake in cells overexpressing LDLR treated with 0.05mg/mL chloroquine to inhibit lysosomal degradation. Conditioned medium containing PCSK9 was normalized to the lowest expressing variant, and added at 1 mL per well on a 6-well dish for 2 hours. Cells were washed in 1X PBS, lysed, and extracts were analyzed via western blotting. **B**. Column analysis representative of 3 independent experiments of quantifications from western blots, calculated as PCSK9 band/LDLR band. All values were set relative to WT control with a value of 1. Column statistics were performed with a one-sample t-test comparing all values to this theoretical value, where the p-value for H553R * = 0.046, and p-value for D374Y * = 0.031.

and that mutating them in tandem (i.e. H553R-H565R) would show a more pronounced increase in uptake or LDLR affinity *in vitro* at neutral pH.

In the subsequent section of this project, we sought to investigate the role of prodomain mutations on PCSK9 activity. In addition to the CTD of PCSK9, the prodomain also contains important regulatory regions with respect to PCSK9 activity for both LDL and LDLR binding. The amino acid tract from 31-52 was previously shown to be critical for LDL association (9), and it behaves as a negative regulator of LDLR binding affinity (87). Herein, we characterized a third area of interest (spanning from residues 106-127) that harbors several natural GOF and LOF mutations. Some of these mutations lacked detailed *in vitro* analyses in the literature, especially in the context of LDL association.

3.2 Prodomain Mutations in PCSK9: Their Functional Consequences

GOF Mutations – L108R and S127R

3.2.1. L108R Mutation Disrupts LDL Binding but Does Not Affect LDLR Binding

The L108R mutation was identified as segregating with a severe FH phenotype in a French family (72). Authors reported that LDLR degradation was increased with this mutation by 2-fold *in vitro* (72). However, there was no previous data in the literature about its effect on LDL binding or LDLR affinity. We assessed LDL binding affinity via a homologous gel-shift competition assay by measuring LDL-bound DyLight 800-labeled WT PCSK9 as a function of increasing concentrations of purified unlabeled competitor (either WT or L108R). Figures 8A and B demonstrate that L108R has a decreased ability to outcompete DyLight 800-labeled WT PCSK9 for binding to LDL, as depicted from the

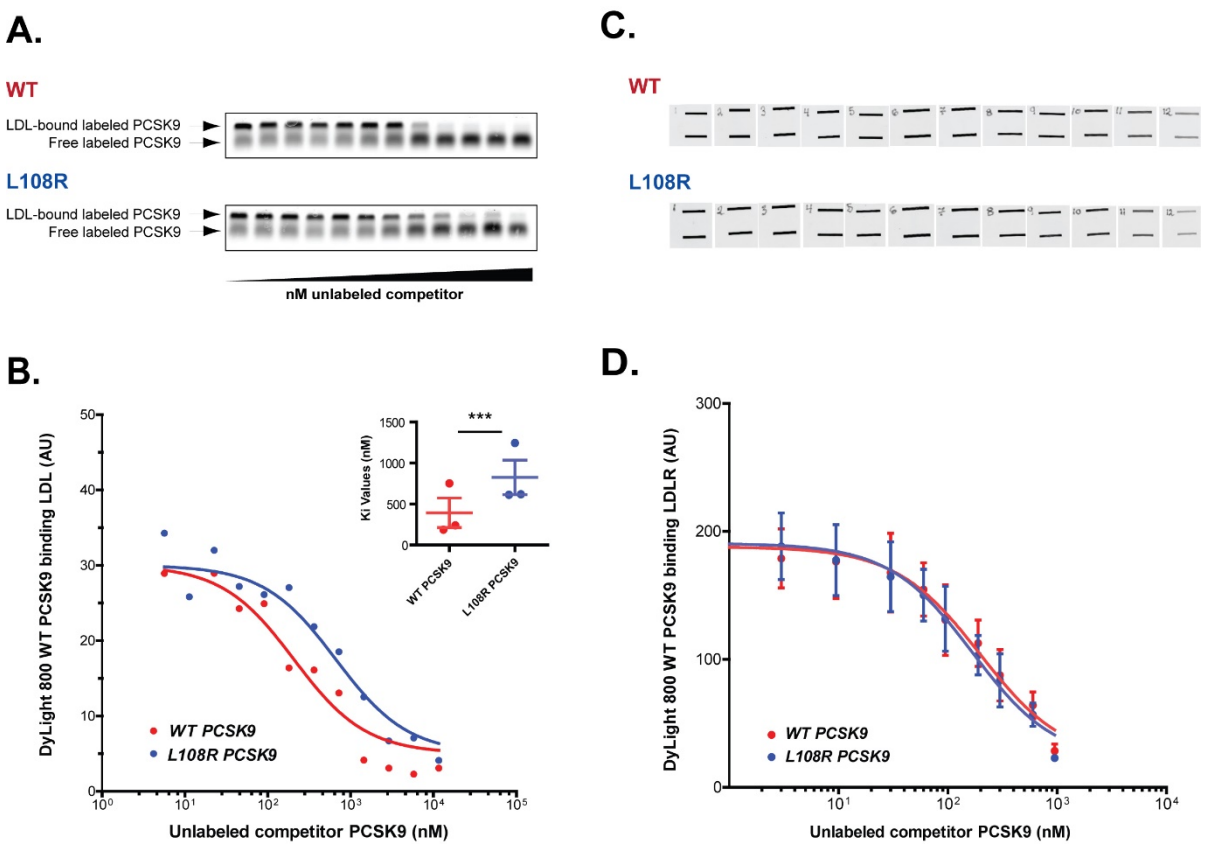

Figure 8. The L108R FH-associated prodomain mutation in PCSK9 inhibits LDL binding but does not affect LDLR binding.

Competition series carried out using DyLight 800-labeled WT PCSK9 with excess of either unlabeled WT or unlabeled L108R. **A.** ***L108R mutation decreases LDL binding affinity.*** Agarose gels used to analyze LDL-bound vs. unbound labeled WT PCSK9. **B**. LDL binding homologous competition curves for purified L108R and WT proteins using PCSK9-free LDL. LDL and labeled WT PCSK9 concentrations kept constant, while an increasing amount of unlabeled competitor was added to the reactions. The curves in part B are generated using the function [binding – competitive, one site, fit K_i] on GraphPad Prism 5.0. The relative K_i for the WT series was determined to be 200.8 nM and 644.2 nM for the L108R series. Differences in mean were calculated by a paired, two-tailed Student's T-test, where p-value = 0.0003. **C.** ***L108R does not affect affinity for LDLR-ECD in vitro.*** Nitrocellulose membranes were blotted with purified LDLR-ECD using a slot-blot apparatus. From membranes 12 - 1, purified, unlabeled competitor PCSK9 was diluted over a range of 3000 to 0.1 nM, with the competitor being either WT or L108R, and DyLight 800-labeled WT PCSK9 at 0.1 µg/mL was competed off. **D**. Binding curves generated from band intensity calculations with the function log(inhibitor) vs. response – variable slope in GraphPad Prism 5. The relative IC_{50} values calculated are 223.0 nM for WT and 189.3 nM for L108R. Statistics were done using a paired two-tailed Student's T-test. Error bars show SEM. Data representative of n=3. Experiments were done during my 4th year Honours thesis in 2017-2018 for the BIM4009 Honours project at the University of Ottawa. Not published.

relative K_i values. The relative K_i for the WT series was determined to be 200.8 nM, and 644.2 nM for the L108R series. Differences in mean were calculated by a paired, two-tailed Student's T-test, where the p-value was 0.0003. The higher K_i indicates that L108R has a lower binding affinity to LDL by about 3-fold relative to WT PCSK9.

To measure L108R's affinity for purified LDLR-ECD, competition-binding assays were carried out using purified proteins with a ligand blot apparatus as previously described for R496W in Figure 5. Figures 8C and D show that there is no significant difference in affinity for LDLR-ECD between WT and L108R PCSK9, as the relative IC_{50} values were calculated to be 223.0 nM for WT, and 189.3 nM for L108R. The difference in IC_{50} values was statistically insignificant when a Student's T-test was performed with the p-value being > 0.05. These results show that the L108R mutation inhibits LDL binding, and does not increase LDLR affinity.

3.2.2. The S127R Prodomain Mutation Does Not Increase Binding Affinity To LDLR

The S127R mutation has been studied quite extensively in the literature. It was one of the first identified FH mutations in the *PCSK9* gene (7, 100). We performed *in vitro* LDLR binding affinity experiments, expecting the affinity to either be increased (56) or unchanged (88, 101). When we carried out our homologous competition assay using purified PCSK9 and LDLR-ECD, we observed that the relative IC_{50} values are not significantly different between WT and S127R (Figure 9A and B). The relative IC_{50} values calculated were 230 nM for WT, and 205 nM for S127R. Statistics were done using a paired, two-tailed Student's T-test and the means were not significantly different. In addition to LDLR affinity, LDLR

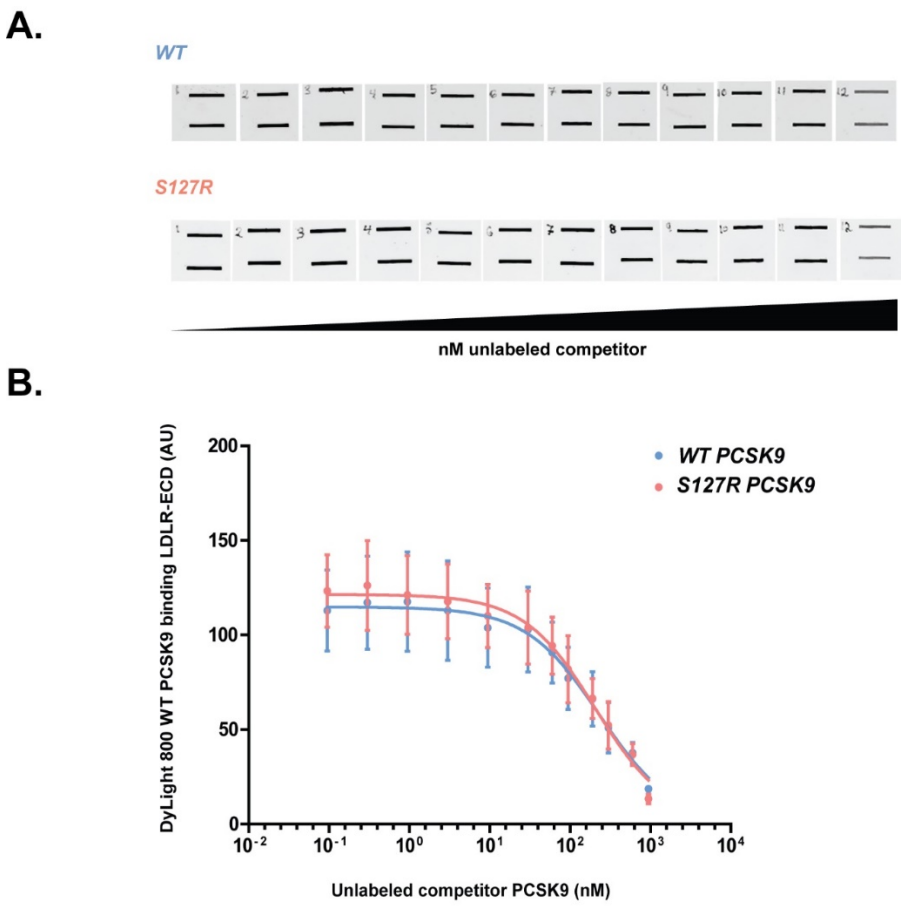

Figure 9. The S127R FH-associated mutation in PCSK9's prodomain does not significantly increase affinity for LDLR-ECD *in vitro.*

A. Nitrocellulose membranes were blotted with purified LDLR-ECD using a slot-blot apparatus. A mixture of 2.5% milk and DyLight 800-labeled WT PCSK9 in low salt TBS-C (pH 7.0) was generated as an incubation buffer. From membranes 12 - 1, purified, unlabeled competitor PCSK9 was diluted over a range of 3000 to 0.1 nM, with the competitor being either WT or S127R, and DyLight 800-labeled WT PCSK9 at 0.1 µg/mL was competed off. Mixtures were added onto membranes and incubated for 2 hours with gentle shaking at room temperature. Blots were then washed and scanned on the LiCor scanner and band intensities calculated using the Odyssey software. **B**. Binding curves generated from average band intensity calculations vs. nM unlabeled competitor with the function log(inhibitor) vs. response – variable slope in GraphPad Prism 5. The relative IC_{50} values calculated are 230 nM for WT and 205 nM for S127R. Statistics were done using a paired, two-tailed Student's T-test. Error bars show SEM. Data representative of n = 3.

degradation activity and PCSK9 uptake are other metrics we used to assess the consequences of the L108R and S127R mutations.

3.2.3. L108R and S127R Slightly Increase LDLR Degradation and PCSK9 Uptake

As both prodomain FH mutations showed no significant changes in LDLR binding affinity in our *in vitro* experiments, at most, we expected modest changes to be observed in LDLR degradation activity and PCSK9 uptake. Hepa1c1c7 mouse hepatoma cells were plated in a monolayer, endogenous *LDLR* expression was induced via the addition of 10μM pravastatin, and cells were cultured in lipoprotein-deficient serum conditions. Purified WT, L108R, L108A, S127R and S127A proteins were added at 5 μg/mL onto respective dishes for 4 hours, followed by biotinylation of cell surface proteins and harvesting of cells. An IP was done on ¾ of the lysates to determine the extent of LDLR degradation by measuring cell surface LDLR levels via western blot. PCSK9 uptake was also measured using the remaining ¼ of the cell lysates. In Figure 10A, the western blot depicts PCSK9 taken up into the cells. Figure 10C is a western blot done on IP reactions containing the biotinylated cell surface proteins used to measure the extent of cell surface LDLR degradation. An untreated control of cells was included in each experiment for baseline measure of induced LDLR expression in the absence of exogenous PCSK9 addition (Figure 10C).

We observed that the FH-associated S127R mutation trends towards increasing PCSK9 uptake slightly (Figure 10A and B) by about 2-fold. It also increases LDLR degradation activity (30-40%) as shown by the decreased band intensity for cell surface LDLR around 150 kDa (Figure 10C), and the column statistics in Figure 10D determined that the p-value for S127R was significant at 0.02. The S127A mutation confers modest differences in activity for PCSK9 uptake (≈ 30-40%) and for LDLR degradation (≈ 10-20%)

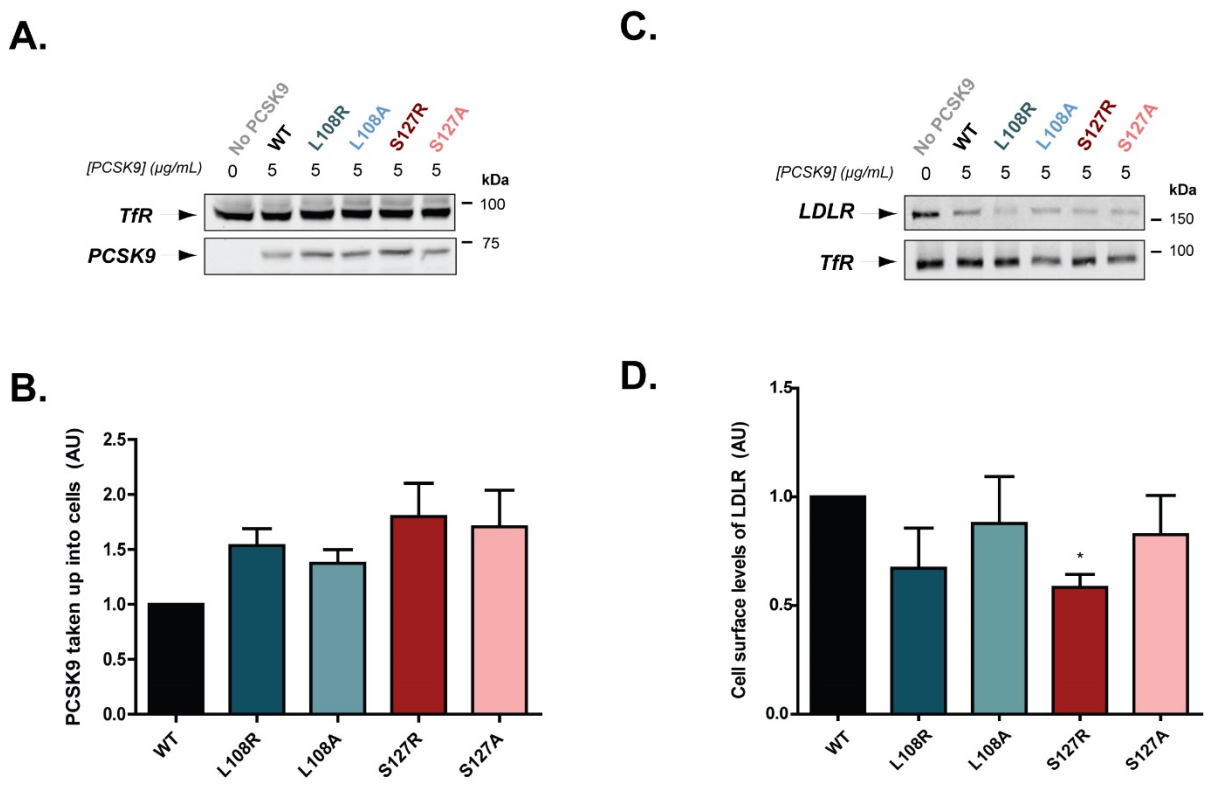

Figure 10. L108R and S127R FH mutations in PCSK9's prodomain slightly increase LDLR-mediated PCSK9 uptake and LDLR degradation activity.

Hepa1c1c7 cells were plated and endogenous LDLR expression was induced via addition of pravastatin. Purified WT, L108R, L108A, S127R and S127A proteins were added at 5 μg/mL onto respective dishes for 4 hours. Cells were then washed and incubated with biotin in biotinylation buffer 2 x for 30 minutes, followed by quenching with glycine in PBS-CM. Western blot detection of proteins allowed in quantifying the amount of PCSK9 internalized into cells, as well as the amount of cell surface LDLR degraded in the presence of each PCSK9 variant. **A**. ***Uptake of PCSK9 into cells is slightly increased for two prodomain FH variants.*** Western blot representative of 1 experiment showing whole cell extracts of LDLR mediated PCSK9 uptake into cells. Transferrin used as a loading control. **B**. Column analysis showing the PCSK9 uptake for various mutants from 3 independent replicates, where differences were not significantly different as tested with column statistics and a one-sample t-test with a hypothetical value of 1. **C**. ***LDLR degradation activity trends towards an increase with L108R and S127R mutations in PCSK9's prodomain***. Western blot showing cell surface LDLR degradation with or without addition of exogenous purified PCSK9. Transferrin receptor used as a loading control. **D**. Column analysis of LDLR degradation for various PCSK9 mutants and WT. Column statistics with one-sample t-test and a hypothetical value of 1 determined that the p-value for S127R * was 0.0201. Data representative of n = 3.

(Figure 10B and D). Both the L108R and L108A mutations have similar but modest effects on PCSK9 uptake (≈ 50% increase). L108R shows approximately 30-40% lower levels of cell surface LDLR, whereas L108A only shows about a 10% difference (Figure 10D). The column statistics analysis determined that the means were not significantly different for L108A or L108R in comparison to WT (Figure 10D). However, there is a slight trend towards higher activity in both the uptake and degradation for L108R.

In conclusion, the LDLR degradation activity and PCSK9 uptake is slightly increased in both S127R and L108R, but the effects are modest when compared to WT PCSK9. These functional assays looking at LDLR association therefore fail to explain the reason for the severe FH phenotype *in vivo* in patients with L108R or S127R. We next sought to identify the effect of these mutations on secretion and processing of PCSK9 along with the additional analysis of the artificial S127P mutation, which was shown to rescue secretion in a previous publication (54).

3.2.4. S127P Rescues Processing and Secretion Events That Are Otherwise Defective in Both S127R and S127A

S127P PCSK9 exhibited normal secretion into cell culture medium in a previous publication (54): a function that is defective with the natural S127R FH variant (73). To replicate this finding, as well as to investigate protein processing events, HEK293 cells were transiently transfected with plasmids coding for various PCSK9 constructs, after which secretion was allowed to occur for 24 hours. The media was then collected, and cells were harvested for western blot analysis and quantification of PCSK9 secretion and processing. The experiment included the pcDNA3.1 vector transfected as a negative control to show that

HEK293 cells do not endogenously express PCSK9, as indicated by absence of a band corresponding to PCSK9 in the control lane (Figure 11A and C).

The processing or maturation is determined by the amount of PCSK9 that has undergone autocatalytic cleavage in cells. The mature form of PCSK9 is observed around 63 kDa in the whole cell extract blot, while the pro PCSK9 form that has not been processed is found higher up, just below 75 kDa (Figure 11A). We observed that S127P, L108R and L108A exhibit normal processing in cells (Figure 11A and B) and effective secretion into the medium (Figure 11C and D) at efficiencies similar to WT. The processing can be observed by western blot analysis, with the mature band around 63 kDa appearing less prominent when the processing is inefficient (Figure 11A). The processing is calculated as the quotient of mature/pro PCSK9 bands for the bar graphs. A column statistics analysis determined that the processing is significantly defective in S127R and S127A (≈ 60-70% less than WT), and is slightly more efficient in L108R (≈ 10% more than WT) as seen in Figure 11B.

The extent of secretion can be visualized by the PCSK9 band in the medium appearing below the 75kDa marker (around 63 kDa) on the western blot in Figure 11C. A column statistics analysis determined that the secretion of S127P, L108R and L108A is not significantly different from WT (Figure 11C and D). The minor furin cleaved form can also be observed at a MW slightly below the mature band and does not appear differentially affected in any of these constructs. The non-covalently associated prodomain dissociates during boiling of the samples for reducing SDS-PAGE, and is found below 20 kDa (Figure 11C). The secretion of S127R and S127A variants is significantly defective compared to WT PCSK9; with a ≈ 60-70% decrease (Figure 11D), mirroring the decrease in processing. These results demonstrate that placing a proline at position 127 in the prodomain allows for

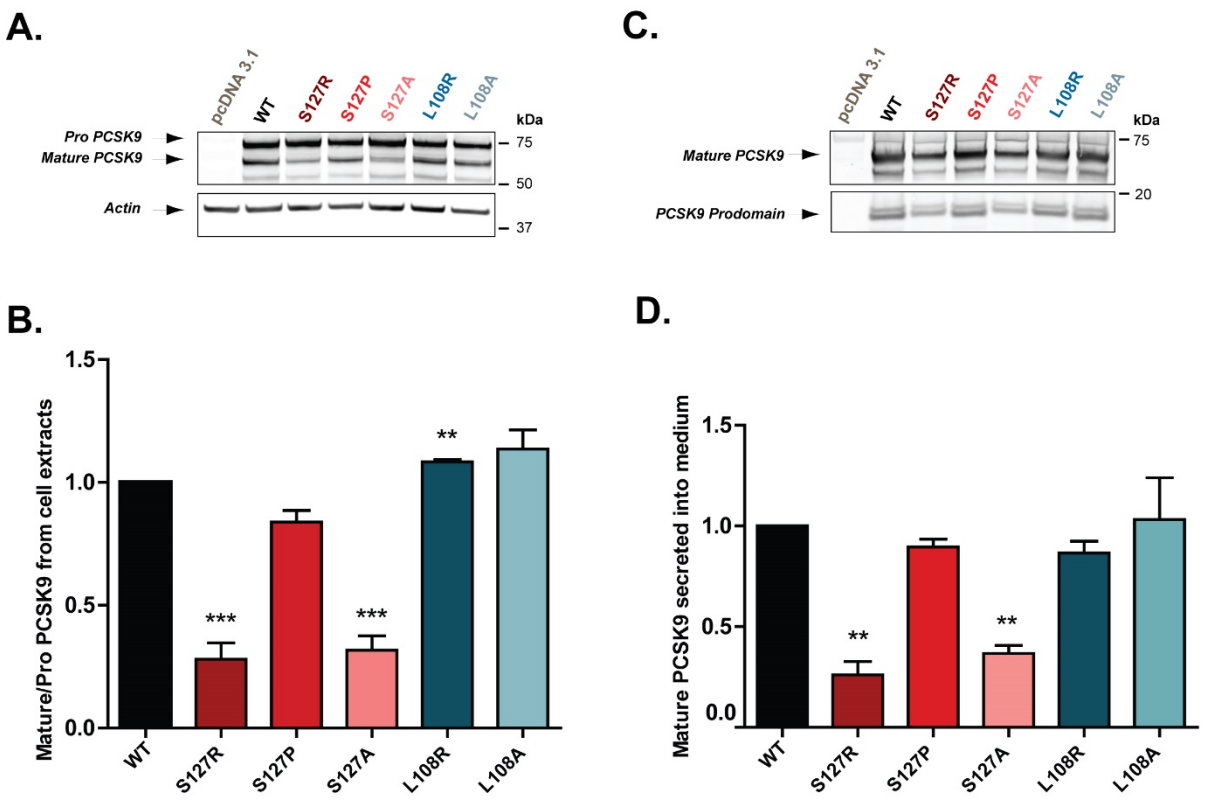

Figure 11. Effects of substitutions at position L108 and S127 on PCSK9 processing and secretion events.

HEK293 cells were transiently transfected with plasmids coding for various PCSK9 constructs, after which secretion was allowed to occur for 24 hours at 37°C. Cultured media was collected and cells were lysed for detection of PCSK9 processing and secretion via western blot. **A & B**. ***S127P confers normal processing, L108R slightly increases processing, and S127R and S127A show defects in processing.*** Western blots and quantifications representing the processing of PCSK9 in cells. Values for graph calculated by mature PCSK9 band/pro PCSK9 band in each lane. A column statistics analysis with a one sample t-test and hypothetical value of 1 (WT) determined that S127R *** had a p-value of 0.0084, S127A *** had a p-value of 0.0072, and L108R ** had a p-value of 0.0124. **C & D**. ***S127P rescues secretion of PCSK9 at efficiency similar to WT, while the S127A and S127R mutations cause significant defects.*** Western blot and graph analyses for amount of secreted PCSK9 into cultured media. Values calculated as quantifications from mature PCSK9 band in medium. A column statistics analysis with a one sample t-test and hypothetical value of 1 (WT) determined that S127R ** had a p-value of 0.0078 and S127A ** had a p-value of 0.0039. Data representative of 3 independent replicates.

processing and secretion to both be at a level comparable to WT PCSK9, in agreement with a previous study (54). To further characterize other functional consequences of this proline substitution, PCSK9 uptake and LDLR degradation activity was analyzed.

3.2.5. S127P Does Not Affect LDLR Degradation or PCSK9 Uptake

As previously described for Figure 10, LDLR degradation and PCSK9 uptake was measured this time for S127P PCSK9 using Hepa1c1c7 cells. Western blot analysis and graphic results are shown in Figure 12 A-D. The artificial S127P mutant exhibits no increase in PCSK9 uptake or in LDLR degradation activity, as shown by the similar band intensity between WT PCSK9 and S127P PCSK9 taken up into cells (Figure 12A), and also the similar amounts in cell surface LDLR levels around 150 kDa (Figure 12C). In fact, it seems that the S127P mutant trends towards slightly less efficient LDLR degradation by ≈ 40-50% compared to WT (Figure 12D). The D374Y mutant was included as a positive control to show the extent of LDLR degradation and PCSK9 uptake in these S127 mutants relative to a highly active FH mutant. The band intensity for D374Y below 75 kDa is the strongest compared to WT and the other two variants (Figure 12A), with the bar graph indicating that uptake is increased by about 5-fold (Figure 12B). The band intensity for LDLR expressed on the cell surface is nearly absent around 150 kDa for D374Y (Figure 12C), and the calculated LDLR expression is ≈ 90% less than WT (Figure 12D).

S127R shows a 2-fold increase in uptake and ≈ 30% reduction in LDLR levels compared to WT. From these results, we conclude that the arginine in S127R is important for the increase in LDLR degradation as previously seen in Figure 10D, as the alanine and proline substitutions did not confer significant changes. To conclude this functional analysis

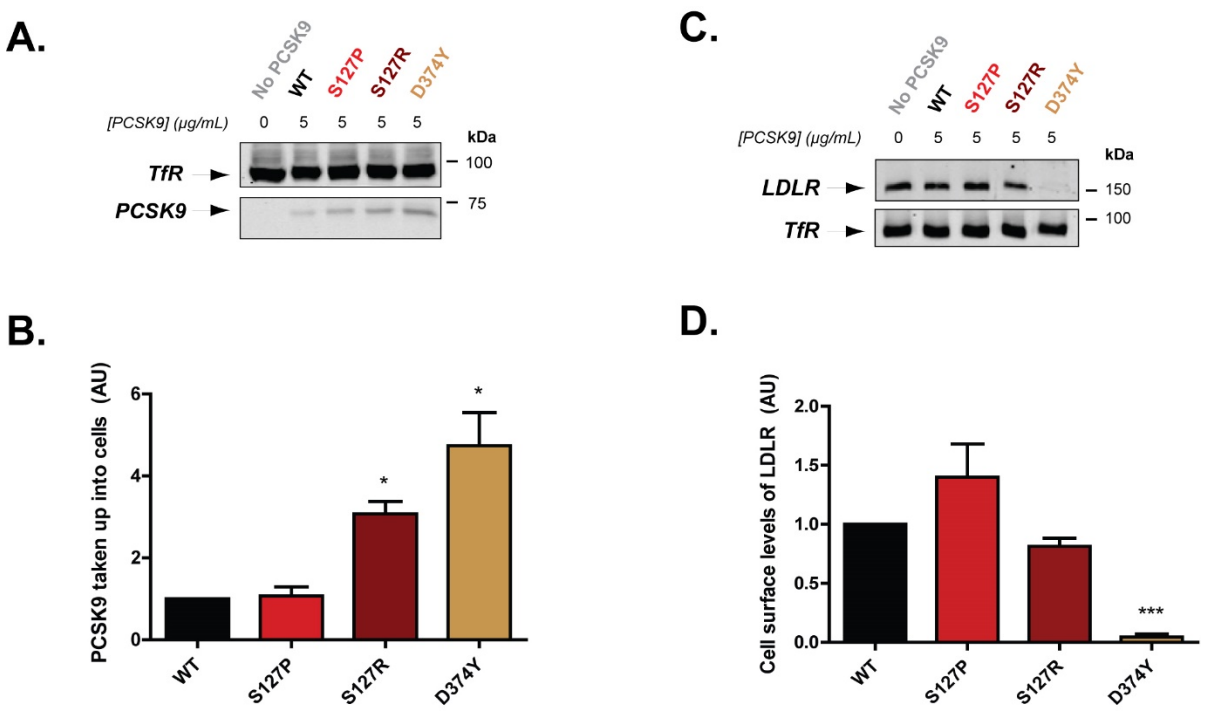

Figure 12. The S127P mutation does not affect PCSK9 uptake or LDLR degradation.

Hepa1c1c7 cells were plated and endogenous LDLR expression was induced via addition of pravastatin. Conditioned medium containing PCSK9 proteins was normalized to the lowest expressing variant, and added onto respective dishes at 5 µg/mL for 4 hours. Cells were then washed and incubated with biotin in biotinylation buffer 2x for 30 minutes, followed by quenching with glycine in PBS-CM. Western blot detection of proteins allowed in quantifying the amount of PCSK9 internalized into cells, as well as the amount of cell surface LDLR degraded in the presence of each PCSK9 variant. **A**. ***S127P mutation does not increase PCSK9 uptake into cells.*** Western blot representative of 1 experiment showing LDLR-mediated PCSK9 uptake into cells. Transferrin was used as a loading control. **B**. Column analysis showing the PCSK9 uptake for various S127 mutants from 3 independent replicates. Column statistics with a hypothetical value set to 1 and a one-sample t-test determined that S127R * p-value = 0.0211 and * D374Y p-value = 0.0437. **C**. ***S127P mutation does not significantly increase LDLR degradation activity.*** Western blot showing cell surface LDLR degradation with or without addition of exogenous PCSK9. Transferrin receptor used as a loading control. **D**. Column analysis of LDLR degradation for various PCSK9 mutants and WT. Column statistics were done using GraphPad Prism 5.0 where all values are compared to WT with a value of 1, followed by a one sample t-test where D374Y *** p-value = 0.0007. Data representative of n = 3.

on the role of the S127 residue in PCSK9 function, we performed LDL binding analysis through Optiprep density gradient centrifugation. We sought to determine whether S127P could compensate for the serine in the context of LDL binding, since it was able to compensate in protein processing and secretion events.

3.2.6. S127A, S127P and S127R Mutations Abolish LDL Binding

Previous work in our lab by Dr. Samantha Sarkar showed that the S127R mutation abolishes LDL binding, as it completely lacks the ability to compete off fluorescent-labeled WT PCSK9 from LDL in our homologous competition assay (data not shown). Similar findings were obtained for the S127A variant. To replicate these findings and to test the consequence of placing a proline at position 127 on LDL binding, we performed Optiprep density gradient centrifugation using conditioned medium containing WT, S127R, S127P or S127A PCSK9. In Figures 13A and B, we observe abolishment of LDL binding for all of these mutants, as shown by complete absence of an LDL-bound PCSK9 band in the LDL layer. We therefore conclude that the native serine residue in PCSK9 is critical for LDL binding. We have now observed several GOF mutations inhibiting LDL binding in both the prodomain (L108R, S127R) and the CTD (R469W, R496W, F515L). Next, we decided to analyze a LOF variant found in our prodomain region of interest in close proximity to L108 and S127. We expressed the mutant via a transient transfection and tested the functional consequence of this natural LOF mutation on LDL binding. We predicted that it might increase binding to LDL: an effect that would be opposite to what we have seen with several GOF *PCSK9* mutations, which would support our overall hypothesis that LDL association of PCSK9 has an inhibitory effect on LDLR degradation activity.

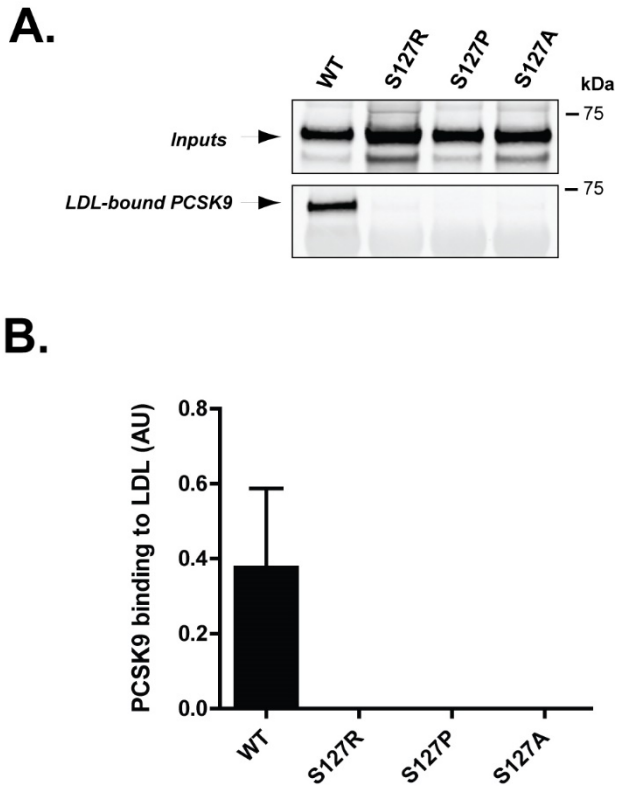

Figure 13. S127R, S127P, and S127A mutations abolish LDL binding.

A. Western blot showing inputs of conditioned medium containing PCSK9 and LDL layers isolated following Optiprep density gradient ultracentrifugation. Incubations were done at 37 °C for 90 minutes with conditioned medium containing PCSK9 and PCSK9-free LDL. A two-hour spin was done after adding Optiprep density gradient solution at 100,000 rpm where the LDL layer could subsequently be visualized and extracted with a needle. Immunoprecipitation of PCSK9 in the LDL layer allowed in quantification of the amounts of PCSK9 bound to LDL in each sample via western blot. Gels were run on 4-12% Bis-Tris gradient gels followed by wet transfer to nitrocellulose membrane. **B.** Quantifications of values from western blots done in 2 independent replicates for the LDL binding experiments, showing mean + SEM. Calculated as LDL bound/input band.

LOF Mutation – G106R

3.2.7. The Natural G106R LOF Mutant Trends Towards Increased LDL Association *in vitro*

LOF mutations in *PCSK9* are associated with decreased plasma LDL-c (78) and in turn, they protect against cardiovascular risk. G106R is a natural LOF mutation (83) that was identified as having severe processing and secretion defects and decreased LDLR degradation activity *in vitro* (85). This mutation lies in close proximity to our region of interest in the prodomain containing GOF mutations L108R and S127R: both of which we have shown to inhibit LDL binding (Figure 8A-B and Figure 13A-B). To test our LDL-binding hypothesis in the context of a LOF mutation, we made conditioned medium containing G106R PCSK9 and then used the same Optiprep density gradient centrifugation protocol as previously described for Figures 4, 6 and 13. With WT PCSK9 as a positive control, we observed that binding to LDL increased ≈ 50-60% with the G106R mutation (Figure 14B), but was not statistically significant ($p > 0.05$). This trend supports our overall hypothesis that PCSK9's association with LDL in the circulation inhibits LDLR degradation activity.

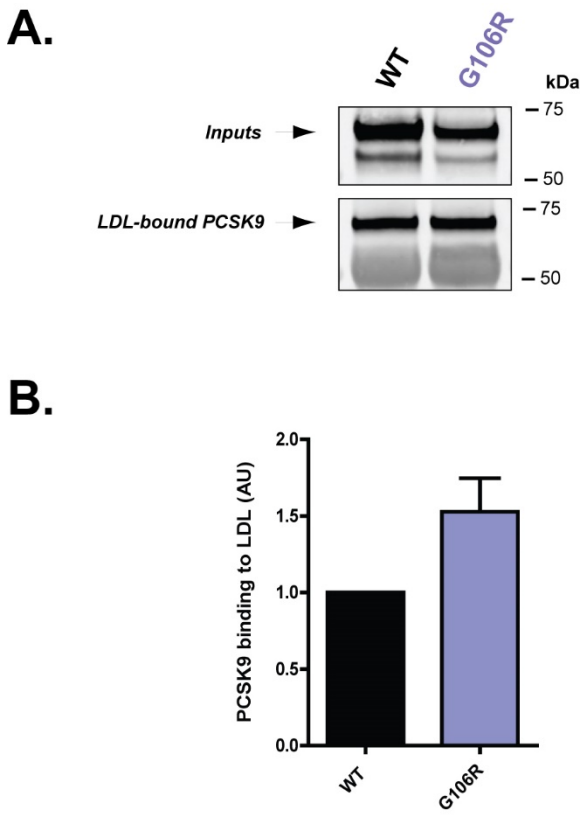

Figure 14. The G106R LOF mutation in PCSK9's prodomain trends towards increased binding to LDL.

A. Western blot showing inputs of conditioned medium containing PCSK9 and LDL layers isolated following Optiprep density gradient ultracentrifugation **B.** Quantifications of values from western blots done in 4 independent replicates for the LDL binding experiments, showing mean + SEM. Calculated as LDL bound/input band with WT value set to 1, and G106R calculated relative to WT. A column statistics analysis with a one-sample t-test determined that there was no significant difference between WT and G106R.

4. Discussion

PCSK9 is an important regulator of plasma LDL-c levels. Since its discovery in 2003 (6, 7), research groups have been working to elucidate PCSK9's molecular mechanisms used for binding to LDLRs. The findings over the last 15 years have allowed for the development of anti-PCSK9 monoclonal antibodies that block the interaction with LDLR in the plasma. More recently, PCSK9's association with LDL has displayed a novel mechanism that contributes to PCSK9 activity *in vitro* (9). To further investigate the potential physiological relevance of this interaction, we sought to characterize the effect of natural *PCSK9* mutations on LDL binding, in order to study the mechanistic effect of these genotypes from patients with known levels of plasma LDL-c. The major findings of this MSc project are that natural GOF mutations in PCSK9 inhibit LDL binding and only modestly affect LDLR binding or degradation events.

We have shown evidence for natural *PCSK9* mutations in the CTD associated with elevated plasma LDL-c inhibiting or abolishing LDL binding (95). We have also identified several prodomain FH mutations that inhibit LDL binding. Furthermore, we have identified a LOF variant associated with lowered LDL-c that shows the opposite effect: trending towards an increase in LDL binding. FH mutations in the CTD seem to be primarily affecting LDL association, and they do not increase LDLR degradation or receptor affinity; which is a trend we also observe with some prodomain FH mutations. Finally, we provide further evidence that LDL-association of PCSK9 may be acting in a classic negative feedback loop on LDLR degradation activity, and that ultimately PCSK9 in the blood

responds to levels of plasma cholesterol in the form of LDL. The implications and next steps following these findings are discussed in the subsequent sections.

4.1. PCSK9's NTR and CTD: Mutations Affecting LDL Binding

The NTR of the PCSK9 prodomain is intrinsically disordered and absent from the available crystal structures. Intrinsically disordered regions (IDRs) in proteins are often functionally important, as increased flexibility makes them more available for protein-protein interactions and post-translational modifications. IDRs can also transiently adopt a more rigid structure under certain conditions (103, 104, 105). The computational model we created in collaboration with Dr. Ariela Vergara-Jaque includes the simulated α-helix of the NTR in Figure 3. An α-helix is predicted to form in the prodomain IDR through allosteric conformational changes upon PCSK9 binding to LDL through lipid and/or protein contacts (95). The prodomain and the CTD are predicted to align and maintain multiple electrostatic interactions perhaps important for stabilizing this auto-inhibited conformation of PCSK9, which might become locked into a more solid state when PCSK9 is associated with LDL. To test this hypothesis, we performed mutagenesis studies and did LDL binding analyses to determine the effect of amino acid substitutions on PCSK9 function. We have shown that the prodomain and CTD both contain specific disease mutations that disrupt the LDL binding function through the alteration of amino acid properties, but to differing degrees of severity. We sought to determine whether these effects on LDL binding perhaps correlated with the lipid phenotypes observed in patients with these natural mutations.

4.1.1. FH-Associated Mutations in PCSK9's CTD Uniquely Affect LDL Binding: The Native R496 Residue Is Required for Fully Functional LDL Association

As shown in Figure 4, GOF mutations in the CTD associated with FH uniquely affect the LDL binding of PCSK9. Both R469W and F515L are natural mutations associated with elevated LDL-c levels (78), and in our studies they both severely inhibit LDL binding (Figure 4A-B), but have no effect on LDLR binding/PCSK9 uptake into cells (Figure 4C-D). In previous cell culture studies, it was shown that all three FH mutations (R469W, R496W, F515L) showed very modest effects on processing and secretion of PCSK9 along with LDLR degradation activity (77, 106, 107), which is in agreement with our observations. The R496W mutation was the most severe in terms of LDL inhibition, where we observed near total abolishment of binding (Figure 4A). This mutation is associated with extremely severe hypercholesterolemia, as indicated by mean total plasma cholesterol of ≈ 300 mg/dL in a Dutch cohort of patients (53). This mutation, however, had no effect on LDLR binding and PCSK9 uptake in cells, and the purified protein used in competition assays did not show greater affinity for LDLR-ECD (Figure 5) when compared to WT. These findings show us that these three CTD mutations are affecting mainly LDL binding, and we predict that inhibition of this function may be a mechanism contributing to the elevated LDL-c phenotype seen in patients. Another FH mutation in this region (N513D) was functionally characterized in our lab by Dr. Zhenkun Hu, and was also determined to uniquely affect LDL association, which was abolished in the same way we saw with the R496W mutation. The LDLR degradation activity, LDLR affinity, and PCSK9 section and processing were unaffected by the N513D mutation (unpublished data).

Introducing other substitution mutations at position 496 allowed for us to determine that the R496 native residue is crucial for LDL binding. An R496Y mutation abolished binding, and an R496Q mutation rescued LDL binding, but only by ≈10% (Figure 6D). An

R496D mutation also abolished binding (data not shown). The slight recovery seen with the Gln substitution might occur because the glutamine side chain is able to hydrogen bond and partially compensate for the natural arginine in the context of an intramolecular interaction within the NTR. However, the poor 10% rescue likely indicates that both the constitutive positive charge *and* the full length and size of the arginine hydrocarbon chain in this position are crucial for proper LDL association. Interestingly, Cameron *et al* identified R496Q PCSK9 in a patient with type III hyperlipoproteinaemia (85). Their *in vitro* assays done with R496Q align with what we observe for R496W: that PCSK9's secretion, processing, and LDLR binding are unaffected by the mutation. The only mechanism that seems to be altered by R496W and R496Q disease mutations is LDL binding; which is highly disrupted with both mutations (Figure 4A and Figure 6D).

4.1.2. Proline Mutations in the NTR Disrupt LDL Binding

Introducing proline mutations into the prodomain's NTR disrupts LDL binding. The L41P and A44P mutations in PCSK9's IDR abolish LDL binding but do not affect LDLR-dependent PCSK9 uptake into cells, indicative of normal LDLR binding affinity (95). We predicted that these proline mutations may be disrupting the helical conformation of the IDR, and in turn disrupt only the LDL association. According to our model, the E39 residue in this region was predicted to form an electrostatic interaction with R496 (95). In this project, an E39P mutation also abolished LDL binding (Figure 6C). As proline side chains lack the ability to hydrogen bond and are structurally rigid due to the cyclic secondary amine, it is possible that this substitution disrupts electrostatic inter-domain interactions with the CTD, or disrupts the entire conformation of the helix. However, these predictions need to be structurally validated. Introducing a small, neutral, nonpolar alanine (E39A) did not

disrupt the LDL binding of PCSK9 (Figure 6C). This leads us to believe that other acidic residues in this stretch of the IDR (32-EDEDGDYEE-40) can potentially compensate for binding to basic residues in the CTD and mediate the appropriate inter-domain interaction. This phenomenon of "electrostatic steering" is also seen in other protein-protein interactions, whereby overall opposing charges in interacting domains promote their association without a strict dependence on individual charged residues (108).

We noticed the armadillo's PCSK9 sequence to have unique amino acids at both positions 39 and 496. These positions are highly conserved across species (109), and in human PCSK9 they are E39 and R496. The armadillo sequence however, has P39 (110) and Q496 instead. This finding struck us as being quite intriguing in relation to the computational model of human PCSK9 that predicted these two specific residues to interact. We tested whether the double E39P-R496Q "armadillo" combination in human PCSK9 might align an NTR-CTD interaction and compensate in the context of LDL binding. However, Dr. Sarkar found that the double mutation did not rescue LDL binding and that it remained disrupted (data not shown). It is therefore possible that the armadillo double variation at these sites is important in some other context of PCSK9 activity, such as protein processing and secretion, or even LDLR association, but this has yet to be investigated.

4.2. Testing the pH Effect: Single Histidine → Arginine Mutations in the CTD

The pH-dependent shift in affinity that WT PCSK9 has for LDLR in an acidic environment has been a major mechanistic question ever since it was discovered (56, 87, 88). To this end, we sought to determine whether our predictive model could perhaps help us with elucidating a mechanism for this effect. Through mutating two conserved histidines

(H553 and H565) to arginines and measuring the PCSK9 uptake into cells, we determined that these two single mutations had no significant increase on LDLR affinity at neutral pH (Figure 7). In addition, we predicted that alanine mutations would blunt the pH effect due to the nonpolar residues being unable to induce a shift in the electrostatic interactions required for relief of PCSK9 auto-inhibition. These mutagenesis experiments were not successful. Furthermore, we were unable to purify the H553R protein via a stable cell line formation, likely due to an error in the gene coding for the Genticin antibiotic resistance.

We were therefore unable to test the H553R mutation in the context of LDLR degradation using purified proteins. This would have been good to measure, because H553R is a natural FH variant and it did slightly increase LDLR-mediated uptake into cells (Figure 7). The H553R mutation had no effect on LDL association (Figure 6C). It is important to remember that the PCSK9-LDLR uptake assay does not adequately detect small-scale changes in affinity, and a measure of PCSK9 uptake includes a measure of the internalization efficiency and receptor-mediated endocytosis, which are much more complex processes than simply measuring the affinity between two proteins. We were mainly looking for large differences in this experiment. This is a qualitative assay, so it is very well possible that if we had been able to purify the protein for competition binding experiments, we would have seen a more significant increase in LDLR affinity. However, the cell-culture uptake experiment represents more physiological conditions than does the ligand blot experiment; whereby the latter uses purified proteins and buffers in non-native conditions. These caveats therefore need to be kept in mind when interpreting this data.

Retrospectively analyzing this CTD region again in the PCSK9 crystal structure, we found another histidine (H551) that might be important in the LDLR degradative function.

Indeed, as shown in a previous publication, there are many histidines in this region, and the *overall* basic charge on the surface of the Cys-His rich CTD is required for LDLR degradation, as single mutations did not show any significant changes in activity (97). It is possible that mutating multiple histidines in tandem (i.e. H551R-H553R, H553R-H565R) would show larger increases in LDLR binding at neutral pH. The H553R mutation is a natural variant whose *in vitro* activity has not been reported in the literature. Although characterized as GOF, it is one of the less severe reported mutations with mean patient LDL-c levels being ≈ 120 mg/dL (78), which is in agreement with our finding that PCSK9 uptake in cell culture is increased only by about 40-50% (Figure 7).

In the future, it would be ideal to continue tests with the Δ31-52 PCSK9 variant, in which LDLR affinity is increased at neutral pH, to confirm that the pH-dependent increase in affinity is indeed blunted when compared to WT PCSK9. This would give us further evidence for an inter-domain interaction being required in pH-dependent LDLR binding. We were lacking an adequate negative control for these competition-binding experiments, as the non-specific binding was very high, and we could not confidently confirm that the effect was blunted (data not shown). Perhaps the use of the LDLR-L318D mutant that is defective in binding PCSK9 would serve as a better negative control. In the co-crystal structure of PCSK9 bound to the EGF-A domain of LDLR, the D374 residue is shown to interact with H306 in the LDLR's EGF-A domain (87, 88, 111), and they are predicted to form hydrogen bonds. It was also predicted that this interaction might be enhanced at low pH, therefore modulating an increase in affinity between PCSK9-LDLR.

Overall, the pH-dependent increase in PCSK9 binding to LDLR may consist of several components, of which a shift in the NTR-CTD inter-domain interaction may play a

partial role. Increased protonation of H306 in LDLR at low pH may be modulating the increase in affinity to PCSK9. The phenomenon of pH-dependent binding was also observed with the D374Y mutant, but it had less of an effect than did WT PCSK9 (56), perhaps meaning that the tyrosine blunts the effect, as binding would be near maximal with this amino acid substitution. Ultimately, intracellularly blunting the pH effect of PCSK9-LDLR binding would represent an ideal route for PCSK9 inhibition with a small molecule. Ideally, it would disrupt the PCSK9-LDLR interaction in endosomes, inducing PCSK9 to release the LDLR before reaching lysosomal fusion, so that PCSK9 is cleared and degraded in the lysosome but the LDLR gets recycled. We made efforts to mutate more histidines in the CTD (i.e. H553A, H565A, H551R, double mutants) however, after months of unsuccessful attempts we transitioned into a separate objective for the remainder of the project.

4.3. The Complexity of Prodomain Mutations: How They Affect PCSK9 Activity

Mutations in the prodomain have heterogeneous effects on PCSK9 activity, making interpretations slightly more challenging. We have identified several key residues in a small surface region of the prodomain that are required for LDL binding, which is novel information in the PCSK9 field. The residues G106, L108 and S127 of the prodomain are predicted to be important for the LDL association of PCSK9, and their proximity on two surface exposed loops is illustrated below in Figure 15. We predict that these residues may play a role in direct interactions with apoB-100, or in other intramolecular interactions perhaps manifested in the PCSK9 protein.

Figure 15. Location of G106, L108 and S127 residues in the PCSK9 prodomain.

Model generated using ROSETTA software by Dr. Ariela Vergara-Jaque with the available crystal structure of PCSK9 at 1.9 Å on PDB – 2QTW (95, 96). The grey helical structure represents a molecular simulation using computational modelling, and the magenta, green, and orange domains represent the prodomain, catalytic, and C-terminal domains of PCSK9, respectively – present in the crystal structure. Three of the prodomain residues important for PCSK9's LDL binding function are highlighted using PyMOL. PCSK9's native residues highlighted are as follows: G106 in yellow, L108 in grey, and S127 in blue. Note the close proximity of these three residues, and their positioning on two juxtaposed helical loops. Importantly, G106R is a LOF mutation that we have observed trends to increase binding to LDL, whereas L108R and S127R are both GOF mutations that decrease and abolish LDL binding affinity, respectively.

4.3.1. L108R Prodomain Mutation Inhibits LDL Binding but Does Not Significantly Affect LDLR Binding Affinity or LDLR Degradation

The L108R mutation was identified in an FH patient with severely high LDL-c levels around 300 mg/dL (53, 72). In that same publication, the authors showed that L108R has a 2-fold higher activity in LDLR degradation *in vitro*, and they reported through predictive modelling that the native Leu might be important in a hydrophobic interaction with L626 in the β-propeller of the LDLR (72). They predicted that the charge of the arginine in L108R might be causing increase in activity towards LDLRs, by shifting this interaction, and instead modulating a salt bridge with Glu605 in the LDLR, thereby increasing the overall affinity.

Through our analysis of LDLR affinity using purified proteins, we determined that L108R does not increase affinity for LDLR *in vitro* (Figure 8C and D), which does not support their predictive modelling (72). However, we tried to replicate their findings for the LDLR degradation activity. We additionally created an alanine mutant (L108A) and measured LDLR degradation with both L108R and L108A. We found that the arginine was important for the 30-40% increase in LDLR degradation (Figure 10D), and that this effect was not seen with L108A. The processing of L108R was also slightly more efficient (Figure 11B) in cells compared to WT PCSK9. However, the major mechanism that seemed to be affected by the L108R mutation was the LDL binding affinity. Using purified proteins, we found that L108R disrupted LDL affinity by 3-fold compared to WT (Figure 8A and B). This is significant in biological terms and it means that L108R might be functioning to cause high LDL-c by disrupting the LDL association and sensing, since the LDLR degradation and PCSK9 processing and secretion were only modestly affected. However, its disruption of

LDL binding compared to R496W for example is not as severe. The effects of the L108R mutation may be ideal to test *in vivo* in the future, as it is associated with one of the more severe disease phenotypes. It is possible that this mutant acts on multiple additive levels by lowering LDL binding affinity several-fold, along with more modest increases in processing and LDLR degradation efficiency.

4.3.2. FH-Associated S127R: Effects on ApoB-100 Secretion, VLDL Production and LDL Association

S127R was the first identified GOF mutation in *PCSK9* associated with FH (7), and patients generally have very high LDL-c ranging between 300-400 mg/dL (53). Many groups have reported findings trying to understand how this mutation causes disease, which has revealed that the mechanisms used are not straightforward, and that S127R seems to regulate multiple complex aspects of PCSK9 function in lipoprotein metabolism. An early kinetic study demonstrated that patients with S127R have 3-fold increases in both apoB-100 secretion and VLDL production when compared to control subjects (100). With our understanding of S127R's LDL binding defect (Figure 13) in the context of LDL binding being inhibitory on PCSK9 activity, it may be that the proportion of S127R PCSK9 in the blood, even if less abundant than WT due to a secretion defect, is actually more active than WT. This increased LDLR degradation could in turn lead to less uptake of lipids/LDL into hepatocytes, which signals for the liver to increase production of VLDL and apoB-100 in a compensating manner. It is possible that S127R's inability to be down regulated or inhibited by LDL binding in the plasma is secondarily causing the increased secretion of apoB-100 and VLDL in humans. However, this is merely speculative and must be tested *in vivo*. We also did not observe a very significant increase in LDLR degradation in cell culture using

S127R (Figure 10D), which supports the hypothesis that the activity levels and mechanisms of S127R would be better understood in an *in vivo* context.

There is a hypothesis that PCSK9 directly interacts with the apoB-100 moiety on LDL; however, the exact locations involved have yet to be shown through chemical cross-linking. Based on previous findings (9, 93, 94), one may have thought that perhaps the S127R variant *directly* increases apoB secretion (100). However, we believe that the increased secretion of apoB-100 seen in patients (100) was due to indirect metabolic effects as mentioned above, since we observe that S127R cannot bind LDL *in vitro* (Figure 13). Furthermore, we observed that S127A and S127P mutations also disrupted LDL binding by fully abolishing it (Figure 13), which means that the native serine has properties, likely related to hydrogen bonding and hydrocarbon chain size, that are crucial for LDL association. In the future, it would be ideal to determine whether S127 is directly involved in binding to apoB-100 through hydrogen bonds, or if it is important for an indirect effect on PCSK9's protein conformation needed when binding to LDL. Further structural studies are required to confirm which scenario is supported.

4.3.3. The S127 Residue in PCSK9's LDLR Degradation and LDLR Affinity

A previous publication showed that the presence of a basic residue at position 127 (S127R and S127K) was required for increased LDLR degradation activity in cell culture (101). Authors found that S127R was 4.3 fold more active in mediating LDLR degradation, as measured by reduction in LDL uptake, which is a much larger effect than what we observed in our conditions (Figure 10D). They also observed an increase in activity with S127K by about 2-fold. We observed that S127A did not confer significant changes in

LDLR degradation or PCSK9 uptake, and that the S127R mutation was required for the 30-40% increase. These authors also observed that S127A did not increase LDLR degradation, which agrees with our findings. An S127D substitution had no effect on degradation activity (101). Adding to this knowledge, we observed that a Pro substitution (S127P) also had no effect on PCSK9 uptake and LDLR degradation (Figure 12). Taken together, our results combined with theirs support the hypothesis that the presence of a long basic side chain at 127 (R127 and K127) is needed for GOF activity in LDLR degradation. This may be manifested through increased hydrogen bonding, or through hydrophobic interactions with the alkyl groups of other residues nearby (Y107, D129) (101); overall stabilizing PCSK9.

In agreement with what we have observed with S127R (Figure 9), Pandit *et al* found that neither Ala, Asp, Arg, Lys, nor Thr substitutions at position 127 significantly affected LDLR affinity (101). However, Cunningham *et al* found that S127R did have increased affinity for LDLR in SPR experiments (56). It is likely that the differences in affinity and discrepancies in the literature are due to variations in the experimental conditions used for measuring affinity. These techniques have differing levels of sensitivity (i.e. SPR > ligand blot), and protein preparations will also inherently vary between batches. It is therefore important to be mindful of these caveats when referring to a relative K_d for various mutants, and it is better to report a range than a single value. Under our conditions using ligand blot competition-binding assays we did not see a difference in affinity for LDLR between S127R and WT PCSK9.

4.3.4. The S127 Residue in PCSK9's Processing and Secretion

PCSK9 maturation involves autoprocessing followed by secretion from cells. Pandit *et al* found that placement of a Lys at 127 conferred a secretion defect (S127K), similarly to S127R and S127A (101). On the other hand, an Asp substitution (S127D) modestly rescued secretion and processing (83%) similar to what we observed with S127P (Figure 11 B and D). It is possible that the hydroxyl groups on serine and aspartic acid are required for secretion and processing, which is why WT and S127D were the only ones with efficient secretion and processing in this previous publication (101). The S127 residue is highly conserved across primates, and it was hypothesized that it may play a role in the recognition of the site for autoprocessing (109). For S127P, the Pro may introduce a tight turn and shift an inter-domain interaction that aligns the protein in such a way that the autoprocessing site is made available, as it would be in WT.

4.3.5. PCSK9's Prodomain and Heparin Sulfate Proteoglycans

It has recently been shown that PCSK9 can bind to HSPGs on the surface of liver cells, aiding as co-receptors in uptake/binding to LDLRs (112). The site on PCSK9 predicted to be required for HSPG binding encompasses an arginine-rich area found between aa 93-139 of the prodomain (112). This is in close proximity to the region where we find the natural FH mutations L108R, S127R and D129G. It is possible that these mutations may enhance binding to HSPGs, and that this may be another mechanism contributing to the GOF phenotypes. However, binding to HSPGs is predicted to be important for LDLR-PCSK9 uptake, so given our findings in this project, we would only expect to see modest effects, since our cell-based assays for L108R and S127R did not show major changes in uptake

(Figure 10 A-B). However, these PCSK9 uptake experiments were done in mouse hepatoma cells, so it would be of interest in the future to test whether human liver cells (i.e. HepG2 or HuH7) incubated with these GOF variants would respond differently and show more significant effects, perhaps by using Heparinase I treatment as a control in the experiment.

Furthermore, in another publication, it was determined that heparin-like molecules (HLMs) can interact with PCSK9 or LDL to mediate the inhibitory effect that PCSK9-LDL association has on LDLR degradation (113). In their model, they propose that PCSK9's HLM association would increase activity towards LDLR and decrease its association with LDL. In this same paper, the S127R mutation was found to increase binding affinity to HLMs, which may be due to the positively charged Arg having enhanced affinity for the negatively charged proteoglycans (113). We found that S127R does not bind to LDL, so it is possible that in addition to this lack of down-regulation through LDL binding in the plasma, its increased association with HLMs/HSPGs also has a negative effect on LDL association, and overall leads to a larger pool of active PCSK9 in the blood.

Taken together, these prodomain mutations affect multiple complex aspects of PCSK9 function. We have observed that LDL binding and PCSK9 processing and secretion are the major functions affected by substitutions at position S127. This is in opposition to the GOF mutations we observed in the CTD (R469W, R496W, and F515L), which seemed to only affect LDL association. Furthermore, we have found that L108R and S127R GOF mutations in the prodomain inhibit LDL binding, similarly to the natural GOF mutant D129G (unpublished data). We conclude that residues L108, S127 and D129 are very important for PCSK9's association with LDL *in vitro*.

4.4. G106R PCSK9: Assessing LDL Binding for a Prodomain LOF Variant

The understanding of LOF mechanisms contributing to lowered PCSK9 activity represents another approach to PCSK9 inhibition. G106R PCSK9 was characterized as a natural LOF variant associated with LDL-c of ≈ 70-100 mg/dL, and was said to segregate with lower plasma LDL in a family study (83). This however, is only a modest decrease in LDL-c. Authors from another group showed that G106R is defectively processed and is not secreted from cells (85). However, under our conditions we see that it is secreted, but with ≈ 50% lower efficiency when compared to WT (data not shown). These authors also found that G106R lowers PCSK9's LDLR degradation activity (85). The literature however did not contain any findings about this mutation's effect on LDL binding. To this end, we were able to obtain enough G106R protein through concentrated conditioned medium to do a qualitative test on LDL binding, and we determined that there is a trend towards an increase in LDL binding by ≈ 50-60% compared to WT (Figure 14).

Although LDL association is increased with this LOF variant, we believe that G106R's secretion defect is the primary mechanism causing LOF activity in PCSK9. We were unable to express and purify G106R on a large scale for LDL affinity experiments due to the secretion defect. Furthermore, it is possible that the integrity and stability of G106R PCSK9 is lower than WT PCSK9, especially in non-native buffer conditions, which makes protein purification very difficult. This may be why we could only use G106R in the form of conditioned medium and could not get any protein through affinity chromatography/gel filtration experiments. Our LDL binding analysis of G106R should therefore be interpreted with these caveats in mind, where a quantitative measure of affinity for LDL could not be

obtained, as the competition-binding experiments require larger amounts of protein that must be purified.

4.5. Conclusions and Proposed Model for Physiological Relevance of PCSK9's Interaction with LDL

Thus far, the residues in PCSK9 that we have confidently determined to play a role in LDL binding include L108, S127, D129, R469, R496 and F515. These amino acids are found in the prodomain and CTD of PCSK9, meaning that it may be possible for these two areas to be mediating the binding interaction with LDL, without affecting LDLR affinity in the catalytic domain (87). Importantly, multiple natural disease mutations in these two regions have shown to negatively affect LDL association *in vitro* with no effect on LDLR binding. Linking *PCSK9* genotypes to known LDL-c phenotypes from patients gives us a basis for understanding the potential physiological relevance of this interaction. Studying GOF mutations allows us to observe more robust effects than what we would observe with LOF variants. We predict that these residues studied in the prodomain and CTD are either a) involved in a direct interaction with apoB-100 on LDL, or b) involved in intramolecular interactions required for locking the auto-inhibited conformation of PCSK9 in the presence of LDL. However, these predictions must be validated through structural studies, potentially by cryogenic electron microscopy.

The general trend for the two prodomain FH mutations studied in this project seems to follow the premise that introducing a charged arginine in this region confers a GOF phenotype through inhibition of LDL binding (L108R, S127R). However, this opposes what is observed with G106R, which is a LOF variant in this same region (Figure 15). In Figure 13, one can observe the importance of the native S127 residue in LDL binding, as it was not

the positive Arg that conferred this GOF effect, yet it was the loss of the Ser, because S127A and S127P also abolished LDL binding. Therefore, any such correlations must be carefully interpreted. In the CTD, switching from basic to very hydrophobic and bulky side chains (i.e. R469W, R496W) conferred LDL binding defects, implying that the charges and side chain sizes in this area are important for proper LDL association. The extent of amino acid changes in terms of their chemical properties is an important factor to keep in mind when predicting the possible nature of these interactions, and the magnitude of their effects on PCSK9's LDL association. There is however, a correlation between the extent of LDL inhibition (i.e. abolishment of binding) and the patient levels of plasma cholesterol in carriers of these GOF mutations (i.e. very high LDL-c with S127R and R496W) (53).

Many natural and artificial PCSK9 mutations are summarized in Table 4.1 along with their consequences on various aspects of PCSK9 activity. The mechanisms used by GOF variants to cause a disease phenotype are very heterogeneous, and it is difficult to generalize even one or two mechanisms that are consistently displayed across all mutations. This heterogeneity highlights the complexity with which various *PCSK9* mutations function in order to ultimately regulate circulating LDL-c and in turn, affect the risk of CVD. Findings on the functional mechanisms of known *PCSK9* mutations were eloquently summarized in a review in 2017 (114).

Taken together, we propose that PCSK9 may lock into its auto-inhibited conformation upon binding to LDL, which overall dampens its ability to mediate LDLR degradation, perhaps through modifying the catalytic domain's affinity for the EGF-A domain. There likely exist active and inactive pools of PCSK9 in the plasma. In healthy individuals, there might be a steady-state equilibrium, where LDL-bound PCSK9 will

Table 4. 1 General qualitative trends of the effects of PCSK9 mutations on functional activity *in vitro*.

Data gathered during this project[1], data that is published[2], data that is not shown but was done in our group[3].

Mutation	*LDLR binding*	*LDL binding*	*LDLR degradation*	*Secretion*	*Processing*
GOF					
L108R[1]	Normal	Inhibited	Increased	Normal	Increased
S127R[1]	Normal	Abolished	Increased	Defective	Defective
D129G[3]	N/A	Abolished	N/A	Defective	Defective
D374Y[2,3]	Increased	Normal	Increased	Normal	Normal
R469W[1,2]	Normal	Inhibited	N/A	Normal	Normal
R496W[1,2]	Normal	Abolished	Normal	Normal	Normal
R496Q[1,2]	Normal	Inhibited	Normal	Normal	Normal
N513D[3]	Normal	Abolished	Normal	Normal	Normal
F515L[1,2]	Normal	Inhibited	N/A	Normal	Normal
H553R[1]	Increased	Normal	N/A	Normal	Normal
LOF					
G106R[1,2]	N/A	Increased	Defective	Defective	Defective
Artificial					
E39A[1]	N/A	Normal	N/A	Normal	Normal
E39P[1]	N/A	Abolished	N/A	Normal	Normal
L108A[1,3]	Normal	Inhibited	Normal	Normal	Normal
S127A[1]	Normal	Abolished	Normal	Defective	Defective
S127P[1]	Normal	Abolished	Normal	Normal	Normal
H565R[1]	Normal	N/A	N/A	Normal	Normal

<u>*Sources of published data:*</u>

D374Y (56)
R496Q, G106R (85)
R469W, R496W, F515L (95)

negatively feed back onto the LDLR degradation pathway when LDL levels increase in the plasma. PCSK9 might be able to sense levels of extracellular cholesterol through binding to LDL, and the purpose of this could be to dampen LDLR degradation activity to prevent further accumulation of plasma LDL. Thus, PCSK9 might play a role as a sensor of LDL buildup and might be cleared as a passive component of LDL through the LDL-LDLR interaction in such conditions (Figure 16). In some patients who have hypercholesterolemia attributable to GOF mutations in *PCSK9*, this regulatory mechanism might be defective, and there could be a shift in the equilibrium towards a larger pool of free plasma PCSK9. Our data supports that some natural *PCSK9* GOF mutations (found in regions crucial for LDL association) inhibit LDL binding, which might increase the pool of active PCSK9 available in the plasma, thereby failing to negatively feed back onto LDLR degradation activity, and ultimately leading to a high LDL-c phenotype.

4.6 Future Directions

To confirm the predicted physiological relevance of our LDL hypothesis *in vivo*, we plan to create adeno-associated viruses expressing *PCSK9* constructs for the variants that we have found to abolish LDL binding, with no effect on LDLR binding *in vitro* (A44P, S127R and R496W). These will be expressed in apoB-100/CETP transgenic mice, which have a human-like lipoprotein profile. The LDL-associated PCSK9 will be measured along with LDLR levels in the liver. If our hypothesis holds true, we expect LDL-bound PCSK9 to be in a low proportion, and for LDLR levels to be low due to a higher proportion of active/free PCSK9 in their plasma. In contrast, we expect this GOF effect would be blunted in control C57Bl/6 mice that have very low LDL levels. The S127R and R496W variants are associated with very high LDL-c in humans (53), and we have observed abolishment of LDL

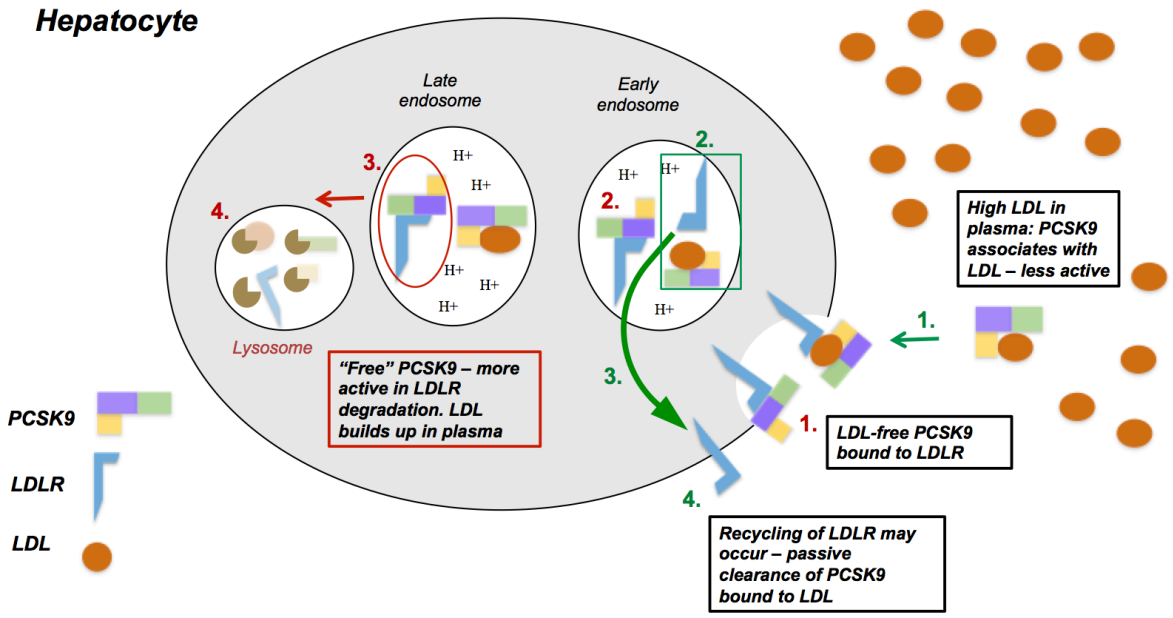

Figure 16. Proposed model for PCSK9's interaction with LDL negatively feeding back on the LDLR degradation function.

1-4 (Red sequence): PCSK9 normally decreases the level of cell surface LDLRs, which leads to less uptake of LDL from the plasma. 1. Free PCSK9 binds to LDLR at the cell surface and together they are internalized into endosomes. 2. PCSK9 and LDLR associate more tightly as the pH decreases in the endosomal system. 3. PCSK9 is unable to dissociate from LDLR, so the complex is shuttled towards lysosomes. 4. PCSK9 and LDLR are both degraded in lysosomes. **1-4 (Green sequence):** Eventually, the build-up of LDL may lead to a higher proportion of LDL-bound (inhibited) PCSK9 in the plasma, thereby negatively feeding back on the initial pathway of cell surface LDLR degradation. 1. LDL and PCSK9 are bound, and LDL will interact with LDLR in the presence of PCSK9. 2. LDL and LDLR are able to dissociate and PCSK9 is still associated with LDL. 3. Recycling of the LDLR, and passive clearance of PCSK9 as a component of LDL (stays in endosomal pathway). 4. LDLR is recycled to the cell surface.

binding for both, perhaps meaning that these variants lack the ability to act as LDL sensors. Our PCSK9-LDL hypothesis will be tested in these mouse models of dyslipidemia.

We also plan to use chemical cross-linking to map the apoB-100 binding site on PCSK9, which will potentially help with the development of novel PCSK9 inhibitors. The goal would be to identify which residues are directly binding to apoB-100, and to exploit this information in order to create a small molecule that could induce plasma PCSK9 to be in a less-active form (i.e. to enhance the inhibitory effect of LDL association). This project has characterized a **third critical region** in PCSK9's prodomain that is important in LDL binding. This region encompasses residues G106, L108, and S127. We have also provided novel evidence for the molecular mechanisms by which natural *PCSK9* mutations affect protein function. We characterized LDLR degradation, LDLR binding, LDL binding, and PCSK9 processing and secretion. These findings add critical information to the PCSK9 field, and allow us to better link known patient genotypes and lipid phenotypes to the highly complex structure-function relationship in PCSK9.

5. References

1. Global Health Estimates 2016: Deaths by Cause, Age, Sex, by Country and by Region, 2000-2016. Geneva, World Health Organization; 2018. Accessed on February 19th 2020 https://www.who.int/news-room/fact-sheets/detail/the-top-10-causes-of-death

2. Law, M. R., Wald, N. J., and Rudnicka, A. R. 2003. Quantifying effect of statins on low density lipoprotein cholesterol, ischaemic heart disease, and stroke: systematic review and meta-analysis. *BMJ (Clinical research ed.)*. 326:1423-1427.

3. Goldstein, J.L. and M.S. Brown. 2009. History of Discovery: The LDL Receptor. *Arterioscler. Thromb. Vasc. Biol.* 29:431–438.

4. Horton, J. D., Cohen, J. C., Hobbs, H. H. 2009. PCSK9. A convertase that coordinates LDL catabolism. *J. Lipid Res.* 50:S172–S177.

5. Seidah, N. G. 2009. PCSK9 as a therapeutic target of dyslipidemia. *Expert Opin. Ther. Targets.* 13:19–28.

6. Seidah, N. G., Benjannet, S., Wickham, L., Marcinkiewicz, J., Jasmin, S. B., Stifani, S., Basak, A., Prat, A., Chretien, M. 2003. The secretory proprotein convertase neural apoptosis-regulated convertase 1 (NARC-1). Liver regeneration and neuronal differentiation. *Proc. Natl. Acad. Sci. U.S.A.* 100:928–933.

7. Abifadel, M., Varret, M., Rabès, J. P., Allard, D., Ouguerram, K., Devillers, M., Cruaud, C., Benjannet, S., Wickham, L., Erlich, D., Derré, A., Villéger, L., Farnier, M., Beucler, I., Bruckert, E., Chambaz, J., Chanu, B., Lecerf, J. M., Luc, G., Moulin, P., Weissenbach, J., Prat, A., Krempf, M., Junien, C., Seidah, N. G., Boileau, C. 2003. Mutations in PCSK9 cause autosomal dominant hypercholesterolemia. *Nat. Genet.* 34:154–156.

8. Rashid, H., Meredith, I.T., Nasis, A. 2017. PCSK9 Monoclonal Antibodies in 2016: Current Status and Future Challenges. *Heart Lung and Circ.* 26:786-798.

9. Kosenko, T., Golder, M., Leblond, G., Weng, W., Lagace, T.A. 2013. Low density lipoprotein binds to proprotein convertase subtilisin/kexin type-9 (PCSK9) in human plasma and inhibits PCSK9-mediated low density lipoprotein receptor degradation. *J. Biol. Chem.* 288:8279–8288.

10. Wang, H.H., Garruti, G., Liu, M., Portincasa, P., Wang, D. Q.-H. 2017. Cholesterol and Lipoprotein Metabolism and Atherosclerosis: Recent Advances in Reverse Cholesterol Transport. *Annals of Hepatology.* 16:s28-s42.

11. Voet, D. and Voet J. G. 2004. Biochemistry. 3rd ed. United States of America: Wiley.

12. Sharpe, L. J. and A. J. Brown 2013. Controlling cholesterol synthesis beyond 3-hydroxy-3-methylglutaryl-CoA reductase (HMGCR). *J. Biol. Chem.* 28:18707-18715.

13. Brown, M.S. and J.L. Goldstein 1997. The SREBP pathway: Regulation of cholesterol metabolism by proteolysis of a membrane-bound transcription factor. *Cell.* 89:331 – 340.

14. Hua, X., Wu, J., Goldstein, J.L., Brown, M.S., Hobbs, H.H. 1995. Structure of the human gene encoding sterol regulatory element binding protein-1 (SREBF1) and localization of SREBF1 and SREBF2 to chromosomes 17p11.2 and 22q13. *Genomics.* 25:667–673.

15. Pai, J.T., Guryev, O., Brown, M.S., Goldstein, J.L. 1998. Differential stimulation of cholesterol and unsaturated fatty acid biosynthesis in cells expressing individual nuclear sterol regulatory element-binding proteins. *J. Biol. Chem.* 273:26138 – 26148.

16. Horton, J.D., Shah, N.A., Warrington, J.A., Anderson, N.N., Park, S.W., Brown, M.S., Goldstein, J.L. 2003. Combined analysis of oligonucleotide microarray data from transgenic and knockout mice identifies direct SREBP target genes. *Proc. Natl. Acad. Sci. U.S.A.* 100:12027–12032.

17. Horton, J.D., Goldstein, J.L., Brown, M.S. 2002. SREBPs: activators of the complete program of cholesterol and fatty acid synthesis in the liver. *J. Clin. Invest.* 109: 1125-1131.

18. Jeong, H. J., Lee, H-S., Kim, K-S., Kim, Y-K., Yoon, D., Park, S W. 2007. Sterol-dependent regulation of proprotein convertase subtilisin/kexin type 9 expression by sterol-regulatory element binding protein-2. *J. Lipid. Res.* 49: 399-409.

19. Lagace, T.A. 2014. PCSK9 and LDLR degradation: regulatory mechanisms in circulation and in cells. *Curr. Opin. Lipid*. 25.

20. Ye, J. and R.A. DeBose-Boyd. 2011. Regulation of Cholesterol and Fatty Acid Synthesis. *Cold Spring Harb. Perspect. Biol.* 3:a004754.

21. Sun, L.P., Li, L., Goldstein, J.L., Brown, M.S. 2005. Insig required for sterol-mediated inhibition of Scap/SREBP binding to COPII proteins in vitro. *J. Biol. Chem.* 280:26483–26490.

22. Radhakrishnan, A., Sun, L.P., Kwon, H.J., Brown, M.S., Goldstein, J.L. 2004. Direct binding of cholesterol to the purified membrane region of SCAP; mechanism for a sterol-sensing domain 1. *Mol. Cell.* 15:259–268.

23. Radhakrishnan, A., Goldstein, J.L., McDonald, J.G., Brown, M.S. 2008. Switch-like control of SREBP-2 transport triggered by small changes in ER cholesterol: A delicate balance. *Cell Metab.* 8:512–521.

24. Yabe, D., Brown, M.S., Goldstein, J.L. 2002. Insig-2, a second endoplasmic reticulum protein that binds SCAP and blocks export of sterol regulatory element-binding proteins. *Proc. Natl Acad. Sci. U.S.A.* 99:12753–12758.

25. Yang, T., Espenshade, P.J., Wright, M.E., Yabe, D., Gong, Y., Aebersold, R., Goldstein, J.L., Brown, M.S. 2002. Crucial step in cholesterol homeostasis: Sterols promote binding of SCAP to INSIG-1, a membrane protein that facilitates retention of SREBPs in ER. *Cell.* 110:489–500.

26. Rader, D.J. and S. Kathiresan. 2018. Chapter 3: Lipoprotein Disorders. *Genomic and Precision Medicine.* 3rd ed. Pages 27-46.

27. Segrest J. P., Garber D.W., Brouillette C. G., Harvey S. C., Anantharamaiah G. M. 1994. The amphipathic alpha helix: a multifunctional structural motif in plasma apolipoproteins. *Adv. Protein Chem.* 45:303-369.

28. Mahley R.W., Innerarity T. L., Rall S. C., Jr., Weisgraber K. H. 1984. Plasma lipoproteins: apolipoprotein structure and function. *J. Lipid Res.* 25:1277-1294.

29. Chan L., Chang B. H., Nakamuta M., Li W. H., Smith L. C. 1997. Apobec-1 and apolipoprotein B mRNA editing. *Biochem. Biophys. Acta.* 1345:11-26.

30. Boren J., Lee I., Zhu W., Arnold K., Taylor S., Innerarity T.L. Identification of the low density lipoprotein receptor-binding site in apolipoprotein B100 and the modulation of its binding activity by the carboxyl terminus in familial defective apo-B100. 1998. *J. Clin. Invest.* 101:1084-1093.

31. Mahley R.W. 1988. Apolipoprotein E: cholesterol transport protein with expanding role in cell biology. *Science.* 240:622-630.

32. Mead, J.R., Irvine, S.A. & Ramji, D.P. 2002. Lipoprotein lipase: structure, function, regulation, and role in disease. *J. Mol. Med*. 80:753–769.

33. Mahley, R. W., Ji, Z. S. 1999. Remnant lipoprotein metabolism: key pathways involving cell-surface heparan sulfate proteoglycans and apolipoprotein E. *J. Lipid Res.* 40:1-16.

34. Frazier-Wood, A. C., Kabagambe, E. K., Wojczynski, M. K., Borecki, I. B., Tiwari, H. K., Smith, C. E., Ordovas, J. M., & Arnett, D. K. 2013. The association between LRP-1 variants and chylomicron uptake after a high fat meal. *Nutrition, metabolism, and cardiovascular diseases.* 23:1154–1158.

35. Toth, P.P. 2003. Reverse cholesterol transport: high-density lipoprotein's magnificent mile. *Curr. Atheroscler. Rep.* 5:386–393.

36. Swenson T. L., Brocia R. W., Tall A. R. 1988. Cholesteryl ester transfer protein has binding sites for neutral lipids and phospholipids. *J. Biol. Chem.* 263:5150-5157.

37. Beisiegel U., Weber W., Ihrke G., Herz J., Stanley K. K. 1989. The LDL-receptor-related protein, LRP, is an apolipoprotein E-binding protein. *Nature.* 341:162–164.

38. Stanford, K. I., Bishop, J. R., Foley, E. M., Gonzales, J. C., Niesman, I. R., Witztum, J. L., Esko, J. D. 2009. Syndecan-1 is the primary heparan sulfate proteoglycan mediating hepatic clearance of triglyceride-rich lipoproteins in mice. *J. Clin. Invest*. 119:3236–3245.

39. Havel, R.S., Eder, H.A., Bragdon, J.H. 1955. The distribution and chemical composition of ultracentrifugally separated lipoproteins in human serum. *J. Clin. Invest.* 34:1345–1353.

40. Rajman, I., Eacho, P.I., Chowienczyk, P.J., Ritter, J.M. 1999. LDL particle size: an important drug target? *Br. J. Clin. Pharmacol.* 48:125–133.

41. Shelness, G.S., Hou, L., Ledford, A.S., Parks, J.S., Weinberg, R.B. 2003. Identification of the Lipoprotein Initiating Binding Domain of Apolipoprotein B. *J. Biol. Chem.* 278:44702-44707.

42. Goldstein, J. L., Ho, Y. K., Basu, S. K., and Brown, M. S. 1979. Binding site on macrophages that mediates uptake and degradation of acetylated low density lipoprotein, producing massive cholesterol deposition. *Proc. Natl. Acad. Sci. U. S. A.* 76:333-337.

43. Michaely, P., Li, W.P., Anderson, R.G., Cohen, J.C., Hobbs, H.H. 2004. The modular adaptor protein ARH is required for low density lipoprotein (LDL) binding and internalization but not for LDL receptor clustering in coated pits. *J. Biol. Chem.* 279:34023-34031.

44. Hobbs, H. H., Brown, M. S., Goldstein, J. L. 1992. Molecular genetics of the LDL receptor gene in familial hypercholesterolemia. *Hum. Mutat.* 1:445–466.

45. Goldstein J.L. and M.S. Brown 1984. Progress in understanding the LDL receptor and HMG-CoA reductase, two membrane proteins that regulate plasma cholesterol. *J. Lipid Res*. 25:1450 – 1461.

46. Lusis, A. J. 2000. Atherosclerosis. *Nature.* 407:233-241.

47. Libby, P., Buring, J.E., Badimon, L. Hansson G.K., Deanfield J., Bittencourt M. S., Tokgözoğlu L., Lewis E.F. 2019. Atherosclerosis. *Nat. Rev. Dis. Primers.* 5:56.

48. Innerarity, T. L., Mahley, R. W., Weisgraber, K. H., Bersot, T. P., Krauss, R. M., Vega, G. L., Grundy, S. M., Friedl, W., Davignon, J., McCarthy, B. J. 1990. Familial defective apolipoprotein B-100. A mutation of apolipoprotein B that causes hypercholesterolemia. *J. Lipid Res.* 31:1337–1349.

49. Abifadel, M., Rabès, J. P., Devillers, M., Munnich, A., Erlich, D., Junien, C., Varret, M., Boileau, C. 2009. Mutations and polymorphisms in the proprotein convertase subtilisin kexin 9 (PCSK9) gene in cholesterol metabolism and disease. *Hum. Mutat.* 30:520–529.

50. Madison B.B. 2016. Srebp2: A master regulator of sterol and fatty acid synthesis. *J. Lipid Res.* 57:333–335.

51. Ramkumar, S., Raghunath, A., Raghunath, S. 2016. Statin Therapy: Review of Safety and Potential Side Effects. *Acta. Cardiol. Sin.* 32:631-639.

52. Reiner, Z., Catapano, A.L., De Backer, G., Graham, I., Taskinen, M-R., Wiklund, O., Agewall, S., Alegria E., Chapman, M.J., Durrington, P., Erdine, S., Halcox, J., Hobbs, R., Kjekshus, J., Filardi, P.P., Riccardi, G.,. Storey, R.F., Wood, D. ESC/EAS Guidelines for the management of dyslipidaemias: The Task Force for the management of dyslipidaemias of the European Society of Cardiology (ESC) and the European Atherosclerosis Society (EAS). 2011. *European Heart Journal.* 32:1769–1818.

53. Hopkins, P. N., Defesche, J., Fouchier, S. W., Bruckert, E., Luc, G., Cariou, B., Sjouke, B., Leren, T. P., Harada-Shiba, M., Mabuchi, H., Rabes, J. P., Carrie, A., van Heyningen, C., Carreau, V., Farnier, M., Teoh, Y. P., Bourbon, M., Kawashiri, M. A., Nohara, A., Soran,

H., Marais, A. D., Tada, H., Abifadel, M., Boileau, C., Chanu, B., Katsuda, S., Kishimoto, I., Lambert, G., Makino, H., Miyamoto, Y., Pichelin, M., Yagi, K., Yamagishi, M., Zair, Y., Mellis, S., Yancopoulos, G. D., Stahl, N., Mendoza, J., Du, Y., Hamon, S., Krempf, M., and Swergold, G. D. 2015. Characterization of Autosomal Dominant Hypercholesterolemia Caused by PCSK9 Gain of Function Mutations and Its Specific Treatment With Alirocumab, a PCSK9 Monoclonal Antibody. *Circ. Cardiovasc. Genet.* 8:823- 831.

54. Benjannet, S., Rhainds, D., Essalmani, R., Mayne, J., Wickham, L., Jin, W., Asselin, M. C., Hamelin, J., Varret, M., Allard, D., Trillard, M., Abifadel, M., Tebon, A., Attie, A. D., Rader, D. J., Boileau, C., Brissette, L., Chrétien, M., Prat, A., Seidah, N. G. 2004. NARC-1/PCSK9 and its natural mutants. Zymogen cleavage and effects on the low density lipoprotein (LDL) receptor and LDL cholesterol. *J. Biol. Chem.* 279:48865–48875.

55. Naureckiene, S., Ma, L., Sreekumar, K., Purandare, U., Lo, C. F., Huang, Y., Chiang, L. W., Grenier, J. M., Ozenberger, B. A., Jacobsen, J. S., Kennedy, J. D., DiStefano, P. S., Wood, A., Bingham, B. 2003. Functional characterization of Narc 1, a novel proteinase related to proteinase K. *Arch. Biochem. Biophys.* 420:55–67.

56. Cunningham, D., Danley, D. E., Geoghegan, K. F., Griffor, M. C., Hawkins, J. L., Subashi, T. A., Varghese, A. H., Ammirati, M. J., Culp, J. S., Hoth, L. R., Mansour, M. N., McGrath, K. M., Seddon, A. P., Shenolikar, S., Stutzman-Engwall, K. J., Warren, L. C., Xia, D., Qiu, X. 2007. Structural and biophysical studies of PCSK9 and its mutants linked to familial hypercholesterolemia. *Nat. Struct. Mol. Biol.* 14:413–419.

57. Piper, D. E., Jackson, S., Liu, Q., Romanow, W. G., Shetterly, S., Thibault, S. T., Shan, B., Walker, N. P. 2007. The crystal structure of PCSK9. A regulator of plasma LDL-cholesterol. *Structure* 15:545–552.

58. Dewpura, T., Raymond, A., Hamelin, J., Seidah, N.G., Mbikay, M., Chretien, M., Mayne, J. 2008. PCSK9 is phosphorylated by a golgi casein kinase-like kinase ex vivo and circulates as a phosphoprotein in humans. *FEBS J.* 275:3480-3493.

59. Benjannet, S., Rhainds, D., Hamelin, J., Nassoury, N., Seidah, N.J. 2006. The Proprotein convertase (PCS) PCSK9 Is Inactivated by Furin and/or PC5/6A. *J. Biol. Chem.* 281:30561-30572.

60. Grefhorst, A., McNutt, M. C., Lagace, T. A., Horton J. D. 2008. Plasma PCSK9 preferentially reduces liver LDL receptors in mice. *J. Lipid Res.* 49:1303–1311.

61. McNutt, M. C., Lagace, T. A., Horton, J. D. 2007. Catalytic activity is not required for secreted PCSK9 to reduce low density lipoprotein receptors in HepG2 cells. *J. Biol. Chem*. 282:20799–20803.

62. Poirier, S., Mayer, G., Poupon, V., McPherson, P. S., Desjardins, R., Ly, K., Asselin, M-C., Day, R., Duclos, F. J., Witmer, M., Parker, R., Prat, A., Seidah, N. G. 2009. Dissection of the endogenous cellular pathways of PCSK9-induced low density lipoprotein receptor degradation: evidence for an intracellular route. *J Biol. Chem.* 284:28856–28864.

63. Lakoski, S. G., Lagace, T. A., Cohen, J. C., Horton, J. D., Hobbs, H. H. 2009. Genetic and metabolic determinants of plasma PCSK9 levels. *J. Clin. Endocrinol. Metab.* 94:2537–2543.

64. Mayne, J., Raymond, A., Chaplin, A., Cousins, M., Kaefer, N., Gyamera-Acheampong, C., Seidah, N. G., Mbikay, M., Chrétien, M., Ooi, T. C. 2007. Plasma PCSK9 levels correlate with cholesterol in men but not in women. *Biochem. Biophys. Res. Commun.* 361:451–456.

65. Welder, G., Zineh, I., Pacanowski, M. A., Troutt, J. S., Cao, G., Konrad, R. J. 2010. High-dose atorvastatin causes a rapid sustained increase in human serum PCSK9 and disrupts its correlation with LDL cholesterol. *J. Lipid Res.* 51:2714–2721.

66. Lambert, G., Ancellin, N., Charlton, F., Comas, D., Pilot, J., Keech, A., Patel, S., Sullivan, D. R., Cohn, J. S., Rye, K.-A., Barter, P. J. 2008. Plasma PCSK9 concentrations correlate with LDL and total cholesterol in diabetic patients and are decreased by fenofibrate treatment. *Clin. Chem.* 54:1038–1045.

67. Browning, J.D. and J.D. Horton 2010. Fasting reduces plasma proprotein convertase, subtilisin/kexin type 9, and cholesterol biosynthesis in humans. *J. Lipid Res.* 51:3359–3363.

68. Dong, B., Wu, M., Li, H., Kraemer, F. B., Adeli, K., Seidah, N. G., Park, S.W., Liu, J. 2010. Strong induction of PCSK9 gene expression through HNF1alpha and SREBP2: mechanism for the resistance to LDL-cholesterol lowering effect of statins in dyslipidemic hamsters. *J Lipid Res.* 51:1486-1495.

69. Dubuc, G. Chamberland, A., Wassef, H., Davignon, J., Seidah, N.G., Bernier, L., Prat, A. 2004. Statins Upregulate PCSK9, the Gene Encoding the Proprotein Convertase Neural Apoptosis-Regulated Convertase-1 Implicated in Familial Hypercholesterolemia. *Atherosclerosis.* 24:1454-1459.

70. Li, H., Dong, B., Lee, H. S., Chen, W., Liu, J. 2009. Hepatocyte nuclear factor 1alpha plays a critical role in PCSK9 gene transcription and regulation by the natural hypocholesterolemic compound berberine. *J. Biol. Chem.* 284: 28885-28895.

71. Shende, V. R., Wu, M., Singh, A. B., Dong, B., Kan, C. F. K., Liu, J. 2015. Reduction of circulating PCSK9 and LDL-C levels by liver-specific knockdown of HNF1α in normolipidemic mice. *J. Lipid Res.* 56:801-809.

72.Abifadel, M., Guerin, M., Benjannet, S., Rabès, J.P., LeGoff, W., Julia, Z., Hamelin, J., C arreau, V., Varret, M., Bruckert, E., Tosolini, L., Meilhac, O., Couvert, P., Bonnefont-Rousselot, D., Chapman, J., Carrié, A., Michel, J. B., Prat, A., Seidah, N. G., and Boileau, C. 2012. Identification and characterization of new gain-of-function mutations in the PCSK9 gene responsible for autosomal dominant hypercholesterolemia. *Atherosclerosis.* 223:394–400.

73. Homer, V.M., Marais, A.D., Charlton, F., Laurie, A.D., Hurndell, N., Scott, R., Mangili, F., Sullivan, D.R., Barter, P.J., Rye, K.A., George, P.M., Lambert, G. 2008. Identification and characterization of two non-secreted PCSK9 mutants associate with familial

hypercholesterolemia in cohorts from New Zealand and South Africa. *Atherosclerosis.* 196:659-666.

74. Leren T.P. 2004. Mutations in the PCSK9 gene in Norwegian subjects with autosomal dominant hypercholesterolemia. *Clin. Genet.* 65:419-422.

75. Allard, D., Amsellem, S., Abifadel, M., Trillard, M., Devillers, M., Luc, G., Kremf, M., Reznik, Y., Girardet, J.P., Fredenrich, A. Junien C., Varret M., Boileau C., Benlian P., Rabès J-P. 2005. Novel mutations of the PCSK9 gene cause variable phenotype of autosomal dominant hypercholesterolemia. *Hum. Mutat.* 26:497.

76. Pisciotta, L., Oliva, C.P., Cefalu, A.B., Noto, D., Bellocchio, A., Fresa, R., Cantafora, A., Patel, D., Averna, M., Tarugi, P., Calandra, S., Bertolini, S. 2005. Additive effect of mutations in LDLR and PCSK9 genes on the phenotype of familial hypercholesterolemia. *Atherosclerosis.* 186:433-440.

77. Chorba, J.S., Galvan, A.M., Shokat, K.M. 2018. Stepwise processing analyses of the single-turnover PCSK9 protease reveal its substrate sequence specificity and link clinical genotype to lipid phenotype. *J. Biol. Chem.* 293:1875-1886.

78. Kotowski, I.K., Pertsemlidis, A., Luke, A., Cooper, R.S., Vega, G.L., Cohen, J.C., Hobbs, H.H. 2006. A spectrum of PCSK9 alleles contributes to plasma levels of low-density lipoprotein cholesterol. *Am. J. Hum. Genet*. 78:410–422.

79. Cohen, J., Pertsemlidis, A., Kotowski, I. K., Graham, R., Garcia, C. K., Hobbs, H. H. 2005. Low LDL cholesterol in individuals of African descent resulting from frequent nonsense mutations in PCSK9. *Nat. Genet*. 37:161–165.

80. Cohen, J. C., Boerwinkle, E., Mosley, T. H., Jr., Hobbs, H. H. 2006. Sequence variations in PCSK9, low LDL, and protection against coronary heart disease. *N. Engl. J. Med.* 354:1264–1272.

81. Zhao, Z., Tuakli-Wosornu, Y., Lagace, T.A., Kinch, L., Grishin, N.V., Horton, J. D., Cohen, J.C., Hobbs, H.H. 2006. Molecular characterization of loss-of-function mutations in PCSK9 and identification of a compound heterozygote. *Am. J. Hum. Genet.* 79:514–523.

82. Humphries, S.E., Neely, R.D., Whittall, R.A., Troutt, J.S., Konrad, R.J., Scartezini, M., Li, K.W., Cooper, J.A., Acharya, J., Neil, A. 2009. Healthy individuals carrying the PCSK9 p.R46L variant and familial hypercholesterolemia patients carrying PCSK9 p.D374Y exhibit lower plasma concentrations of PCSK9. *Clin. Chem.* 55:2153-2161.

83. Berge, K. E., Ose, L., Leren, T. P. 2006. Missense Mutations in the PCSK9 Gene Are Associated With Hypocholesterolemia and Possibly Increased Response to Statin Therapy. *Atheroscler. Throm. Vasc. Biol.* 26:1094-1100.

84. Sun, X.M., Eden, E.R., Tosi, I., Neuwirth, C.K., Wile, D., Naoumova, R.P., Soutar, A.K. 2005. Evidence for effect of mutant PCSK9 on apolipoprotein B secretion as the cause of unusually severe dominant hypercholesterolemia. *Hum. Mol. Genet.* 14:1161–1169.

85. Cameron, J., Holla, O.L., Ranheim, T., Kulseth, M.A., Berge, K.E., Leren, T.P. 2006. Effect of mutations in the PCSK9 gene on the cell surface LDL receptors. *Hum Mol Genet.*

15:1551-1558.

86. Zhang, D.-W., Lagace, T. A., Garuti, R., Zhao, Z., McDonald, M., Horton, J. D., Cohen, J. C., Hobbs, H. H. 2007. Binding of proprotein convertase subtilisin/kexin type 9 to epidermal growth factor-like repeat A of low density lipoprotein receptor decreases receptor recycling and increases degradation. *J. Biol. Chem.* 282:18602–18612.

87. Kwon, H. J., Lagace, T. A., McNutt, M. C., Horton, J. D., Deisenhofer, J. 2008. Molecular basis for LDL receptor recognition by PCSK9. *Proc. Natl. Acad. Sci. U.S.A.* 105:1820–1825.

88. Fisher, T. S., Lo Surdo, P., Pandit, S., Mattu, M., Santoro, J. C., Wisniewski, D., Cummings, R. T., Calzetta, A., Cubbon, R. M., Fischer, P. A., Tarachandani, A., De Francesco, R., Wright, S. D., Sparrow, C. P., Carfi, A., Sitlani, A. 2007. Effects of pH and low density lipoprotein (LDL) on PCSK9-dependent LDL receptor regulation. *J. Biol. Chem.* 282: 20502–20512.

89. Nguyen, M.-A., Kosenko, T., Lagace, T.A. 2014. Internalized PCSK9 dissociates from recycling LDL receptors in PCSK9-resistsnt SV-589 fibroblasts. *J. Lipid. Res.* 55:266-275.

90. Institute for Clinical and Economic Review. PCSK9 Inhibitors for Treatment of High Cholesterol: Effectiveness, Value, and Value-Based Price Benchmarks Draft Report 2015. 1-116.

91. Luo, Y., Warren, L., Xia, D., Jensen, H., Sand, T., Petras, S., Qin, W., Miller, K. S., Hawkins, J. 2009. Function and distribution of circulating human PCSK9 expressed extrahepatically in transgenic mice. *J. Lipid Res.* 50:1581–1588.

92. Fan, D., Yancey, P. G., Qiu, S., Ding, L., Weeber, E. J., Linton, M. F., Fazio, S. 2008. Self-association of human PCSK9 correlates with its LDLR-degrading activity. *Biochemistry.* 47:1631–1639.

93. Sun, H., Samarghandi, A., Zhang, N., Yao, Z., Xiong, M., Teng, B.B. 2012. Proprotein convertase subtilisin/kexin type 9 interacts with apolipoprotein B and prevents its intracellular degradation, irrespective of the low-density lipoprotein receptor. *Atheroscler. Throm. Vasc. Biol.* 32:1585-1595.

94. Hori, M., Ishihara, M., Yuasa, Y., Makino, H., Yanagi, K., Tamanaha, T., Kishimoto, I., Kujiraoka, T., Hattori, H., Harada-Shiba, M. 2015. Removal of plasma mature and furin-cleaved proprotein convertase subtilisin/kexin type 9 by low-density lipoprotein apheresis in familial hypercholesterolemia: development and application of a new assay for PCSK9. *J. Clin. Endocrinol. Metab*. 100:E41-E49.

95. Sarkar, S.K., Foo, A.C.Y., Matyas, A., Asikhia, I., Kosenko, T., Goto, N. K., Vergara-Jaque, A., Lagace, T.A. 2020. A transient amphipathic helix in the prodomain of PCSK9 facilitates binding to low-density lipoprotein particles. *J. Biol. Chem.* 295: 2285-2298.

96. Hampton, E.N., Knuth, M.W., Li, J., Harris, J.L., Lesley, S.A., Spraggon, G. 2007. The self-inhibited structure of full-length PCSK9 at 1.9 Å reveals structural homology with resistin within the C-terminal domain. *Proc. Natl. Acad. Sci. U. S. A.* 104:14604-14609.

97. Holla, O.L., Cameron, J. Tveten, K., Strom, T.B., Berge, K.E., Laerdahl, J.K., Leren, T.P. 2011. Role of the C-terminal domain of PCSK9 in degradation of the LDL receptors. *J. Lipid Res.* 52:1787-1794.

98. Grimsley, G.R., Scholtz, J.M., Pace, N.C. 2008. A summary of the measured pK values of the ionizable groups in folded proteins. *Protein Science.* 18:247-251.

99. Geisow, M.J. and W.H. Evans. 1984. pH in the endosome: Measurements during pinocytosis and receptor-mediated endocytosis. *Exp. Cell Research.* 150:36-46.

100. Ouguerram, K., Chetiveaux, M., Zair, Y., Costet, P., Abifadel, M., Varret, M., Boileau, C., Magot, T., Krempf, M. 2004. Apolipoprotein B100 metabolism in autosomal-dominant hypercholesterolemia related to mutations in PCSK9. *Atheroscler. Throm. Vasc. Biol*. 24:1448-1453.

101. Pandit, S., Wisniewski, D., Santoro, J.C., Ha, S., Ramakrishnan, V., Cubbon, R.M., Cummings, R.T., Wright, S.D., Sparrow, C.P., Sitlani, A., Fisher, T.S. 2008. Functional analysis of sites within PCSK9 responsible for hypercholesterolemia. *J. Lipid Res.* 49:1333-1343.

102. Timms, K.M., Wagner, S., Samuels, M.E., Forbey, K., Goldfine, H., Jammulapati, S., Skolnick, M.H., Hopkins, P.N., Hunt, S.C., and Shattuck, D. M. 2004. A mutation in PCSK9 causing autosomal-dominant hypercholesterolemia in a Utah pedigree. *Hum. Genet.* 114:349–353.

103. Wright, P. E., and Dyson, H. J. 2009. Linking folding and binding. *Curr. Opin. Struct. Biol.* 19: 31–38.

104. Wright, P. E., and Dyson, H. J. 2015. Intrinsically disordered proteins in cellular signalling and regulation. *Nat. Rev. Mol. Cell Biol.* 16:18–29.

105. Ahrens, J. B., Nunez-Castilla, J., and Siltberg-Liberles, J. 2017. Evolution of intrinsic disorder in eukaryotic proteins. *Cell. Mol. Life Sci.* 74:3163–3174.

106. Fasano, T., Sun, X.M., Patel, D.D., Soutar, A.K. 2009. Degradation of LDLR protein mediated by 'gain of function' PCSK9 mutants in normal and ARH cells. *Atherosclerosis.* 203:166-171.

107. Geschwindner, S., Andersson, G.M., Beisel, H.G., Breuer, S., Hallberg, C., Kihlberg, B.M., Lindqvist, A.M., O'Mahony, G., Plowright, A.T., Raubacher, F., Knecht, W. 2015. Characterization of de novo mutations in the C-terminal domain of proprotein convertase subtilisin/kexin type 9. *Protein Eng. Des. Sel.* 28:117-125.

108. Kristensen, K. K., Midtgaard, S.R., Mysling, S., Kovrov, O., Hansen, L.B., Skar-

Gislinge, N., Beigneux, A.P., Kragelund, B.B., Olivecrona G., Young, S.G., Jorgensen, T.J.D., Fong, L.G., Ploug, M. 2018. A disordered acidic domain in GPIHBP1 harboring a sulfated tyrosine regulates lipoprotein lipase. *Proc. Natl. Acad. Sci. U.S.A.* 115:E6020-6029.

109. Ding, K., S. J. McDonough, and I. J. Kullo. 2007. Evidence for positive selection in the C-terminal domain of the cholesterol metabolism gene PCSK9 based on phylogenetic analysis in 14 primate species. *PLoS ONE*. 2:e1098.

110. Holla, O. L., Laerdahl, J.K., Strom, T.B., Tveten, K., Cameron, J., Berge, K.E., Leren, T.P. 2011. Removal of acidic residues of the prodomain of PCSK9 increases its activity towards the LDL receptor. *BBRC.* 406:234-238.

111. Lagace, T. A., D. E. Curtis, R. Garuti, M. C. McNutt, S. W. Park, H. B. Prather, N. N. Anderson, Y. K. Ho, R. E. Hammer, and J. D. Horton. 2006. Secreted PCSK9 decreases the number of LDL receptors in hepatocytes and in livers of parabiotic mice. *J. Clin. Invest.* 116:2995–3005.

112. Gustafsen, C., Olsen, D., Vilstrup, J., Lund, S., Reinhardt, A., Wellner, N., Larsen, T., Andersen, C. B. F., Weyer, K., Li, J. P., Seeberger, P. H., Thirup, S., Madsen, P., and Glerup, S. 2017. Heparan sulfate proteoglycans present PCSK9 to the LDL receptor. *Nat. Commun.* 8:503.

113. Galvan, A.M. and J.S. Chorba. 2019. Cell-associated heparin-like molecules modulate the ability of LDL to regulate PCSK9 uptake. *J. Lipid Res.* 60: 71-84.

114. Dron, J.S. and R.A. Hegele. 2017. Complexity of mechanisms among human proprotein convertase subtilisin-kexin type 9 variants. *Curr. Opin. Lipid*. 28:161-169.

6. Contribution of Collaborators

Dr. Lagace founded the project idea. Previous lab members made all of the PCSK9 mutations used for experiments that are not listed in the primers table (Table 2.1). All of the protocols described in the methods section had been established prior to me beginning my project. I completed all of the experiments, data collection and data analyses myself, with help from Tanja and Dr. Lagace. I received extensive feedback from Dr. Lagace throughout my master's project and in the process of writing this thesis. I also received edits and suggestions from Tanja for my materials and methods.

Dr. Samantha Sarkar completed the LDL binding studies mentioned but not shown: S127R (competition binding curves), D129G (another prodomain FH variant), and the E39P-R496Q "armadillo" combination mutation. She also repeated the LDL binding twice for E39A and E39P mutations (the representative experiment shown in Figure 6C was done by me). Dr. Ariela Vergara-Jaque generated the computational model seen in Figures 3 and 15 with the PCSK9 crystal structure (96) and molecular simulations for the NTR using the ROSETTA software (95). I generated the rest of the figures myself through GraphPad Prism, Adobe Illustrator and/or PowerPoint. The data for L108R PCSK9 is not published (LDL and LDLR affinity data – Figure 8) and was completed by me during my Honours thesis for the BIM project at uOttawa in 2017-2018 titled, "Investigation into the molecular mechanisms underlying the L108R gain-of-function mutation in proprotein convertase subtilisin/kexin type 9."

7. Curriculum Vitae

Academic Background & Awards

- **The University of Ottawa Heart Institute (2018-2020)**

MSc in Biochemistry – Lipoprotein Receptor Biology Lab (Supervisor Dr. Thomas Lagace)
Admission Scholarship – Graduate (2018-2020)
Excellence Scholarship (2019)
Queen Elizabeth II Graduate Scholarship in Science and Technology (2019)

- **The University of Ottawa (2014-2018)**

BSc (Hons) in Biomedical Sciences (Neuroscience) – Magna Cum Laude
Merit Scholarship (2016)
Dean's Honour list (2017, 2018)
Admission Scholarship – Undergraduate (Received in 2014 – Renewed in 2017, 2018)

Publications

Sarkar, S.K., Foo, A.C.Y., *** Matyas, A**., Asikhia, I., Kosenko, T., Goto, N. K., Vergara-Jaque, A., Lagace, T.A. 2020. A transient amphipathic helix in the prodomain of PCSK9 facilitates binding to low-density lipoprotein particles. *J. Biol. Chem.* 295:2285-2298.

Oral Presentations

*** Matyas A**, Sarkar S K, Kosenko T, Lagace T A. "FH associated mutations in PCSK9 disrupt LDL binding and increase LDLR degradative functions," The Canadian Vascular and Lipid Summit. Oct 2019, Banff, AB, Canada.

Poster Presentations

*** Matyas A**, Sarkar S K, Kosenko T, Lagace T A. "Understanding the role of PCSK9's inter-domain interactions in hypercholesterolemia," uOttawa BMI Poster Day, May 2019.

*** Matyas A**, Sarkar S K, Lagace T A. "Investigation into the molecular mechanisms underlying the L108R gain-of-function mutation in proprotein convertase subtilisin/kexin type 9," uOttawa BIM Honours Poster Session, April 2018.

Work & Volunteer Experience

Communications Coordinator – Ottawa Heart / UOHI Trainee Committee (2019-2020)
Volunteer Science Educator – Let's Talk Science (2018-2020)
Undergraduate Research Assistant – Ottawa Heart Institute (2017, 2018)
Pharmacy Assistant – Marina Pharmacy (2016-2018)